Early-Life RSV-Infection Alters Local and Systemic Immune Cell Populations in Neonates through TSLP Production

by

Carrie-Anne Malinczak

A dissertation submitted in partial fulfillment
of the requirements for the degree of
Doctor of Philosophy
(Molecular and Cellular Pathology)
in the University of Michigan
2019

Doctoral Committee:

Professor Nicholas W. Lukacs, Chair
Associate Professor Jane Deng
Associate Professor David Lombard
Professor Bethany B. Moore

Carrie-Anne Malinczak

carrieam@umich.edu

ORCID iD: 0000-0003-3377-5921

Acknowledgements

As with any major life accomplishment, I have many people to thank. First, my mentor Nick Lukacs. Throughout my career, I have worked with many mentors and Nick is by far, without a doubt, the best mentor I have ever had. My career path has been atypical, having returned to academia to pursue a Ph.D. degree, after spending nearly 20 years working in industry. When choosing a lab, it was crucial for my success that I find a fit that would accommodate my family life. He made it possible to focus on work/life balance with little stress. I could not have done this without his support as well as that of the entire Lukacs lab!

To everyone in the Lukacs lab, I owe many thanks. Andrew was my side-kick, working on nearly every *in vivo* endpoint with me. Sue is a great source of technical and experimental expertise and she made sure the RSV stock remained replenished. Catherine was a mentor of mine from the very beginning when I started my rotation. Finally, Wendy became a very solid confidante both scientifically and personally. She was there through all the projects and a great support for me personally, knowing how difficult work-life balance can be at times.

I also had collaborators in other labs that offered significant support including Matt for flow training and Ron for ChIP analysis. I also want to recognize Abhijit (Chinnaiyan Lab) for the assistance with ATAC-seq work and the Zemans lab, especially Steve, for the support in the structural analysis work.

My committee members Beth, Dave, and Jane have also been instrumental in supporting my work and for giving advice on next stages of my career.

I am also very fortunate to have the support of my parents who showed me that by having a

Table of Contents

List of Figures

List of Appendices

Abstract

Respiratory syncytial virus (RSV), a ubiquitous human pathogen, infects nearly all children by the age of two. It produces severe lower respiratory tract disease, including bronchiolitis, and is characterized by excessive mucus production and immune-mediated lung damage. Severe RSV bronchiolitis in infancy is strongly correlated with development of recurrent wheezing later in childhood, and boys are twice as likely to be affected than girls. These findings suggest persistent immune system alterations well beyond the time of viral clearance, especially in boys. RSV has the ability to evade the type-1 immune response and prime toward a pathologic Th2/Th17 response. Immunopathology associated with severe RSV infection is believed to be the cause of significant airway diseases later in life. However, sex differences associated with these changes and/or if systemic alterations are occurring along with local lung alterations have not been previously defined.

Our studies here show that early-life RSV infection leads to differential long-term effects based upon the sex of the neonate, leaving male mice prone to exacerbation upon secondary allergen exposure while overall protecting female mice. During initial viral infection, we observed better viral control in the female mice with correlative expression of interferon-β that was not observed in male mice. Additionally, we observed persistent immune alterations in male mice at 4 weeks post-infection. These alterations include Th2 and Th17-skewing, innate cytokine expression (*Tslp* and *Il33*), and infiltration of innate immune cells (DC and ILC2). Upon exposure to allergen, beginning at 4 weeks following early-life RSV-infection, male mice show severe

allergic exacerbation while female mice appear to be protected; knockdown of TSLP signaling using TSLPR-/- mice abrogated allergen exacerbation in male mice.

We also show that long-term systemic alterations are occurring following early-life RSV-infection. Bone marrow-derived dendritic cells (BMDC) isolated from early-life RSV-infected male mice at 4 weeks post-infection retained expression of maturation markers (*Cd80/86, Ox40l*). Chemokines/ cytokines associated with the inflammatory response during RSV-infection were also persistently expressed along with *Kdm6b* and *Tslp*. Knockdown of TSLP signaling using TSLPR-/- male mice abrogated this activated phenotype and led to enhanced T cell IFN-γ production. ATAC-seq data indicated differences in the chromatin landscape of WT and TSLPR-/- BMDC, showing more open regions of chromatin near anti-viral type-1 genes, *Mid1, Spp1,* and *Cxcl11* in TSLPR-/- BMDC. qPCR showed increased expression of *Mid1*, *Ifnb* and *Il12a*.

Further evaluation of BMDC showed *KDM6* demethylases were upregulated upon RSV-infection. KDM6 Chemical inhibition (GSK J4) in BMDC decreased production of chemokines and cytokines associated with the inflammatory response during RSV-infection and decreased maturation marker (CD80/86, MHCII) expression, similar to the TSLPR-/- BMDC phenotype. RSV-infected BMDC treated with GSK J4 altered co-activation of T cell cytokine production. Airway sensitization of naïve mice with RSV-infected BMDCs exacerbate a live challenge with RSV infection but was inhibited when BMDCs were treated with GSK J4 prior to sensitization. Finally, *in vivo* treatment with GSK J4 during RSV-infection reduced immunopathology.

Collectively, these studies highlight the importance of proper anti-viral immune responses to limit RSV-driven Th2 immunopathology and future disease by limiting persistent alterations of the immune system. These data validate neonatal sex-differences to RSV and indicate that sex of

the neonate should be considered during RSV disease treatment. These studies identify TSLP as

a promising therapeutic target, especially in boys hospitalized with severe RSV.

Chapter 1: Introduction

1.1. Respiratory Syncytial Virus Infection

1.1.1 Virus genome and immune evasion

Respiratory syncytial virus (RSV) is often the first clinically relevant pathogen encountered in life, with nearly all children infected during the first 2 years of life[1,2] . RSV infection is the leading cause of childhood hospitalization and increases the risk for developing childhood asthma and recurrent wheezing[1,3]. RSV can also adversely affect the elderly and immunocompromised individuals, causing severe lower respiratory tract infection and pneumonia[4–6]. RSV is a single-stranded RNA virus belonging to the Paramyxoviridae family. The RSV genome consists of 10 genes that can encode 11 different proteins: the fusion glycoprotein (F), G glycoprotein (G), small hydrophobic protein (SH), a matrix protein (M) and 2 matrix protein variants (M2-1 and M2-2), a nucleoprotein (N), a phosphoprotein (P) and the large RNA polymerase protein (L) as well as 2 non-structural proteins (NS1 and NS2)[7,8]. The F, G and SH proteins form the viral envelope while the M proteins, N, P and L proteins associate with the single-stranded RNA.

The RSV-F and G proteins are the main virulence factors which mediate airway epithelial cell penetration during RSV infection[7–9]. The G protein facilitates attachment to glycosoaminoglycans present on the surface of target cells, while the F protein mediates fusion of the viral envelope and cell plasma membrane, releasing the nucleocapsid into the cytoplasm[9,10]. Upon entry, the L protein initiates transcription of the negative-sense RNA[7,11]. Virion assembly then takes place at the plasma membrane, where the nucleocapsid localizes with viral envelope proteins expressed on the host cell membrane. Virions bud off of the apical surface of polarized alveolar epithelial cells,

where they form clusters of long filaments that extend from the cell surface, which form the syncytia associated with RSV infection[7,11].

RSV has the ability to evade the immune response via multiple mechanisms. The non-structural proteins (NS1 and NS2) are able to inhibit both the innate and adaptive immune system[12,13]. NS1 is a known inhibitor of type-1 interferon, which is required for viral clearance[14–16]. Additionally, NS1 can antagonize both dendritic cell maturation and T cell responses[17,18], while NS2 can bind RIG-I and degrade STAT-2 to further inhibit type-1 interferon[12,13]. Finally, the G glycoprotein has multiple methods for being immunomodulatory, such as the production of a secretory G form that acts as an antigen decoy to inhibit antibody-mediated viral effects[11,19].

The remarkable ability of RSV to evade and alter the immune system is likely what leads to the clinical relevance of this pathogen. Despite only a single RSV serotype and 2 antigenic subpopulations (A and B), immunologic memory following RSV infection is often short-lived and sub-optimal and therefore, re-infection throughout life is common[7,8,11]. Additionally, early-life RSV infection is associated with childhood wheezing related to respiratory viral infection exacerbation, allergies and asthma[1,3]. Currently, there is no available vaccine for RSV and therefore, elucidating the mechanisms and pathways involved in RSV-driven immunopathology and subsequent lung pathologies later in life is of critical importance.

1.1.2. Epidemiology

The health burden costs of RSV infection account for over 3 million hospitalizations and approximately 100,000 deaths per year in children under 5, worldwide[20,21]. Studies have shown that up to 68% of infants may be infected with RSV in their first year of life and nearly all children will be infected by 2 years of age[22]. In healthy infants, those that are 3-6 months of age during peak RSV season are most at risk. The main line of defense during early life is maternally-derived

neutralizing antibodies; however, these antibodies appear to be insufficient, decrease as the infant ages and completely wane within 6 months of age[22].

RSV infection is almost always symptomatic, with most infections leading to mild upper respiratory tract infections or otitis media[22]. However, severe lower respiratory tract infections, most often bronchiolitis, may also occur and may be life-threatening. It is suggested that 15-50% of childhood infections involve the lower respiratory tract with ~5% requiring hospitalization[22,23] and up to 10% of those hospitalized will end up in the intensive care unit due to severe disease[11,22]. RSV is believed to be the most frequent viral cause of lower respiratory tract infection in children and is implicated in up to 80% of all bronchiolitis cases[22,23]. Bronchiolitis is the cause of nearly 20% of infant hospitalization in the United States[22], indicating that RSV is a significant health care burden, even in industrialized countries.

RSV-related death is a significant cause of mortality in developing countries and individuals with pre-existing conditions and is believed to be the second most likely cause of death by a single pathogen in children under 1 year of age, worldwide[22,24]. In addition to a severe primary infection, RSV re-infection is common throughout life and up to 75% of infants infected by 12 months of age will become re-infected before they reach the age of 2. Symptoms of the disease wane with re-infection; however, the elderly, immunocompromised individuals, and those with chronic conditions are at high risk of developing lower respiratory tract infections making RSV a significant cause of morbidity and mortality in these individuals[22,24].

There is currently no vaccine available or a sufficient option for anti-viral therapy, partially due to our incomplete understanding of how severe immunopathology is developed. In the 1960s, a vaccine trial was conducted with suboptimal optimal results; vaccinated infants became severely exacerbated upon exposure to live virus leading to severe disease as well as 2 infant deaths[25–27].

3

There is however, a monoclonal antibody (Palivizumab) that does show success when given to high risk infants prophylactically, leading to decreased hospitalization compared to control groups as well as decreased incidence of subsequent wheezing[28]. However, at least half of all children that are hospitalized due to severe RSV are previously healthy individuals[22] that would not qualify for prophylactic treatment; therefore, identifying mechanisms leading to disease and furthermore, novel treatment options for the general population is a critical unmet need.

1.1.3. RSV-driven immunopathology

RSV predominantly infects ciliated epithelial cells in the airways but can also lead to infection in the sub-epithelium and neighboring immune cells, such as dendritic cells[29,30]. The major histopathologic characteristics of RSV infection include acute bronchiolitis, mucosal swelling of the airways, and airway obstruction caused by sloughed epithelial cells and mucus production[6,22,30]. Recent pre-clinical and clinical data, suggest that severe RSV disease is associated with an altered innate and adaptive immune response, characterized by excessive Th2 and Th17 immune responses[20,31–36]. Numerous studies have shown that RSV plays a role in reducing innate cytokine production that is necessary for appropriate anti-viral responses[20,35,37,38]. Both viral replication as well as RSV-associated immunopathology can lead to RSV disease symptoms and probing these and potentially other underlying disease mechanisms that are supported by clinical data will be important for therapeutically targeting the immune environment.

Initial RSV response is driven by innate cytokines, such as IL-25, IL-33 and thymic stromal lymphopoietin (TSLP) that are released from the airway epithelial cells following infection. These cytokines have the ability to activate the immune response through interactions with dendritic cells, T cells and innate lymphoid cells[39–43]. During a typical viral infection, the immune response is strongly dictated by dendritic cells (DC) because they activate the immune system and instruct

T cells toward distinct T helper type responses [44]. RSV can skew the immune response away from anti-viral and towards a Th2-type response by inhibiting the production of IFN-β and subsequently decreasing the Th1 response[45]. This lack of an anti-viral response as well as skewing towards dysregulated Th2/Th17 has been correlated with severe disease[20,31,35]. Additionally, studies with neonatal RSV infection have demonstrated that there are persistent, long-term alterations in the lung that include increased mucus production and increased populations of immune cells[46,47].

1.1.3.1. Th2 response

1.1.3.1.1. T cells

The differentiation of specific T cell subsets was discovered in mice[48–50] and subsequently shown in humans[51]. T cell-mediated immunity occurs in successive antigen-driven and cytokine-driven steps. First, T cells are activated by specific antigens presented by peptide-MHC complexes on the surface of antigen presenting cells (ie. Dendritic cells). Next, these activated T cells are induced to clonally expand by the cytokine Interleukin-2 (IL-2), and subsequently differentiate into CD4+ T cells as a result of a specific subset of cytokines engaging and activating their respective cytokine receptors[52,53]. Distinct cytokine profiles reflect different T cell functions and include: Th1-type, which primarily produce IFN-γ; Th2-type characterized by the production of the cytokines IL-4, IL-5 and IL-13, and Th17-type, which produce mainly IL-17 and IL-22. The overall role of T cells differs in that Th1 are mainly involved in cell-mediated immunity[54] and the anti-viral response[55,56] whereas Th2 is responsible for humoral immunity and B cell development of the antibody response[54]. The Th17 arm of the immune response is largely involved in antibacterial and mucosal immunity[57]. A successful immune response requires a balance of these subsets and inappropriate immune response skewing has been linked to the development of pathologic responses, such as that observed following RSV infection[20,31,35].

For example, the Th2 immune response has been implicated in severe RSV disease as well as the development of many lung pathologies, such as allergy and asthma[20,35,58]. The Th2 response promotes the infiltration of eosinophils and neutrophils into the lungs leading to an inflammatory-allergic cellular environment which dampens effector functions, such as the secretion of IFN-γ[35,36]. As a result, clearance of RSV is delayed and instead, viral spreading is promoted. The specific cytokines involved in this response include IL-4, IL-5 and IL-13 which have been shown to perform both independent as well as overlapping roles, leading to antibody class switching to IgE, eosinophil recruitment and mucin production; characteristics of both severe RSV disease as well as asthma that can lead to airway hyperreactivity which is associated with poor lung function[35,58].

IL-4/IL-13

Interleukin-4 (IL-4) is a multifunctional cytokine that plays a critical role in the immune response and shares sequence homology, cell surface receptors, intracellular signaling, and partial functional effects on cells with another Th2-type cytokine, IL-13[59,60]. Both IL-4 and IL-13 are produced by activated T cells as well as mast cells, basophils, eosinophils and innate lymphoid type-2 cells (ILC2)[39,59,60]. IL-4 is best known for defining the Th2 phenotype as well as regulating cell proliferation, apoptosis, and expression of numerous genes in various cell types[60]. Additionally, IL-4/IL-13 are involved in antibody class-switching to IgE by recruiting and activating IgE-producing B cells that mediate diseases such as allergy and asthma[60–62]. These cytokines are also both involved in inflammation and mucus production associated with the type-2 immune response.

The IL-4 alpha receptor (IL-4Rα) is a unique member of the common-gamma chain (γ_c) family of receptors[59] with the ability to signal within three different receptor complexes, known as Type I and Type II receptors[63–65]. On cells of hematopoietic stem cell origin, the Type I receptor

6

comprises IL-4Rα and γ_c[59]. Type I receptor complexes are only formed by IL-4 and are more active in regulating Th2 development. In non-hematopoietic stem cells, IL-4 can use the Type II complex, comprising IL-4Rα and IL-13Rα1[66]. Type II receptor complex is also a functional receptor for IL-13[67] which largely explains the overlap of the biological effects of IL-4 and IL-13[68]. Type II receptor complex formed by either IL-4 or IL-13 is more active in regulating cells that mediate airway hypersensitivity and mucus secretion[63]. Interestingly, IL-13 appears to have its own distinct role in allergic inflammation, acting as a key regulator of allergen-induced airway inflammation, and goblet cell metaplasia[68].

IL-5

The Th-2 associated cytokine IL-5 was initially identified by its ability to support the growth and terminal differentiation of mouse B cells *in vitro*; it has now been shown to exert pleiotropic activities on various target cells including B cells, eosinophils, and basophils. IL-5 is produced by both hematopoietic and non-hematopoietic cells including T cells, granulocytes, and natural helper cells and exerts its effects via receptors that comprise an IL-5-specific α and common β-subunit[69]. IL-5 is involved in the recruitment of eosinophils and contributes to inflammation and epithelial cell sloughing within the airways[70]. IL-5 regulates eosinophilia within the lung as well as in the circulation and amplifies chemotaxis into the airways. Moreover, in the presence of antigen, IL-5 provides fundamental signals for eosinophil degranulation and assists in the induction of airway hyperreactivity (AHR) [70,71].

In addition to inflammation, epithelial cell sloughing and AHR, the Th2 immune response is also involved in mucus production. Excessive secretion of mucus in the airways is an important cause of morbidity and mortality in diseases such as asthma, chronic obstructive pulmonary disease (COPD), and cystic fibrosis[72]. In patients and experimental animal models with these

airway diseases, including RSV, increased numbers of goblet cells (mucus-producing cells) line the surface airway epithelium of the lung, defined as goblet cell metaplasia[72]. Mucus production within the lungs of mice is largely driven by the mucus genes: *Gob5* and *Muc5ac*. The expression of *Muc5ac* is used as a marker for goblet cells and *Gob5* expression has been shown to be increased in the lungs of asthmatics[72]. Additionally, it has been determined that the overexpression of *Gob5* can lead to increased expression of *Muc5ac*[72]. Mucus cell metaplasia in airway diseases is accompanied by significant airway inflammation, therefore, inflammatory cells and their secreted mediators are believed to directly act on airway epithelial cells to induce goblet cell formation. In asthma, Th2 cytokines, such as IL-4 and IL-13 play important roles in directly causing *Muc5ac* expression in airway cells but IL-13 seems to have the more prominent role. IL-4 has also been shown to induce mucin expression *in vitro* and *in vivo*[72], but is not critical to mucus cell hyperplasia. IL-13, on the other hand, has been shown to act directly on airway epithelial cells to increase *Muc5ac* expression as well as lead to goblet cell metaplasia[72].

1.1.3.1.2. Innate Lymphoid Type-2 Cells (ILC2)

Importantly, T cells are not the only cells capable of producing Th2-type cytokines. Some of the additional cell types, include mast cells, eosinophils, neutrophils and basophils. Another significant producer of Th2 cytokines are the innate lymphoid 2 cells (ILC2), known to be involved in lung disease pathogenesis. ILC2 are a rare population of innate cells of lymphoid origin, but unlike T cells or B cells do not contain an antigen receptor and are therefore, non-specific innate responding cells. It has been suggested that ILC2 are far more potent than CD4+ T cells in their induction of type-2 cytokines; in fact, it is estimated that ILC2 produce 10 times more cytokine than T cells on a per cell basis[73].

Innate lymphoid cells play key roles in lymphoid tissue development as well as the initiation of inflammation and more complex roles during the immune response, including the transition from innate to adaptive immunity and chronic inflammation[39,74]. Remarkably, dysregulation of this rare population has been linked with chronic pathologies, including asthma and autoimmunity[39]. The early expression of ILC2 leads to eosinophilia (IL5), mucus production (IL-13) and lung repair (amphiregulin)[74,75]. ILC2 are the main source of IL-13 during helminth expulsion but are also known to expand during allergic lung inflammation[74].

Innate cytokines, including thymic stromal lymphopoietin (TSLP), IL-25 and IL-33 are known inducers of ILC2 differentiation[39,40,76]. ILC2 are increased in RSV infected lungs and these cells produce IL-5 and IL-13, cytokines important in the development of airway inflammation and mucus production as described above[46,47]. The secretion of these innate cytokines following infection of airway epithelial cells by RSV leads to the initial activation of the immune response, including the activation of dendritic cells (DC, described below) as well as ILC2[43]. Stier et al[73], link the early induction of effector ILC2 to the development of airway hyperreactivity and mucus production associated with RSV through TSLP-driven induction of IL-13 producing ILC2[73]. Age-related IL-33 production was shown to be necessary to induce ILC2 and lead to Th2-driven immunopathology following neonatal RSV infection[47]. In addition to the RSV-driven immunopathology, this innate cytokine/ILC2 mechanism has also been implicated in pathologies related to early-life rhinovirus infection[77].

Furthermore, ILC2 have also been linked to adaptive immunity[78]. For example, ILC2 response is required for DC polarization of CD4+ Th2 memory during allergic responses[79]. ILC2s were found to act upstream of DCs, making them essential for DC production of CCL-17, a chemoattractant for memory Th2 cells demonstrating that ILC2 are critical for orchestrating an

efficient localized memory Th2 cell response in collaboration with tissue-resident DC[79]. During allergic lung inflammation following papain exposure, ILC2 are necessary for CD4+ T cell polarization[80]. Here, IL-33 mediated ILC2 development was required for IL-13 driven migration of DC to the lung draining lymph nodes where they primed T cells towards Th2.

1.1.3.2. Th17 response

In addition to Th2-type immunity, RSV also leads to a pathogenic Th-17 response. The Th17 immune response is involved in regulating inflammation but also modulates lung and airway structural cells during the pathogenesis of asthma and COPD[81]. During anti-bacterial immunity, Th17 immunity is crucial for neutrophil recruitment to limit bacterial infection[82]. Th17 responses are also involved in the development of mucus production and goblet cell hyperplasia by leading to the upregulation of *Muc5ac*[83,84]. Signaling through STAT-3, activated by IL-6 and IL-23 as well as IL-1β and TGFβ are required for induction of Th17 cells[81]. Cell types capable of producing IL17-associated cytokines include CD4+ T cells, γδ T cells, ILC3, and neutrophils[81].

The IL-17 family of cytokines consists of 6 family members IL-17A-F[85,86]; IL-17A and IL-17F show the strongest proinflammatory role and are involved in many diseases of autoimmunity as well as asthma[86]. The percentage of Th17 cells as well as the plasma concentrations of IL-17 increase with disease severity and elevated IL-17A levels correlate with increased AHR in patients with asthma[81]. Additionally, IL-17 has also been reported to modulate airway structural cells, leading to tissue remodeling[81]. IL-17A induces the expression of two mucin genes (*Muc5ac* and *Muc5b*) in bronchial human and murine epithelial cells and overexpression of IL-17F in mice results in goblet cell hyperplasia and mucin gene expression. Moreover, IL-17A and IL-17F induce several profibrotic cytokines, such as IL-6 and TGF-β[81].

In the case of RSV infection, IL-17A was determined to be upregulated during human infection with RSV as well as in mouse models of disease[31]. Mouse modeling showed that IL-17A was pathogenic through its role in driving mucus production and inflammation as well as inhibition of CD8+ cytotoxic T cells during RSV infection and inhibition of IL-17A led to increased viral clearance and decreased pathology. Additionally, this study showed that IL-17 is involved in exacerbated allergic responses following RSV infection through mucus production, inflammation and increased Th2 responses. These data indicated that Th-17 is involved in both pathologic responses following RSV infection as well as exacerbations later in life, including allergy and asthma[31].

1.1.3.3. Dendritic Cell Role During RSV

Dendritic cells (DC) play a crucial role in the development of the immune response and link innate and adaptive immunity by instructing T cells toward a Th1 (anti-viral), Th2 (anti-parasitic or allergy-associated) or Th17 (anti-bacterial or autoimmunity) type response. DC are sentinel cells present in the lung during steady-state conditions that constantly monitor the lungs for foreign pathogens or antigens. Upon RSV infection, DCs acquire viral antigen either through direct infection or indirectly from dying infected cells. They then undergo maturation and migrate to the lung-draining lymph nodes (LDLN) where they present antigen to naive T cells. Mouse DC are divided into conventional DC (cDC) which are CD11c+/MHCII+ and plasmacytoid DC (pDC) which are CD11c^{int}/B220+[87]. Plasmacytoid DC show a protective role during RSV infection largely through the production of Type-1 IFN[29,88]. Conventional DC within the lung are further divided into CD11b+ and CD103+ both of which have been implicated in pathogenic inflammatory responses during RSV infection[29]; with CD103+ shown to drive very strong Th2 responses[89]. During a typical viral response, the DC instruct T cells toward anti-viral Th1 via the

production of Type-1 interferon (IFN), such as IFN-β, which leads to the production of IFN-γ and proper viral clearance[15]. However, RSV has the ability to dampen type-1 immunity as described previously through multiple mechanisms, including direct inhibition of type-1 interferon as well as the use of an antigen decoy to evade the immune system[7,12,19]. In the absence of type-1 immunity, the DC produce cytokines and chemokines that skew the response towards Th2/Th17[7,11,36].

It has been shown that the numbers of cDC and pDC increase in the lung following RSV infection in both human and mouse[11,29]. Analysis of nasal washes collected from children during an RSV infection determined that DC were increased in the lung and furthermore, levels of cDC in the blood were decreased, correlating with recruitment to sights of infection[29]. Interestingly, correlations have been shown between absolute number of cDC and increased levels of inflammatory cytokines (i.e. IL6, CCL2) supporting cDC as a source of inflammation within the nasal cavity during RSV infection[29]. In addition, mouse studies indicate an increase in mature DC that contain RSV RNA within the lung draining lymph nodes (LDLN); evidence that DC have the ability to acquire DC, mature and navigate to the LDLN to activate naïve T cells.

RSV infection of DC leads to maturation of the infected cell as well as neighboring DC along with the upregulation of MHC and co-stimulatory molecules, such as CD80 and CD86[29,90]. RSV-infected DC produce pro-inflammatory cytokines such as IL-1β, IL-6, IL-12, type-1 IFN and TNFα as well as chemokines such as CCL2, CCL3 and CCL5. However, despite maturation and this pro-inflammatory milieu, these DC lack an ability to properly activate and polarize naïve T cells[29,90]. Two different models have been described to support this phenomenon, including RSV-secretion of an immunosuppressive factor and disruption of synapse formation between DC and naïve T cell[29,35]. However, it is likely that a combination of both models exists to inhibit proper T

cell activation which leads to a decrease in T cell production of important anti-viral cytokines, such as IL-2 and IFN-γ, leading to an imbalanced immune response, skewing away from Th1 anti-viral immunity toward a predominantly Th2/Th17 pathogenic response.

The different DC subsets (pDC and cDC) have been shown to play differential roles in the RSV immune response. The pDC population has a protective role through production of IFN-α for viral clearance as well as regulation of the Th2 response, limiting airway hyperreactivity and mucus production[29,88,91]. On the other hand, cDC have been implicated in promoting the Th2 response by upregulation of CCR6 and CCL20 secretion leading to the recruitment of Th2 cells to the lung[29,92]. Furthermore, while cDC are necessary for a proper inflammatory response against pathogens, sheer absolute numbers of cDC have been proven to lead to a pathogenic response during RSV infection[92]. These data suggest that a critical balance is required between pDC and cDC for proper inflammatory and viral responses within the lungs.

In summary, RSV infects airway epithelial cells leading to secretion of innate cytokines such as IL-25, IL-33 and TSLP, which promotes induction of the immune response by activating dendritic cells, the main link to the adaptive immune response. Dendritic cells then instruct the T cells toward a skewed Th2/Th17 response, through the secretion of immunopathology-linked cytokines and a lack of type-1 IFN production. In addition, the innate cytokines (IL-33, IL-25 and TSLP) are also able to directly act on T cells as well as the innate lymphoid cells to further enhance a Th2 response. Together, this leads to the immunopathology associated with RSV, including goblet cell metaplasia/mucus production as well as inflammation within the airways (**Figure 1-1**).
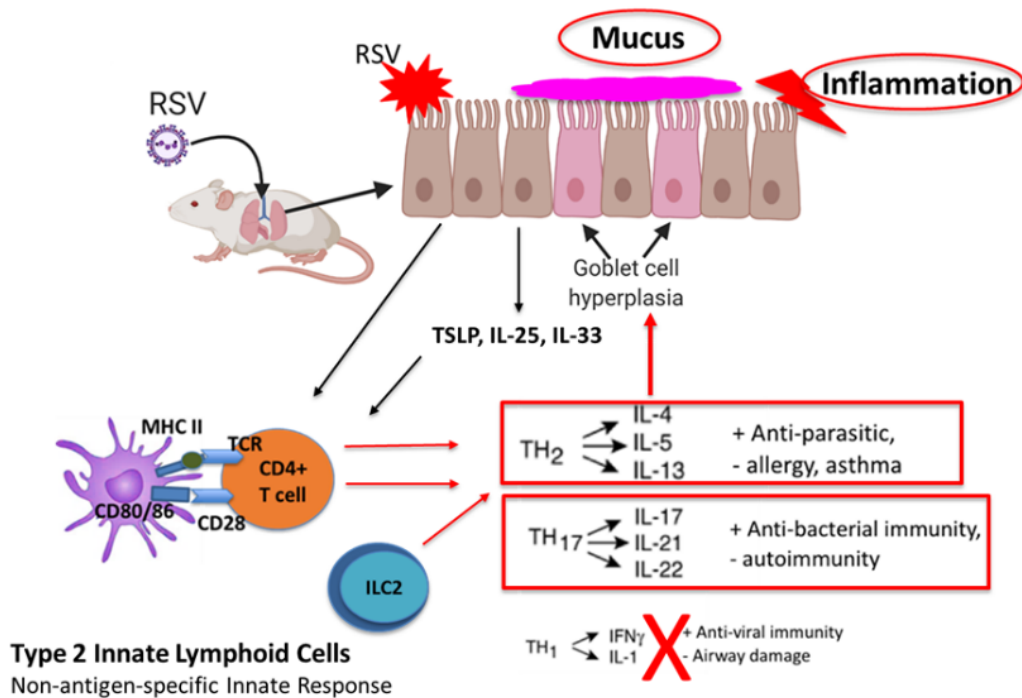
Figure 1- 1. Overview of RSV-infection.
Figure created with BioRendor.com

1.2. Early-life RSV and asthma

Along with the initial disease complications associated with the primary RSV infection, RSV-driven Th2/Th17 skewing has also been implicated in leading to airway restructuring linked to exacerbated allergic responses later in life[93]. Up to 48% of infants who were hospitalized for severe RSV-associated bronchiolitis and/or lower respiratory tract infection go on to develop asthma during their childhood[94,95]. Asthma is the most common chronic childhood illness, affecting approximately 5 million children under 18 years of age, including 1.3 million children under 5[96]. During childhood, males have higher occurrences of asthma and wheezing than do females at a 2:1 ratio[97]. Additionally, males are approximately twice as likely to become hospitalized than females due to severe RSV infection[23]. Thus, the risk for severe RSV infection and RSV-associated asthma development is higher in males than in females[98].

1.3. TSLP in RSV and asthma pathogenesis

As indicated above, innate cytokines such as IL-25, IL-33 and TSLP are implicated in lung pathologies such as those associated with RSV infection and asthma. Many studies have indicated a role for these innate cytokines in respiratory viral complications, asthma development, as well as viral exacerbations of existing asthma[99–101]. Allergen challenge, following neonatal rhinovirus infection identified that both IL-33 and TSLP are required for IL-25-induced ILC2 production of IL-13 leading to mucus metaplasia but TSLP was necessary for maximal ILC2 gene expression even in the presence of IL-25 and IL-33[76]. Additionally, experimental asthma pathogenesis was shown to persist in IL-33R knockout mice (ST2-/-) due to increased expression of TSLP that enhanced ILC2 production of IL-13; abrogation of this response was only possible with the addition of an anti-TSLP antibody[102]. Finally, in an allergen challenge model conducted on adult human subjects with allergic asthma, administration of an anti-TSLP monoclonal antibody (AMG 157) reduced allergen-induced bronchoconstriction and airway inflammation, suggesting a key role for TSLP in allergen-induced airway responses in asthmatics[103]. Collectively, these studies make it plausible that TSLP, IL-25 and IL-33 cooperate and regulate each other during initial disease progression but TSLP may be more significant in the development of subsequent diseases later in life. Furthermore, it has been shown that increased TSLP mRNA in bronchial epithelial cells of asthmatics directly correlates with degree of airflow obstruction[104] and GWAS studies show a strong association between TSLP and severe asthma[105,106]. Therefore, here, we have focused on the cytokine TSLP.

TSLP is an early responding innate cytokine that plays a critical role in the regulation of immune responses and in the differentiation of hematopoietic cells. TSLP was originally identified in the culture supernatant of a thymic stromal cell line as a growth factor for B cell

lymphopoiesis[107,108]. TSLP signals through a heterodimeric receptor complex consisting of an interleukin-7 (IL-7) receptor α chain and TSLP receptor (TSLPR) (also known as cytokine receptor-like factor 2 (CRLF2)). The TSLP/TSLPR axis can activate multiple signal transduction pathways including JAK/STAT and PI-3 kinase[108]. Aberrant TSLP/TSLPR signaling has been associated with a variety of human diseases including asthma, atopic dermatitis, nasal polyposis, inflammatory bowel disease, eosinophilic esophagitis and leukemia[108–110]. Factors such as toll-like receptor ligands, viruses, microbes, allergens, helminths, and chemicals trigger TSLP production[111]. Proinflammatory cytokines, Th2-related cytokines, and IgE also induce or enhance TSLP production, indicating multiple feedback loops[108,111]. The transcription factors NF-κB and AP-1 (BATF) are critical for TSLP regulation[108,111].

Stimulation by TSLP induces the phosphorylation and activation of JAKs, which then regulate the activity of STAT factors, including STAT1, STAT3, STAT4, STAT5a, STAT5b and STAT6[108,112]. The activation of these signaling pathways, leads to multiple TSLP-driven immune responses. For example, pro-inflammatory cytokines such as IL-6 are induced through IRF4/STAT3 that can lead to cell proliferation, dendritic cell migration and subsequently airway inflammatory responses[112]. Additionally, the activation through NFKBIA leads to upregulation of the OX-40L on dendritic cells to drive Th2 responses and airway inflammation upon interaction with OX-40 on Th2 cells[41,112].

TSLP has a wide range of immune cell targets, including ILC2, DC and T cells. The initial biologic function of TSLP demonstrated that it interacted with DC to promote Th2 cell differentiation and thus promoted allergic disease[113,114]. TSLP can also act directly on Th2 cells as well as ILC2, causing them to produce Th2-type cytokines, such as IL-5 and IL-13 to enhance inflammation and mucus production[73] In addition, TSLP signaling instructs DCs to produce CCL-

17 and CCL-22[41], chemokines that recruit Th2 cells through interaction with the CCR4 receptor. Finally, in response to TSLP, cDCs will themselves produce TSLP that further interacts with DCs and ILC2, creating a feedback loop that is independent of epithelial cell-derived TSLP[115,116].

TSLP is upregulated following RSV infection of lung epithelial cells[117]. During neonatal RSV-infection, TSLP mediates immunopathology through OX-40/Th2 signaling[118], as well as exerts direct effects upon ILC2 cells to enhance inflammation and mucus production[73]. When TSLP was neutralized during neonatal RSV infection, the severity of a later exacerbated RSV infection was mitigated[118], indicating that TSLP may be creating a broadly altered immune environment.

1.4. Dendritic Cell Alteration Following Early-life RSV and Long-Term Alterations

Many studies over the years have identified several DC-linked chemokines (CCL2, CCL3, CCL5, CxCL1, CxCL2) that contribute to the pathogenesis of asthmatic disease, the RSV-induced exacerbation, and the clearance and resolution of the ongoing pathology[7,92,119]. In addition, chemokine receptors (CCR6, CCR7) have been identified that regulate recruitment of specific immune cells involved in the response to RSV and/or allergen-induced asthma-like responses[92,120,121]. Furthermore, RSV predisposes animals to more severe allergen responses[58,89]. The most prominent cell that appears to be involved in chronic disease that is enhanced/exacerbated by RSV is the inflammatory/myeloid dendritic cell (mDC). In contrast, as described above, the pDC is a protective subset that promotes a more appropriate anti-viral response. It has previously been identified that RSV-exposed mDC are sufficient to promote a more severe and accelerated disease environment when exposed to allergens[37,89] . Understanding how RSV infection influences DC function to alter the immune environment is critical to understanding how these responses impact pulmonary pathogenesis, leading to exacerbations later

in life. It is likely that RSV and other viral infections, including rhinovirus, uncover an underlying phenotype and reinforce the immune environment by further altering pathogenic immune responses, possibly through the phenomenon of trained immunity.

Immunologic memory is a powerful tool for host defense against pathogens. In the case of classical adaptive immunity, T and B cells develop a highly diverse repertoire of antigen-specific receptors by somatic gene rearrangement. However, the general view that only adaptive immunity can build immunologic memory has recently been challenged by a phenomenon termed *trained immunity* or *innate immune memory*[122,123]. Trained immunity involves innate cells such as myeloid cells (including dendritic cells), natural killer (NK) cells, and innate lymphoid cells (ILCs) and their interactions with pattern recognition receptors (PRRs) and effector cytokines. In contrast to classical adaptive memory, the increased responsiveness to secondary stimuli during trained immunity is not specific for a particular pathogen and it is mediated through signals involving transcription factors and epigenetic reprogramming. Finally, trained immunity relies on an altered functional state of innate immune cells that persists for weeks-to-months after the elimination of the initial stimulus[122,123].

Unlike lymphocytes, innate immune cells do not express rearranging antigen receptor genes, but they do express PRRs and other receptors that allow them to recognize and respond to pathogens (pathogen-associated molecular patterns, PAMPs) and endogenous danger signals (damage-associated molecular patterns, DAMPs)[124,125]. Although these responses are not as specific as antigen receptors, there is evidence that expression of distinct members of PRR families (Toll-like receptors, NOD-like receptors, C-type lectin receptors, RIG-I-like receptors) on macrophages and dendritic cells may trigger specific immune responses based on the pathogen encountered[124,125]. Some of the first evidence of trained immunity in macrophages came from

studies of LPS-induced tolerance where gene-specific chromatin modifications were associated with silencing of genes coding for inflammatory molecules, while priming other genes coding for antimicrobial molecules[126]. These findings suggested that macrophages could be primed by LPS to become more or less responsive to subsequent activation signals. This observation was expanded by studies that demonstrated that exposure of monocytes/macrophages to *C. albicans* or β-glucan enhanced their subsequent response to stimulation with unrelated pathogens or PAMPs, leading to the term trained immunity[122,127]. Training was demonstrated to be accompanied by significant reprogramming of chromatin marks.

A distinguishing feature of trained innate immunity is the ability to mount a qualitatively different and often much stronger transcriptional response when challenged with pathogen or danger signals. In myeloid cells, many loci encoding inflammatory genes are in a repressed configuration[128,129] and upon primary stimulation, massive changes are observed in these loci with alterations driven by the recruitment of transcription factors (i.e. NF-κB, AP-1, and STAT family members) to enhancers and gene promoters, which are usually pre-marked by myeloid lineage-determining transcription factors such as PU.1[122]. Transcriptions factors then recruit coactivators (i.e. histone chromatin remodelers) that locally modify chromatin to make it more accessible to transcriptional machinery[128,129].

Maintenance of this enhanced accessibility may lead to a more efficient induction of genes primed by the initial stimulation[126]. The persistence of histone modifications deposited at promoters or enhancers after the initial stimulus may impact the secondary response[122,127]. Therefore, the observed long-term persistence of some histone modifications in myeloid cells after removal of the initial activation stimulus may reflect either stability of these marks or the

sustained activation of the upstream signaling pathways and transcription factors that control their deposition (i.e. PU.1, STAT, IRF).

1.5. Epigenetics Following RSV Infection

The concept that our immune responses are influenced by environmental factors including microorganisms, pollution, diet and pathogen exposure is important for understanding disease progression. Epigenetic modifications can directly target DNA or target the histone proteins that comprise the nucleosomes that the DNA is wrapped around. Chromatin that is wound around histones is regulated by the nature of the modifications to the protein tails of the histone core components, including H2A, H2B, H3, and H4. These modifications (methylation, acetylation, ubiquitination, phosphorylation, etc) determine the transcriptional status of the gene loci by exposing or sequestering the gene promoter region. Approximately 100 enzymes have been identified that modify histone proteins and subsequently control whether genes are in a transcriptionally active (open) or transcriptionally silenced (closed) configuration. A group of epigenetic enzymes ("writers") add distinct chemical groups (methyl, acetyl, or phosphate) to histones to determine whether the chromatin is "open" or "closed". In addition to the enzymes that add these groups, studies have identified that there are also enzymes the take these same groups away ("erasers"). While epigenetic modifications to histones can have long-term effects on the gene expression profile of a cell, these writers and erasers can provide modifications that allow for greater plasticity during cell activation. The amino acid that is most often modified in histones is lysine and its position in the histone tail can determine if the added modification allows an active (open) or silenced (closed) configuration of the gene. For example, the addition of methyl groups on lysine (K) 4 of histone (H) 3 (i.e. H3K4) leads to activation of gene transcription, whereas H3K27 methylation is a repressive mark[130]. This process is controlled by

methyltransferases (writers) that add methyl groups and demethylases (erasers) that remove them. There is already evidence that epigenetic modulation directs the differentiation and maturation of immune cells. For example, the cytokines typically produced by Th2 cells (IL-4, IL-5 and IL-13) are suppressed in Th1 cells through histone modification[131,132]. In addition, Th17 cells have increased H3K4 methylation at the IL-17 promoter[132]. In DCs, IL-12 production is decreased following severe sepsis due to decreased H3K4 methylation[133]. KDM5B, an H3K4 demethylase, is upregulated following RSV infection of DCs[37]. Since H3K4me3 is an activating mark, this demethylase acts as a transcriptional repressor to specific gene targets. RSV infection induces KDM5B expression, which in turn induces changes in DCs that create a pathogenic T cell mediated immune response due to the regulation of critical innate cytokines, especially Type I IFN. Together these studies have characterized how a single epigenetic modification can alter an ongoing immune response that has significant impact on subsequent allergic airway responses.

Another key epigenetic gene modifier is H3K27 tri-methylation, which represses gene transcription and removal of this mark by KDM6 demethylases leads to active gene transcription. H3K4 methylation is crucial for active gene transcription, while H3K27 methylation appears to fine tune gene transcription [130,134]. In addition to the canonical role of H3K27 demethylation, KDM6 also contributes to gene activation by modulation of H3K4 methylation through stabilization of the MLL complex [135,136] and guides gene transcription by binding POLII to enhance its movement along genes [137,138]. Many studies have linked KDM6 demethylation of H3K27 and immune cell regulation. For instance, KDM6b has been strongly implicated in macrophage M2 polarization[134]. Additionally, inhibition of KDM6a/b enzymatic activity has been shown to lead to decreased inflammation during experimental autoimmune encephalitis by creating a tolerogenic DC phenotype[134,139]. Altogether, these studies show that immune epigenetic programs control

several chromatin modifying enzymes that alter the ability of the immune response to function appropriately.

1.6. Summary and Specific Aims

Respiratory syncytial virus (RSV) is often the first clinically relevant pathogen encountered in life, with nearly all infants infected within the first 2 years of life[2,23]. RSV infection is the leading cause of childhood hospitalization, and increases the risk for developing childhood asthma and recurrent wheezing[1,3]. In addition to causing this exacerbated lung disease, RSV is also directly associated with a significant amount of health burden costs and mortality, accounting for over 3 million hospitalizations and 66,000-199,000 deaths per year, in children under 5, worldwide[20,21]. Recent data, including that from our laboratory, suggest that severe RSV disease is associated with an altered innate and adaptive immune response, characterized by excessive Th2 and Th17 immune responses. Numerous studies have shown that RSV has a role in reducing innate cytokine production necessary for appropriate anti-viral responses[20,35,37,38].

Both direct viral replication as well as indirect immunopathology can lead to RSV disease symptoms. RSV can skew the immune response away from anti-viral and towards a Th2 type response by inhibiting the production of IFN-β and subsequently decreasing Th1[45] (**Figure 1-1**). This lack of anti-viral response as well as skewing towards dysregulated Th2/Th17 has been correlated with severe disease[20,31,35], possibly leading to airway restructuring and this restructuring has been linked to exacerbated allergic responses later in life[93]. How RSV alters the immune system to influence these responses is currently unknown. Determining what factors are altered upon initial infection may lead to a greater understanding of how the immune response is affected later in life to lead to exacerbated disease.

It has been suggested that up to 48% of infants who were hospitalized for severe RSV-associated bronchiolitis and/or lower respiratory tract infection may go on to develop asthma during their childhood[94]. Asthma is the most common chronic childhood illness and during childhood, males have higher occurrences of asthma and wheezing[97]. Additionally, males are approximately twice as likely to become hospitalized than females due to severe RSV infection[23]. Therefore, the risk for both severe RSV infection as well as RSV-associated asthma development may be higher in males than in females.

How RSV alters the immune system to influence immune responses later in life and why males are more susceptible to both severe infection as well as childhood asthma is currently unknown. Previous studies with neonatal RSV infection have demonstrated that there are persistent changes in the lung that include mucus production and increased immune cell populations that persist in the lung, including type 2 innate lymphoid cells (ILC2) that produce IL-5 and IL-13, known to contribute to the immunopathologic Th2 responses that are associated with severe RSV infection and asthma[46,47]. Epithelial cell-derived cytokines, including thymic stromal lymphopoietin (TSLP), IL-25 and IL-33 are known inducers of ILC2 differentiation[39,40,76]. TSLP drives Th2-type responses via its influence on DCs, T cells, and ILC2s [41,42,140] and in some cases, may be required for CD4+ Th2 memory[42]. RSV infection has been shown to lead to increased expression of TSLP[117,118], which has also been implicated in asthma pathogenesis[141–143]. In fact, TSLP has been suggested as a possible biomarker in pediatric asthmatics[144]. Additionally, it has been shown that RSV infection leads to activated IL-13 producing ILC2s that are dependent on TSLP[73]. The studies described here will examine the modulated immune responses during neonatal RSV infection that include alteration of immune cell phenotypes and subsequent persistent changes leading to the altered development of allergic responses. We hypothesize that *early-life*

RSV infection alters local and systemic immune cell populations in neonates through TSLP production. These studies will utilize the human chimeric RSV A2 strain with Line 19 F fusion protein which has been shown to enhance viral load, mucus hypersecretion and airway hyperreactivity in mouse models[145]. A neonatal mouse model was developed to evaluate early-life RSV infection as well as secondary allergic disease (**Figure 2-5**). Determining what factors are altered during early-life exposure and how to control RSV infection to limit these changes, may lead to possible interventions to decrease the incidence of childhood asthma.

We first examined the **role of TSLP following early-life RSV infection and subsequent allergic responses later in life to determine if differences exist between male and female mice**. We hypothesized that males will be more susceptible to RSV infection and have a stronger immune response to allergen upon subsequent challenge and that exacerbation will be dependent on TSLP. Our results show that male mice have decreased viral control with increased viral gene expression over the course of primary infection whereas females clear the virus much quicker. Correlating with increased viral clearance in female mice, IFN-β is expressed only in female mice but not male mice. Upon allergen challenge later in life, male mice show an exacerbated allergic response to cockroach allergen (CRA) while female mice are protected. Furthermore, testing in TSLPR-/- mice abrogated the exacerbated response in male mice, supporting a role for TSLP in male-specific allergic exacerbation following early-life RSV infection.

We next examined **how early-life RSV infection leads to systemic changes of the immune system, specifically in the bone-marrow-derived dendritic cell (BMDC) population**. We hypothesized that RSV will lead to phenotypic alterations of BMDC that will cause changes in pro-inflammatory cytokine production and more highly reactive BMDC that migrate into the lungs during secondary exposures to propagate enhanced disease. Our data show that BMDC from

early-life RSV infected mice show differential pro-inflammatory responses compared to naïve mice, producing higher levels of pro-inflammatory cytokines and chemokines, such as IL-6 and CCL3 and male mice retain signs of activation, including upregulation of CD80/86 and MHC II as far out as 4 weeks post-infection. Interestingly, BMDC from early-life RSV-infected female WT mice and TSLPRKO-/- male mice do not show this phenotype and appear more like BMDC from naïve mice. These data indicate that the BMDC from early-life RSV-infected male mice remain in a persistently activated/inflammatory state and knockdown of TSLP signaling abrogates this phenotype. Furthermore, ATAC-seq data indicated that changes in the BMDC were linked to accessibility of the chromatin landscape in WT vs TSLPR-/- mice and showed links to genes within the Type-1 IFN pathway, such as *Mid1* as well as transcription factors involved in Th2 pathogenesis, specifically IRF4. In addition, we observe that RSV-infected BMDC from TSLPR-/- mice are capable of driving strong T cell production of IFN-γ upon co-culture with T cells isolated from RSV-infected animals. These data indicate that early-life RSV-infection leads to systemic alterations in the bone marrow related to TSLP signaling and inhibition of type-1 interferon which may be linked to persistent transcriptional modifications.

Finally, we examined **epigenetic regulation of BMDC following RSV infection and the role of lysine demethylases, KDM6A/B**. Data from our previous BMDC studies, indicated that BMDC isolated at 4 weeks post-early-life RSV-infection retain upregulation of the epigenetic enzyme, Kdm6b, even at baseline; therefore, we further examined the role of the Kdm6 family of enzymes during RSV infection. We hypothesized that RSV infection will lead to the upregulation of the H3K27 demethylases, KDM6A and KDM6B that will alter BMDC phenotype leading to RSV-driven immunopathology. These data show that following RSV infection *in vivo*, KDM6A/B are upregulated in CD11c+ cells within the lungs. Additionally, *in vitro* experiments show that

BMDC are also capable of upregulating these enzymes following RSV infection. The inhibition of KDM6 enzymatic activity by GSK J4 leads to a decrease in pro-inflammatory cytokine and chemokine expression in BMDC and a shift in T cell response, partially through alteration of APC function (decreased expression of CD86 and MHCII). Airway sensitization of naïve mice with RSV-infected BMDCs exacerbated a live challenge with RSV infection but this exacerbation was inhibited when BMDCs were treated with GSK J4 prior to sensitization. Finally, *in vivo* treatment with GSK J4 during RSV infection reduced inflammatory CD11c+ DC (CD11b+/MHCII+ and CD11b+/CD86+) in the lungs along with IL-13 levels and overall inflammation. These results suggest that KDM6 expression in DC enhances pro-inflammatory innate cytokine production to promote an altered Th2 immune response following RSV infection that leads to more severe immunopathology.

Chapter 2: Sex-Associated TSLP-Induced Immune Alterations Following Early-Life RSV Infection Leads to Enhanced Allergic Disease

2.1. Abstract

Many studies have linked severe RSV infection during early-life with an enhanced likelihood of developing childhood asthma, showing a greater susceptibility in boys. Our studies show that early-life RSV infection leads to differential long-term effects based upon the sex of the neonate; leaving male mice prone to exacerbation upon secondary allergen exposure while overall protecting female mice. During initial viral infection, we observed better viral control in the female mice with correlative expression of interferon-β that was not observed in male mice. Additionally, we observed persistent immune alterations in male mice at 4 weeks post infection. These alterations include Th2 and Th17-skewing, innate cytokine expression (*Tslp* and *Il33*), and infiltration of innate immune cells (DC and ILC2). Upon exposure to allergen, beginning at 4 weeks following early-life RSV-infection, male mice show severe allergic exacerbation while female mice appear to be protected. Due to persistent expression of TSLP following early-life RSV infection in male mice, genetically modified TSLPR-/- mice were evaluated and demonstrated an abrogation of allergen exacerbation in male mice. These data indicate that TSLP is involved in the altered immune environment following neonatal RSV-infection that leads to more severe responses in males during allergy exposure, later in life. Thus, TSLP may be a clinically relevant therapeutic target early in life.

2.2. Introduction

Respiratory syncytial virus (RSV) is often the first clinically relevant pathogen encountered, with nearly all children infected during the first 2 years of life[1,2]. This viral infection is the leading cause of childhood hospitalization and increases the risk for developing childhood asthma and recurrent wheezing[1,3]. The health burden costs of RSV infection account for over 3 million hospitalizations and approximately 100,000 deaths per year in children under 5, worldwide[20,21]. Recent pre-clinical and clinical data, including data from our laboratory, suggest that severe RSV disease is associated with an altered innate and adaptive immune response, characterized by excessive Th2 and Th17 immune responses[20,31–36]. Numerous studies have shown that RSV plays a role in reducing innate cytokine production that is necessary for appropriate anti-viral responses[20,35,37,38]. Both viral replication as well as immunopathology can lead to RSV disease symptoms and probing these and potentially other underlying disease mechanisms that are supported by clinical data will be important for therapeutically targeting the immune environment.

During a viral infection, the immune response is strongly dictated by dendritic cells (DC) because they activate the immune system and instruct T cells toward distinct T helper type responses [44]. RSV can skew the immune response away from anti-viral and towards a Th2-type response by inhibiting the production of IFN-β and subsequently decreasing the Th1 pro-inflammatory response[45]. This lack of an anti-viral response as well as skewing towards dysregulated Th2/Th17 has been correlated with severe disease[20,31,35], leading to airway restructuring linked to exacerbated allergic responses later in life[93]. Up to 48% of infants who were hospitalized for severe RSV-associated bronchiolitis and/or lower respiratory tract infection go on to develop asthma during their childhood[94,95]. Asthma is the most common chronic childhood illness, affecting approximately 5 million children under 18 years of age, including 1.3

million children under 5[96]. During childhood, males have higher occurrences of asthma and wheezing than do females at a 2:1 ratio[97]. Additionally, males are approximately twice as likely to become hospitalized than females due to severe RSV infection[23]. Thus, the risk for severe RSV infection and RSV-associated asthma development is higher in males than in females[98].

How RSV alters the immune system to influence these observed responses is currently not well defined. Previous studies with neonatal RSV infection have demonstrated that there are persistent changes in the lung that include increased mucus production and increased populations of immune cells. Specifically, type 2 innate lymphoid cells (ILC2) are increased in RSV infected lungs and these cells produce IL-5 and IL-13, cytokines important in the development of inflammation and mucus production[46,47]. Innate cytokines, including thymic stromal lymphopoietin (TSLP), IL-25 and IL-33 are known inducers of ILC2 differentiation[39,40,76]. TSLP is a known driver of Th2-type responses through its influence on DCs, T cells, and ILC2s [41,42,140] and may be required for CD4+ Th2 memory[42]. RSV infection has been shown to lead to increased expression of TSLP[117,118], which has also been implicated in asthma pathogenesis[141–143]. In fact, TSLP has been suggested as a possible biomarker in pediatric asthmatics[144]. Additionally, it has been directly shown that RSV infection leads to activated IL-13 producing ILC2s that are dependent on TSLP[73]. However, the mechanisms by which early life RSV infection alters immune responses related to allergen sensitization have yet to be elucidated.

In the present study, we examined the modulated immune responses due to neonatal RSV infection that include alteration of immune cell phenotypes and subsequent persistent changes leading to the altered development of allergic responses. Specifically, we demonstrate for the first time that early-life RSV infection alters immune cell populations in neonates in a sex dependent manner through TSLP production to affect the early development of type 2 immune responses

resulting in enhanced allergic responses later in life. These results suggest that clinically targeting TSLP during early-life RSV exposure may prevent RSV-induced immune environment changes and thus may decrease the incidence of childhood asthma.

2.3. Materials and Methods

2.3.1. Animals

All experiments involving the use of animals were approved by the University of Michigan animal care and use committee. Male and female BALB/c mice, 6 to 8 weeks of age, were purchased from The Jackson Laboratory (Bar Harbor, ME) and used as breeders for experimental animals. TSLPR-/- mice were kindly provided by Dr. Steven Ziegler and adult mice bred in-house were used as breeders. Male and female mice (WT and TSLPR-/-), born in-house were used for all experiments. All mice were maintained under standard pathogen-free conditions.

2.3.2. RSV-infection

A chimeric RSV A2 strain with recombinant Line19 fusion protein was used for all experiments as previously described[145]. Male and female Balb/c and TSLPR-/- mice were infected intranasally (5 µL/animal) with 1.5×10^5 pfu of RSV A2/L19-F at 7 days of age.

Analysis of the viral response was performed at 2-8 days and 14 days post-infection to determine primary response and resolution, respectively. Long-term analysis was performed at 4 weeks post-infection (**Figure 2-1**).
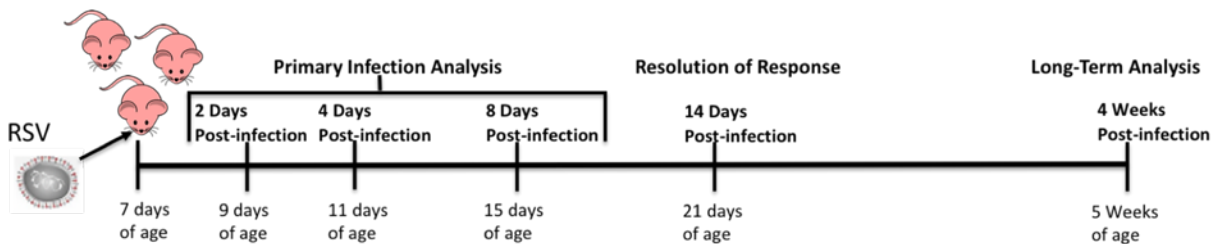
Figure 2- 1. Neonatal RSV-infection Experimental Model

2.3.3. Mouse Cockroach Allergen (CRA) Asthma Model

The allergen used was a clinical grade, skin test cockroach allergen (CRA) (Hollister-Stier, Spokane, WA) as previously described[146,147]. Mice were sensitized intratracheally with 500 protein nitrogen units (pnu) of CRA, over 3 consecutive days. Next, mice were challenged intratracheally with 500 pnu of CRA on days 14, 20, 22, and 23 after initial CRA sensitization. On day 24, one day after the last allergen challenge, animals were sacrificed, and samples were taken. The same model was used in the TSLPR-/- mice.

2.3.4. Quantitative RT-PCR

Lung tissue was homogenized in TRIzol reagent and RNA was extracted using TRIzol reagent (Invitrogen, Carlsbad, CA). cDNA was synthesized using murine leukemia virus reverse transcriptase (Applied Biosystems, Foster City, CA) and incubated at 37℃ for one hour, followed by incubation at 95℃ for 10 min to stop the reaction. Real-time quantitative PCR (qPCR) was multiplexed using Taqman primers, with a FAM-conjugated probe to measure transcription of *Gob5, Muc5ac, Il4, Il5, Il13, Il17a, Ifng, Tslp, Il25, Il33*. Fold change was quantified using $2^{-\Delta\Delta}$ cycle threshold (CT) method. Custom primers were designed to measure Muc5ac and Gob5 mRNA levels as described[120]. All reactions were run on a 7500 Real-Time PCR System (Applied Biosystems).

2.3.5. Lung Histology

The 2 middle lobes of the right lung were perfused with 10% formalin for fixation and embedded in paraffin. Five-micrometer lung sections were stained with periodic acid-Schiff (PAS) to detect mucus production, and inflammatory infiltrates. Photomicrographs were captured using a Zeiss Axio Imager Z1 and AxioVision 4.8 software (Zeiss, Munich, Germany)

2.3.6. Flow Cytometry

The lungs were removed, and single cells were isolated by enzymatic digestion with 2.5 mg/ml Liberase™ (Roche) and 20 U/ml DNaseI (Sigma, St. Louis, MO) in RPMI 1640 for 45 min at 37°C or 1 mg/mL collagenase (Roche) and 20 U/ml DNaseI (Sigma, St. Louis, MO) in RPMI 1640 + 10% FCS for 60 min at 37°C. Tissues were further dispersed through an 18-gauge needle (5-ml syringe), RBCs were lysed and samples were filtered twice through 100-μm nylon mesh. Cells were resuspended in PBS. Live cells were identified using LIVE/DEAD Fixable Yellow Dead Cell Stain kit (Thermo Fisher Scientific, Waltham, MA), then washed and resuspended in PBS with 1% FCS. Fc receptors were blocked with purified anti-CD16/ 32 (clone 93; BioLegend, San Diego, CA). Surface markers were identified using Abs (clones) against the following antigens, all from BioLegend: anti-Cd11c (N418), MHC II (M5/114.15.2), Cd11b (M1/70), OX-40L (RM134L), Cd3 (145-2C11), Cd4 (GK1.5), Cd8 (53-6.7), Cd25 (3C7), Cd90 (53-2.1), cKit (2B8), ST2 (D1H9), Gr-1 (RB6- 8C5), B220 (RA3-6B2), Ter119 (Ter-119). For innate lymphoid cell staining, lineage markers were anti-CD3, CD11b, B220, Gr-1, and TER119. ILC2: CD45+/Lin-/ CD90+/ ST2+. Data was collected using a NovoCyte flow cytometer (ACEA Bioscience, Inc. San Diego, California). Data analysis was performed using FlowJo software (Tree Star, Oregon, USA).

2.3.7. Mediastinal lymph nodes in vitro restimulation and cytokine production assay

Mediastinal lymph nodes (mLN) were enzymatically digested using 1 mg/ml collagenase A (Roche) and 20 U/ml DNaseI (Sigma-Aldrich) in RPMI 1640 with 10% FCS for 45 min at 37°C. Tissues were further dispersed through an 18-gauge needle (1-ml syringe). RBCs were lysed, and samples were filtered through 100-μm nylon mesh. Cells (5×10^5) from mLN cells were plated in 96-well plates and restimulated with 1.5-3.0 x 10^5 pfu of RSV or 300 pnu of CRA for 48 hours.

IL-4, IL-5, IL-13, Il-17a and IFN-γ levels in supernatants were measured with a Bio-Plex cytokine assay (Bio-Rad Laboratories).

2.3.8 RNAscope for formalin fixed paraffin embedded (FFPE) tissue

Lungs were perfused with 10% formalin for fixation and embedded in paraffin (FFPE). RNAscope 2.5 duplex detection kit for FFPE samples (ACDbio, Newark, CA) was used to perform RNAscope as previously described[148]. Probes to detect *Tslp* (target region 10-1149) and *Il33* (target region 2-947) were used with green chromogen detection.

2.3.9. Measurement of airway hyperreactivity

Airway hyperreactivity was measured using mouse plethysmography, that is specially designed for the low tidal volumes (Buxco Research Systems), as previously described[121,146]. Briefly, the mouse to be tested is anesthetized with sodium pentobarbital and intubated via cannulation of the trachea with an 18-gauge metal tube. The intubated mouse was ventilated at a volume of 200 μL at a rate of 120 breaths/min. The airway resistance was measured in the closed plethysmograph by directly assessing tracheal pressure and comparing the level to corresponding box pressure changes. These values were monitored and immediately transformed into resistance measurements using computer-assisted calculations. Once baseline levels had stabilized and initial readings were taken, a methacholine challenge was given via iv tail vein injection (375 μg/kg of methacholine) as previously described[121,146]. After the methacholine challenge, the response was monitored, and the peak airway resistance was recorded as a measure of airway hyperreactivity.

2.3.10. Mucus Scoring Analysis

Slides from PAS-stained lungs were blind-coded and scored by an individual observer to quantify mucus on a scale of 1-4. Scoring is as follows: 1 = Minimal/No Mucus; 2 = Slight: Multiple

airways with goblet cell hyperplasia and mucus; 3 = Moderate: Multiple airways with significant

mucus and some plugging; 4 = Severe: significant Mucus plugging.

2.3.11. Statistical analysis

Data were analyzed by Prism 7 (GraphPad Software). Data presented are mean values ± SEM.

Comparison of two groups was performed with an unpaired, two-tailed Student *t*-test.

Comparison of three or more groups was analyzed by one-way ANOVA, followed by two-tailed

Student *t*-test for individual comparisons. A *p*-value <0.05 was considered significant.

2.4. Results

2.4.1. Neonatal RSV infection of male and female mice leads to a strong Th2/Th17-type immune response with delayed resolution in male mice

To evaluate the immune response to early-life RSV infection, male and female neonatal mice were

infected intranasally with RSV (A2/L19-F (1.5 x10^5 pfu)) at 7 days of age (**Figure 2-1**). Following

infection, both males and females had mucus and inflammation present within their lungs peaking

around 4-8 days post-infection with decreased mucus observed by 14 days post-infection (**Figure**

2-2A,B). Age-matched male and female control mice show little to no signs of mucus production

within the lungs at these time points (**Appendix 1; Figure A1-1A,B**), indicating viral induction of

mucus. Additionally, at 14 days post-infection, lymphoid aggregates or bronchus associated

lymphoid tissue (BALT) was observed in male mice, but not female mice (**Figure 2-2A**). An

increase in viral gene expression was observed in male compared to female mice on day 4 of

infection (**Figure 2-2C**) with female but not male mice having an increase in interferon-β gene

expression (**Figure 2-2D**), a critical cytokine required for viral clearance[15]. Lung draining lymph

nodes, harvested from neonatally-infected mice at 8 days post RSV-infection, showed a strong

Th2 and Th17-type immune response, with no discernible difference between males and females

(**Figure 2-2E**). However, upon analysis at 14 days post-infection, males showed higher cytokine responses in restimulated lymph nodes compared to females (**Figure 2-2F**). These data indicate that both male and female neonatal mice elicit an RSV-driven Th2/Th17-type immune response but male mice displayed a lack of viral control with a delay in immune contraction compared to female mice.
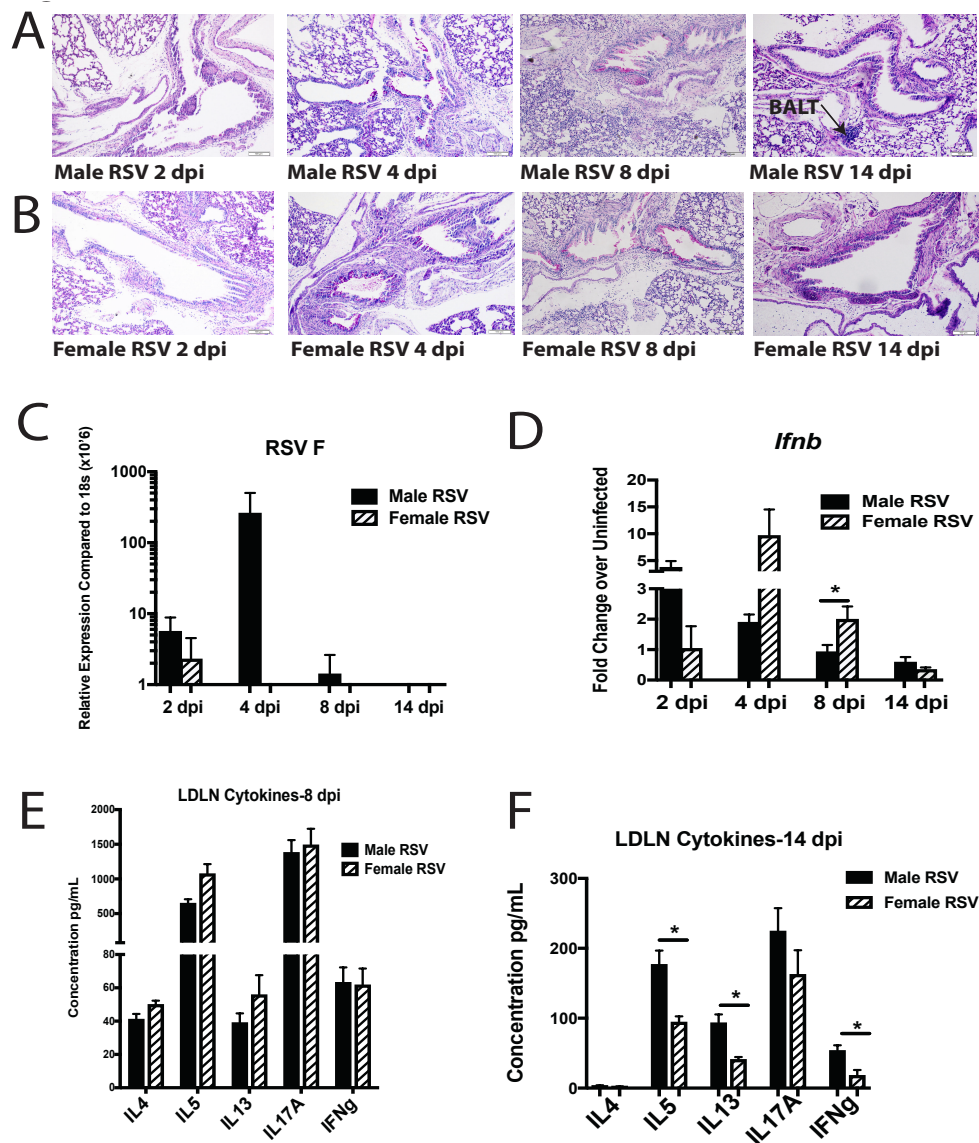
Figure 2- 2. Neonatal RSV infection of male and female mice leads to a strong Th2/Th17-type immune response with delayed resolution in male mice.
Male and Female mice were infected with RSV at 7 days of age and tissues collected at 2, 4, 8 or 14 days post-infection to evaluate primary response and resolution of Th2/Th17 response. **A, B**. Lungs were embedded in paraffin and Periodic acid-Schiff stain (PAS) was performed to visualize mucus (bright pink staining) Representative photos shown. **C, D**. Lungs were homogenized and

mRNA extracted to determine RSV F and interferon-β gene expression, respectively (N ≥ 3) **E, F**. Lung draining lymph nodes were processed into single cell suspension and re-stimulated with RSV in vitro for 48 hours to determine cytokine protein levels (N ≥ 4). Data represent Mean ± SEM (Representative of at least 2 individual experiments). * = p < 0.05

2.4.2. Male mice infected with RSV during early-life show signs of lung immunopathology that persists for up to 4 weeks post-infection

Further evaluation of persistent immune alterations was performed at later time points after neonatal RSV infection in male and female mice (**Figure 2-1**). Uninfected, age-matched (5-week old) mice were used as controls and no differences were observed between the sexes (**Appendix 1; Figure A1-2**). However, significant differences were observed at 4 weeks post-early-life RSV-infection, with persistent lung immunopathology, including visible signs of mucus still present in the lungs of male mice (**Figure 2-3A**) but not female mice (**Figure 2-3B**). In correlation with lung pathology, males had increased expression of the mucus gene, *muc5ac*, compared to neonatally RSV-infected females (**Figure 2-3C**). The number of mice that displayed visible mucus and overexpressed *muc5ac* compared to naïve at 4 weeks post-infection was 78% of early-life infected male mice (7/9) and 15% of female mice (2/13) (**Figure 2-3C**). In addition, the results showed persistent gene expression of Th2-type and *Il17a* in males compared to females (**Figure 2-3D**). Innate cytokines TSLP, IL-25 and IL-33, which are all strong drivers of Th2-type responses[113,149,150] were also evaluated and indicated that early life RSV infected male mice showed persistent gene expression of *Tslp* and *Il33* compared to female mice (**Figure 2-3E**). To determine the location of the *Tslp* and *Il33* within the male lungs, as these cytokines are strongly linked to asthma pathogenesis, studies were performed using RNAscope technology. *Tslp* expression was observed within the bronchial airway epithelial cells, while *Il33* was limited to the alveolar epithelial cell areas (**Figure 2-3F-K**). Thus, early-life RSV infection in male mice leads to persistent Th2/Th17 skewing within the local lung environment, while females resolve this response and have a local lung environment similar to previously uninfected mice.

36
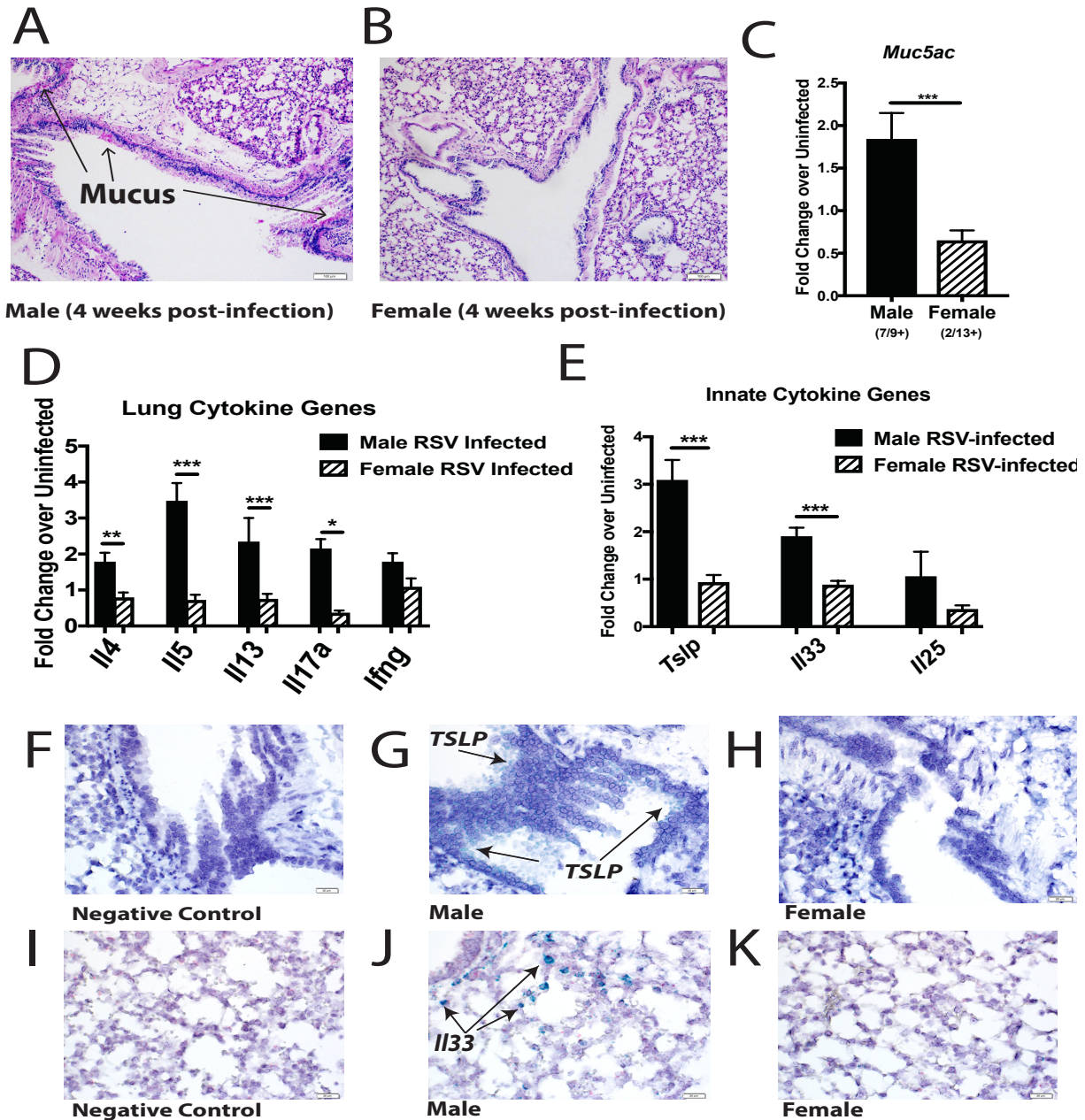
Figure 2- 3. Male mice infected with RSV during early-life show signs of lung immunopathology that persists for up to 4 weeks post-infection.
Male and Female mice were infected with RSV at 7 days of age and tissues collected at 4 weeks post-infection to evaluate long-term alterations. **A,B**. Lungs were embedded in paraffin and Periodic acid-Schiff stain (PAS) was performed to visualize mucus (bright pink staining). Representative photos shown **C-E.** Lungs were homogenized and mRNA extracted to determine gene expression compared to age/sex-matched uninfected controls ($N = \geq 9$) **F-K**. RNAscope was performed to determine location of *Tslp* and *Il33* within male lungs (stained in green). Representative photos shown. Data represent Mean ± SEM (Representative of or pooled from 2 individual experiments). * = $p < 0.05$; ** = $p < 0.01$; *** = $p < 0.001$.

2.4.3. Differential immune cell populations in the lungs of male and female mice with early-life RSV infection

Due to the persistent immunopathology observed in the lungs from early-life RSV-infected male mice, we next examined immune cell populations that may lead to these alterations at 4 weeks post-infection. Age-matched (5-week old) naïve animals were used as controls. Naïve male and female animals showed similar immune cell populations at 5 weeks of age, indicating no inherent differences between the sexes. In contrast, lungs from male mice at 4 weeks post-neonatal RSV infection contained increased Cd11c+/Cd11b+ and Cd103+ DC populations (**Figure 2-4A,B**). Interestingly, female mice at 4 weeks post-neonatal RSV infection also have decreased Cd103+ DC compared to naïve female mice (**Figure 2-4B**). Additionally, early-life RSV infected males contain significantly more OX-40L+ cells than early-life infected females (**Figure 2-4A-C**), which have been implicated in severe neonatal RSV responses as well as asthma[118,151,152]. We also observed that males had significantly more ILC2, which can produce Th2-type cytokines (**Figure 2-4D,E**). However, no differences were observed in CD4+ or CD8+ T cells (**Figure 2-4F,G**). This phenotypic immune alteration in males may allow for the continued production of potentially pathogenic cytokines within the local environment.
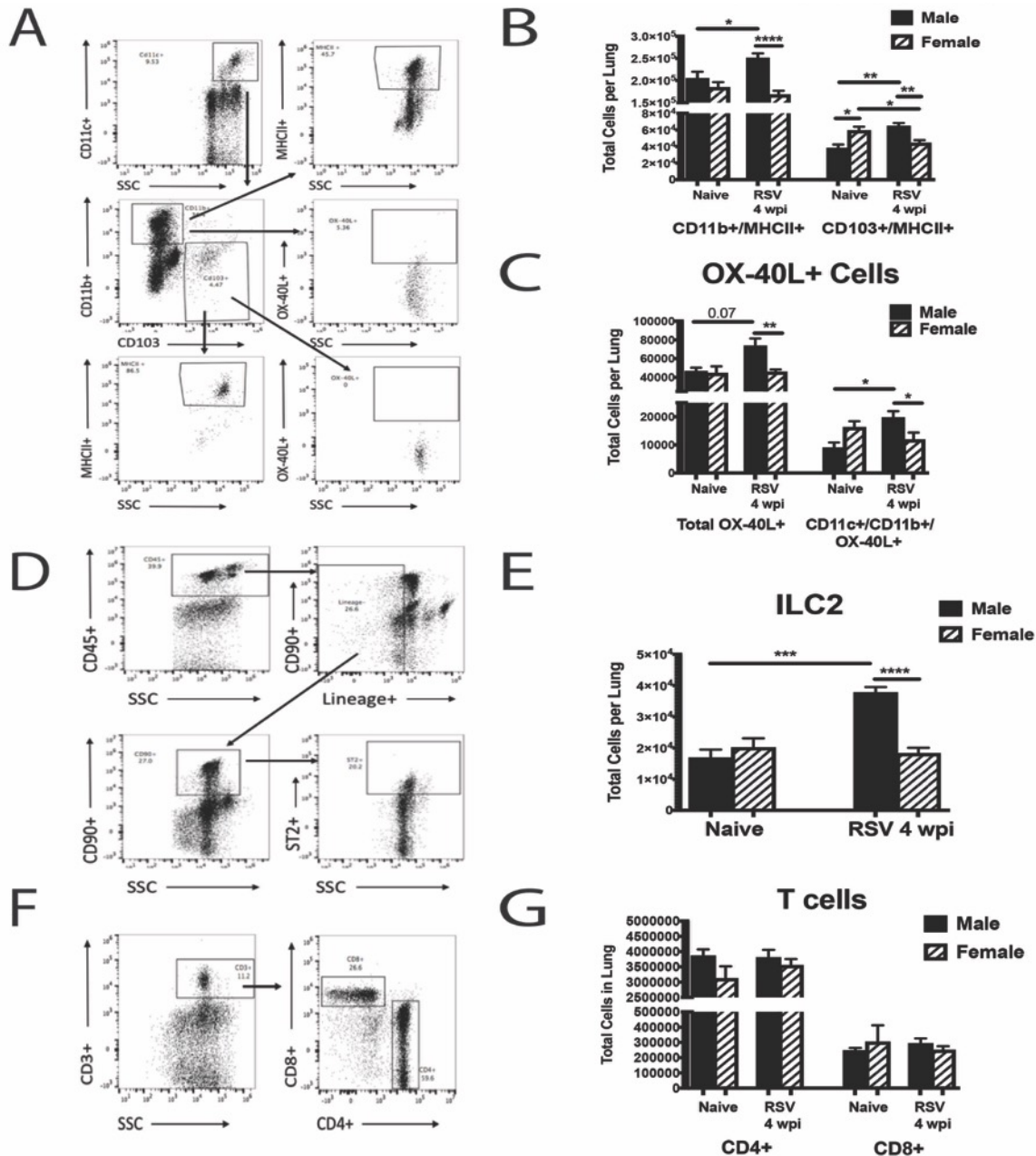
Figure 2- 4. Differential immune cell populations in the lungs of male and female mice with early-life RSV infection.
Male and Female mice were infected with RSV at 7 days of age and lungs collected at 4 weeks post-infection to evaluate cell populations. Lungs were processed into single-cell suspension and stained for flow cytometry analysis. **A**. Gating strategy for dendritic cells **B**. CD11c+ dendritic cell types (N ≥ 9) **C**. OX-40L+ cells (N ≥ 9) **D**. Gating strategy for innate lymphoid cells **E**. Innate lymphoid cell populations (N = 5) **F**. Gating strategy for T cells **G**. T cell populations (N ≥ 9). Data represent Mean ± SEM (Representative of or pooled from 2 individual experiments). * = p < 0.05; ** = p < 0.01; *** = p < 0.001; **** = p < 0.0001.

2.4.4. Early-life RSV infection leads to exacerbated allergic response in male mice

Five-week old mice that were previously infected with RSV at 7 days of age were sensitized and

challenged with cockroach allergen (CRA) to determine if prior infection with RSV alters the

immune response to allergens later in life (RSV/CRA). CRA was administered via intratracheal instillation into the lungs over 3 consecutive days, starting at 4 weeks post-infection, followed by 4 challenges 2 weeks later to elicit an allergic response (**Figure 2-5A**). Naïve age-matched animals were used as controls and administered CRA in the same manner. Lung histology showed that RSV/CRA males have severe pathology and increased mucus compared both to mice given only CRA and female mice given RSV/CRA (**Figure 2-5B**). Airway hyperreactivity (AHR) was significantly higher in the males given RSV/CRA (**Figure 2-5C**) compared to all other groups indicating more severe lung physiology responses. A correlative increase in mucus score was also observed in the RSV/CRA male mice (**Figure 2-5D**) and interestingly, a decreased mucus score was observed in RSV/CRA female mice compared to both RSV/CRA male mice as well as CRA only female mice (**Figure 2-5D**). Additionally, mucus-associated genes, *gob5* and *muc5ac*, as well as gene expression of *Il13* were significantly increased in lungs from male mice given RSV/CRA, compared to female mice (**Figure 2-5E**). Increased infiltration of inflammatory myeloid-type cells as well as ILC2 were observed in male mice given RSV/CRA compared to females given RSV/CRA, with no differences in T cell numbers (**Figure 2-5F-G**). However, analysis of the CRA-specific response analyzed by cytokine production from isolated lymph node cells showed that male mice infected with RSV during early life had significantly more Th2 and IL-17A cytokine production upon CRA re-challenge when compared to females, suggestive of a shift in T cell responsiveness to the allergen (**Figure 2-5H**). No differences were observed between uninfected males and females tested (**Appendix 1; Figure A1-3**), indicating that the baseline allergic response is equivalent between male and female mice. Altogether, these data indicate that the effects of early-life RSV-infection lead to sex-specific alterations that persist long-term in male mice.
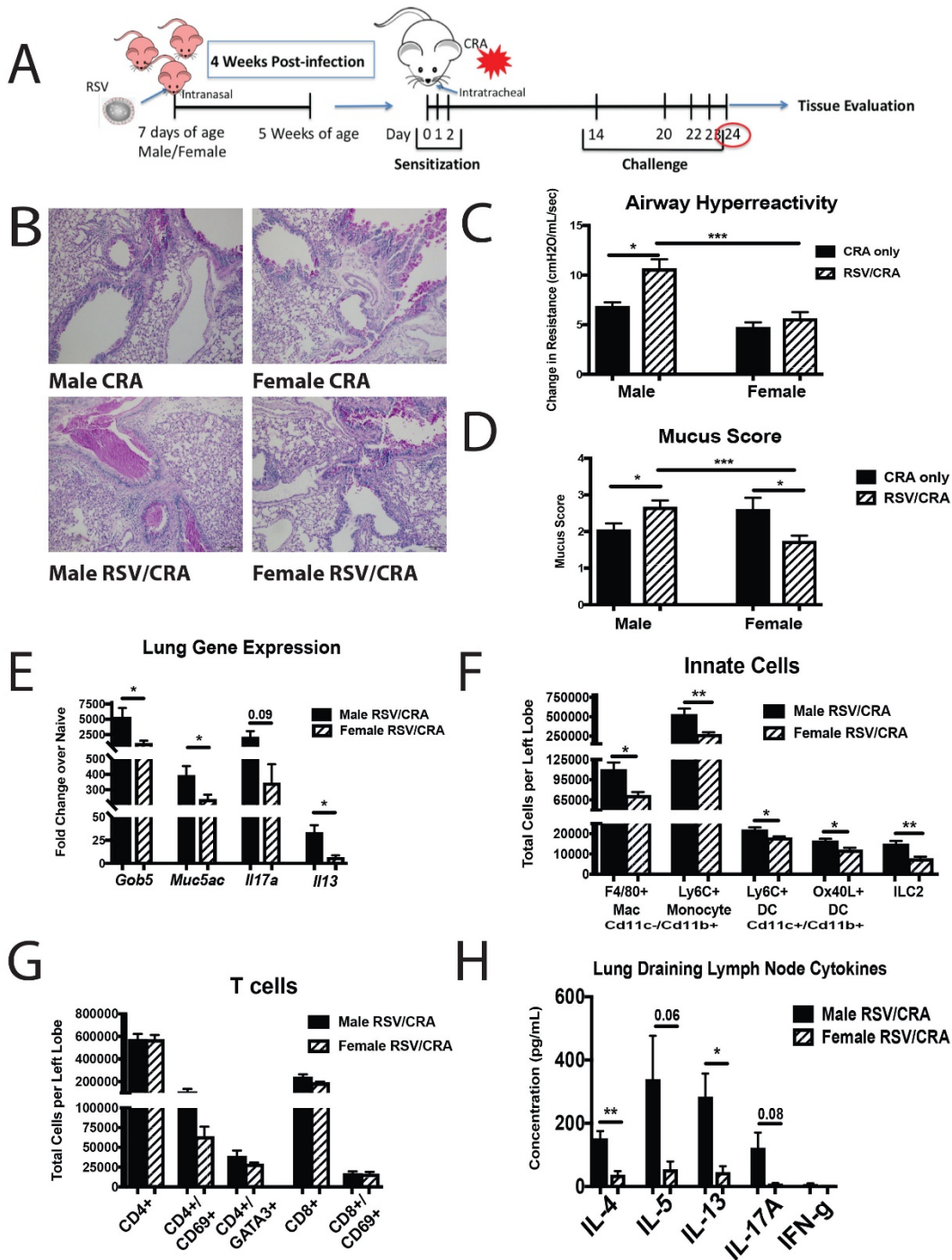
Figure 2- 5. Early-life RSV infection leads to exacerbated allergic response in male mice.
Male and Female mice were infected with RSV at 7 days of age and secondary allergen challenge initiated at 4 weeks post-infection. **A**. Experimental Design **B.** Lungs were embedded in paraffin and Periodic acid-Schiff stain (PAS) was performed to visualize mucus (bright pink staining). Representative photos shown **C.** AHR was determined using full-body plethysmography and methacholine challenge (N ≥ 3) **D**. Subjective mucus scoring was performed on blinded histological slides on a scale of 1-4 for mucus production (N ≥ 8) **E.** Lungs were homogenized and mRNA extracted to determine mucus and cytokine gene expression compared to age/sex-matched naïve controls (N ≥ 3) **F,G**. Lungs were processed into single-cell suspension and stained for flow cytometry analysis. (N ≥ 4) **H.** Lung draining lymph nodes were processed into single cell suspension and re-stimulated with CRA in vitro for 48 hours to determine cytokine protein levels (N ≥ 3). Data represent Mean ± SEM (Representative of or pooled from 2-3 individual experiments). * = $p < 0.05$; ** = $p < 0.01$; *** = $p < 0.001$

41

2.4.5. Deletion of TSLP receptor leads to decreased immune responses following CRA exposure in male mice with early-life RSV infection

Based on our observed correlative evidence of TSLP expression with persistent Th2/Th17-skewing, we evaluated the sex-associated role of TSLP in the immune exacerbation observed following CRA exposure in mice. Male and female TSLP receptor knockout (TSLPR-/-) mice were RSV infected during early-life, followed by a CRA challenge initiated 4 weeks later (**Figure 2-5A**). Histologic evaluation showed decreased mucus in the lungs of TSLPR-/- male mice compared to WT male mice given early RSV followed by the CRA challenge (**Figure 2-6A**). Furthermore, AHR was decreased in TSLPR-/- male mice with a previous neonatal RSV infection (**Figure 2-6B**), indicating improved lung function compared to WT male mice. Consistent with histology, a decrease in mucus score (**Figure 2-6C**) as well as mucus gene expression (**Figure 2-6D**) was observed in TSLPR-/- male mice compared to WT male mice given RSV/CRA. The results also demonstrated a decrease in *Il13* cytokine gene expression levels within the lungs of TSLPR-/- compared to WT male mice given RSV/CRA (**Figure 2-6E**). Correlating with the decreased *Il13* expression, a decrease in ILC2 was observed in the TSLPR-/- male mice given RSV/CRA (**Figure 2-6F**) with no changes in CD4+ T cell numbers (**Figure 2-6G,H**). Additionally, male TSLPR-/- RSV-infected/CRA challenged mice had decreased CRA-specific Th2 cytokine production in the lung draining lymph nodes compared to WT mice (**Figure 2-6I**). Of interest, similar to previous studies[153], we found no difference in the male or female mice given only CRA when TSLPR-/- mice were compared to WT mice (**Appendix 1; Figure A1-3**), suggesting that the TSLP-induced environment created by an early life RSV infection was critical. Importantly, unlike male mice, females were not exacerbated following RSV-infection alone and thus were independent of TSLP, supporting a sex-specific role for this pathway.
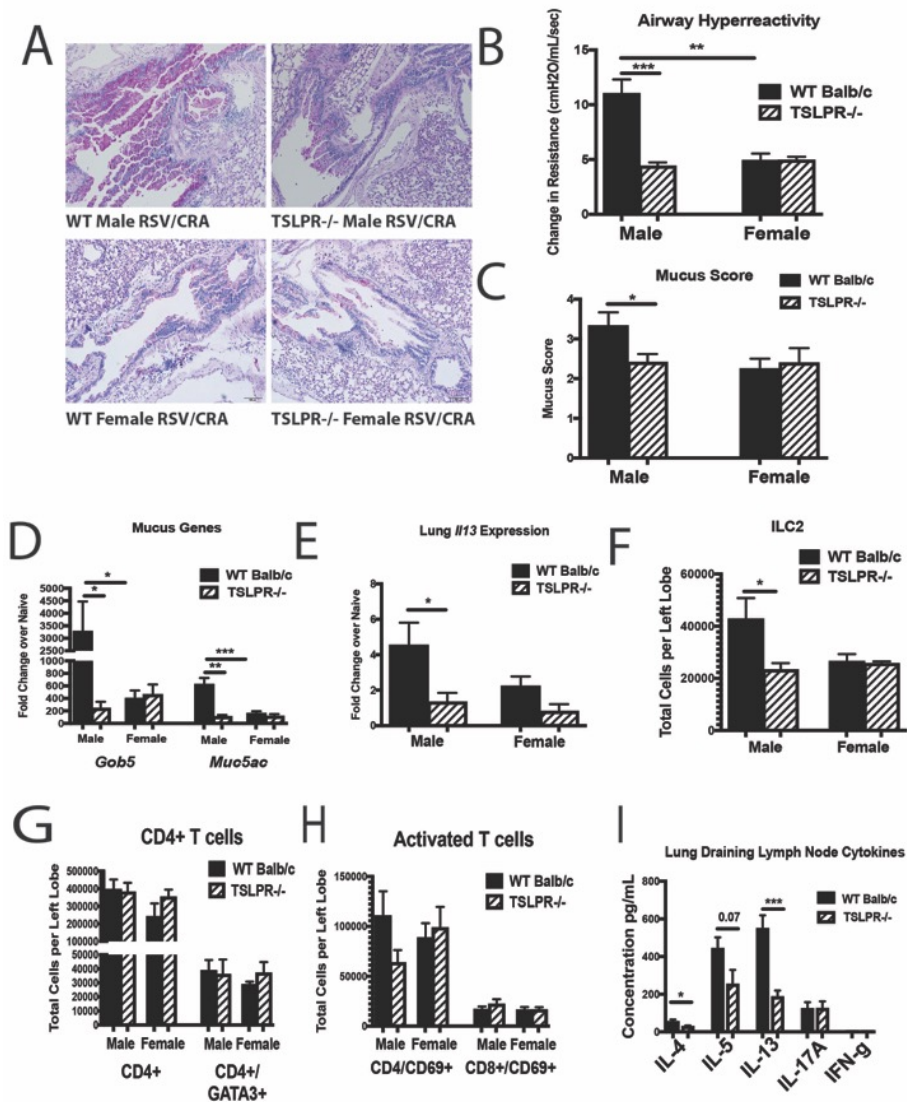
Figure 2- 6. Deletion of TSLP receptor leads to decreased immune responses following CRA exposure in male mice with early-life RSV infection.
Male and Female TSLPR-/- mice were infected with RSV at 7 days of age and secondary allergen challenge initiated at 4 weeks post-infection. **A**. Lungs were embedded in paraffin and Periodic acid-Schiff stain (PAS) was performed to visualize mucus (bright pink staining). Representative photos shown **B**. AHR was determined using full-body plethysmography and methacholine challenge (N ≥ 3) **C**. Subjective mucus scoring was performed on blinded histological slides on a scale of 1-4 for mucus production (N ≥ 6) **D, E**. Lungs were homogenized and mRNA extracted to determine mucus and cytokine gene expression compared to age/sex-matched naïve controls (N ≥ 3) **F-H**. Lungs were processed into single-cell suspension and stained for flow cytometry analysis (N ≥ 3) I. Lung draining lymph nodes in single cell suspension were re-stimulated with CRA *in vitro* for 48 hours to determine cytokine protein levels (N≥ 3). Data represent Mean ± SEM (Representative of or pooled from 2-3 individual experiments). *=p<0.05; **=p<0.01; ***=p<0.001.

2.5. Discussion

Clinically, data suggest that severe RSV infection during early-life enhances the likelihood of developing childhood asthma by 3-5 fold[1,154]. Most children are infected with RSV within the first 2 years of life and up to 3-5% of children become hospitalized due to complications from severe disease[23]. Studies suggest that ~50% of children hospitalized during severe RSV infection go on to develop childhood asthma[94,95]. Additionally, clinical data show that boys are more susceptible to RSV, hospitalized at a 2:1 ratio compared to girls, and are more than twice as likely to develop childhood asthma[2,23,155]. Here we show that male mice infected neonatally with RSV have poorer viral control than female mice of the same age and that at 4 weeks post-early-life RSV-infection, male mice show a persistent signature of RSV-driven Th2/Th17 immunopathology, mucus and an altered immune environment that leads to an exacerbated allergic phenotype associated with TSLP driven mechanisms. Thus, these studies outline 2 important concepts; 1) early RSV infection results in an altered immune phenotype in the lung that is dependent upon sex; and 2) the persistence of the early innate cytokine, TSLP, has a role in the altered immune environment and may be a clinically relevant target early in life.

TSLP is an early responding, innate cytokine, that can drive Th2-type responses and is upregulated following RSV infection of lung epithelial cells[117]. During neonatal RSV-infection, TSLP mediates immunopathology through OX-40/Th2 signaling[118], as well as having direct effects upon ILC2 cells, causing them to produce Th2-type cytokines, IL-5 and IL-13 to enhance inflammation and mucus production[73]. When TSLP was neutralized during neonatal RSV infection, the severity of a later exacerbated RSV infection was mitigated[118], indicating that TSLP may be creating a broadly altered immune environment. Additionally, TSLP has been implicated in the pathogenesis of asthma. Increased TSLP mRNA in bronchial epithelial cells of asthmatics

directly correlates with degree of airflow obstruction[104] and GWAS studies show a strong association between TSLP and severe asthma[105,106]. The TSLP SNP, rs1837253 on the T allele, which leads to decreased epithelial cell production of TSLP, has been identified in boys to reduce the risk of developing atopic asthma and airway hyperresponsiveness as well as protection from allergic rhinitis[156–158]. This same TSLP mutation shows no protective effect in girls, suggesting that the role of TSLP in asthma may be more significant in boys than girls. Our data expands on these clinical findings, showing a significant correlation between RSV-induced TSLP and the subsequent development of viral-associated allergic asthma later in life in male mice, following early-life RSV-infection.

TSLP has a wide range of immune cell targets, including ILC2, DC and T cells. The initial biologic function of TSLP demonstrated that it interacted with DC to promote Th2 cell differentiation and thus promoted allergic disease[113,114]. TSLP stimulation of CD11b+ DC upregulates OX-40L that interacts with OX-40 on CD4 T cells to promote a Th2 response[151,152]. The survival and maintenance of ILC2 that produce Th2-type cytokines, depends on the presence of TSLP[159,160]. In addition, TSLP signaling instructs DCs to produce CCL-22[41], a chemokine that recruits Th2 cells through its interaction with the CCR4 receptor. Finally, in response to TSLP, DCs will themselves produce TSLP that further interacts with DCs and ILC2, creating a feedback loop that is independent of epithelial cell-derived TSLP[115,116]. The data provided in our studies, using TSLPR-/- mice, indicated that TSLP signaling is responsible for the increased presence of innate immune cells in the lungs of male mice conditioned with a neonatal RSV infection. Interestingly, the TSLPR-/- mice had a similar allergen response in the lungs compared to WT male and female mice when no neonatal RSV infection was given. These data recapitulate previous data indicating that although TSLP is involved in the development of Th2 cells, the long-term

allergen responses are not altered in its absence[153]. Similarly, TSLP was not necessary to develop

chronic Th2 driven parasitic helminth granulomatous responses[161]. Thus, TSLP may be central to

the development of chronic type 2 immune responses when a stimulus, such as RSV infection,

promotes an altered immune environment that predisposes tissue to development of allergic

responses. This is likely more significant in neonates that have an immature immune environment

that can be more easily skewed to an altered immune phenotype.

The upregulation of another innate cytokine, IL-33, was also associated with the early RSV

infection in male mice. While we have not further explored the role of IL-33 in the sex difference

in the altered immune environment, it may also contribute. Interesting, the expression of TSLP

mRNA was more highly evident and associated with bronchial epithelial cell area in male mice at

4-weeks post-infection, whereas IL-33 appeared to be more contained and associated with alveolar

areas as assessed by RNAscope. Many studies have indicated a role for these innate cytokines in

respiratory viral complications, asthma development, as well as viral exacerbations of existing

asthma[99–101]. It is evident that these cytokines have distinctive as well as additive effects on ILC2

responses[76,102,159]. Allergen challenge, following neonatal rhinovirus infection identified that both

IL-33 and TSLP are required for IL-25-induced ILC2 production of IL-13 leading to mucus

metaplasia but TSLP was necessary for maximal ILC2 gene expression even in the presence of IL-

25 and IL-33[76]. Additionally, experimental asthma pathogenesis was shown to persist in IL-33R

knockout mice (ST2-/-) due to increased expression of TSLP that enhanced ILC2 production of

IL-13; abrogation of this response was only possible with the addition of an anti-TSLP antibody[102].

Finally, in an allergen challenge model conducted on adult human subjects with allergic asthma,

administration of an anti-TSLP monoclonal antibody (AMG 157) reduced allergen-induced

bronchoconstriction and airway inflammation, suggesting a key role for TSLP in allergen-induced

airway responses in asthmatics[103]. Collectively, these studies as well as our data presented here make it plausible that TSLP, IL-25 and IL-33 cooperate and regulate each other during initial disease progression but TSLP may be more significant in the development of subsequent diseases later in life. Given the availability of anti-TSLP in human trials, a therapeutic intervention in infants with severe RSV may be highly beneficial, especially for boys.

These novel data recapitulate the clinical observations where males are more likely to develop severe respiratory complications and childhood asthma than are girls. This suggests that early-life RSV-infection in males leads to persistent TSLP-associated Th2/Th17 immune-driven pathology within the lungs, while the same early-life infection in females allows for appropriate Th2/Th17 resolution thereby protecting females from later asthma pathogenesis. This phenomenon may be due to poorly controlled viral replication and decreased viral clearance in males following the initial infection, possibly due to lack of type-1 interferon production, which is critical for viral clearance as well as resolution of Th2/Th17 immune responses[15,162,163]. Correlating with our findings, it has previously been shown that female plasmacytoid dendritic cells (pDC) isolated from human peripheral mononuclear cells express higher levels of type-1 interferons (IFNα/β) compared to male pDC following TLR7 stimulation[164]. While another study has shown that type-3 interferon (IFNλ) has the ability to upregulate TSLP expression[165], the role of type-1 interferons and TSLP has not been fully elucidated. Furthermore, previous studies with bronchial epithelial cells from asthmatics have shown that TSLP and interferon-β have an inverse relationship, showing a bias towards low interferon- β but high TSLP, while the reverse is true for healthy individuals[166]. These results may suggest that targeting TSLP during early-life RSV infection, especially in male infants hospitalized with severe disease, may limit these changes and may decrease the incidence of childhood asthma.

Chapter 3: Early-Life RSV Infection Leads to Long-Term Systemic Alterations of BMDC Through Persistent Expression of TSLP

3.1. Abstract

Many studies have linked severe RSV infection during early-life with enhanced immune responses upon secondary exposures, such as during RSV re-infection and childhood asthma. Innate immune cell populations (i.e. antigen presenting cells) have been shown to be capable of immune memory following pathogen exposure that leads to alterations of the immune response later in life. Here we show that long-term systemic alterations are occurring following early-life RSV-infection. Bone marrow-derived dendritic cells (BMDC) isolated from early-life RSV-infected male mice at 4 weeks post-infection retained expression of maturation markers, such as *Cd80/86* and *Ox40l*. Chemokines and cytokines associated with the inflammatory response during RSV infection were also persistently expressed (i.e. *Ccl3, Ccl5, Il6*) along with *Kdm6b* and *Tslp*, previously shown to lead to enhanced inflammatory responses as well as secondary responses following RSV-infection, respectively. The addition of recombinant TSLP to naïve BMDC cultures showed a similar response to BMDC isolated from early-life RSV mice, indicating a role for TSLP in the persistent BMDC phenotype. Furthermore, knockdown of TSLP signaling using TSLPR-/- male mice abrogated this activated phenotype and led to enhanced Th1 responses. Finally, ATAC-seq data indicated differences in the chromatin landscape of WT and TSLPR-/- BMDC, showing more "open" regions of chromatin near anti-viral type-1 genes (*Mid1, Spp1, Cxcl11*) in TSLPR-/- BMDC while more accessibility was observed near genes linked to RSV disease (*Cxcl1, Cxcl2, Areg*) in the WT BMDC with a link to IRF4 signaling, a transcription factor associated with a Th2-

type response and TSLP signaling. These data indicate that TSLP is involved in persistently altering the immune system in the bone marrow following early-life RSV-infection, leading to altered immune responses later in life. Thus, targeting TSLP during early-life may be clinically relevant.

3.2. Introduction

Respiratory syncytial virus (RSV) is a ubiquitous pathogen that infects nearly all infants by age two, is the leading cause of bronchiolitis in children worldwide[1,2] and is the second most likely cause of death in children under the age of one by a single pathogen[24]. According to the CDC, approximately 60,000 pediatric hospitalizations in children under the age of 5 in the United States each year are due to RSV, estimating an annual cost of over $300,000,000[2,20,167] making RSV a significant source of morbidity and health care burden. Currently, no vaccine against RSV is available and research in this area has been slow and cumbersome due to a lack of significant understanding of the virus as well as previous vaccine trial failure. In the late 1960s, attempts to vaccinate children with formalin-inactivated RSV vaccine caused severe exacerbated disease upon re-infection with live RSV due to enhanced inflammatory disease and mucus production[25–27]. Furthermore, several epidemiological studies link severe RSV infection with the later development of hyper-reactive airway disease, including asthma, that persists even years after the initial viral infection has resolved[1,3,20]. The inability to properly respond to RSV infection in these patients may be due to altered innate immune responses that can determine the subsequent pathogenic responses.

RSV can skew the immune response away from anti-viral and towards a Th2-type response by inhibiting dendritic cell production of IFN-β and subsequently decreasing the less pathogenic anti-viral Th1 response[45]. The reduction of anti-viral responses as well as skewing towards

dysregulated Th2/Th17 has been correlated with severe disease[20,31,168], leading to airway alterations linked to exacerbated allergic responses later in life [93]. Many studies over the years have identified several DC-linked chemokines (CCL2, CCL3, CCL5, CxCL1, CxCL2) that contribute to the pathogenesis of asthmatic disease, the RSV-induced exacerbation, and the clearance and resolution of the ongoing pathology[7,92,119]. It has previously been identified that RSV-exposed mDC are sufficient to promote a more severe and accelerated disease environment when exposed to allergens[37,89]. Understanding how RSV infection influences DC function to alter the immune environment is critical to understanding how these responses impact pulmonary pathogenesis, leading to exacerbations later in life. It is likely that RSV uncovers an underlying phenotype to reinforce the immune environment by further altering pathogenic immune responses, possibly through the phenomenon of trained immunity.

How RSV alters the immune system to influence these observed responses is currently not well-defined. Previous studies with neonatal RSV infection, including those from our laboratory, have demonstrated that there are persistent changes in the lung that include increased mucus production, increased populations of immune cells and persistent expression of inflammatory cytokines[47,91,169]. Specifically, the innate cytokine, thymic stromal lymphopoietin (TSLP), a known driver of Th2-type responses through its influence on DCs, T cells, and ILC2s [41,42,140] is persistently expressed[169]. RSV infection has been shown to lead to increased expression of TSLP[117,118], which has also been implicated in asthma pathogenesis[141–143]. Our lab has previously shown that male mice infected neonatally with RSV have poorer viral control than female mice of the same age and that at 4 weeks post-early-life RSV-infection, male mice show a persistent signature of RSV-driven Th2/Th17 immunopathology, mucus and an altered local immune environment in the lung that leads to an exacerbated allergic phenotype associated with TSLP

driven mechanisms[169]. Additionally, it has been directly shown that TSLP interacts with the transcription factor IRF4 to drive DC-specific Th2 responses[170,171] as well as ILC2-linked Th2 lung repair and disease[140,172]. However, whether early life RSV infection has the ability to persistently alter the systemic immune system has yet to be elucidated.

In the studies in this chapter, we examined TSLP-driven modulated systemic immune responses due to neonatal RSV infection that include persistent alteration of BMDC cell populations. Specifically, we demonstrate that RSV infection leads to persistent upregulation of TSLP in BMDC, leading to a persistently "activated" phenotype, including upregulation of maturation markers (CD80/86 and OX-40L) and the continued expression of inflammatory cytokines and chemokines. Knockdown of TSLP signaling abrogates this activated phenotype, leaving the BMDC population in a similar activation state as naïve BMDC and allowing for T cell production of IFN-γ. Furthermore, ATAC-seq analysis determined that WT BMDC have less accessibility in promoter regions near type-1 immune genes, suggesting decreased ability of these BMDC to mount the appropriate anti-viral response in the presence of TSLP. These data indicate that TSLP is involved in inhibition of the anti-RSV response as well as persistently altering the immune system at a systemic level in the bone marrow following early-life RSV-infection leading to trained immunity. Thus, targeting TSLP and overall DC function may be crucial for limiting long-term RSV-driven disease pathologies.

3.3. Materials and Methods

3.3.1. Animals

All experiments involving the use of animals were approved by the University of Michigan animal care and use committee (protocol PRO0000888, exp. 02/14/2022). Male and female BALB/c mice, 6 to 8 weeks of age, were purchased from The Jackson Laboratory (Bar Harbor, ME) and used as

breeders for experimental animals and for collection of adult BMDC. TSLPR-/- mice on BALB/c background were kindly provided by Dr. Steven Ziegler and adult mice bred in-house were used as breeders and for collection of adult BMDC. Male neonatal mice (WT and TSLPR-/-), born in-house were used for all early-life experiments. All mice were maintained under standard pathogen-free conditions.

3.3.2. RSV-infection

A chimeric RSV A2 strain with recombinant Line19 fusion protein was used for all experiments as previously described[145]. Male and female Balb/c and TSLPR-/- mice were infected intranasally (5 µL/animal) with 3×10^5 pfu of RSV A2/L19-F at 7 days of age.

Long-term analysis of BMDC was performed at 4 weeks post-infection.

Viral stocks were grown in Hep-2 cells and concentrations determined by plaque assay. Virus was ultra-centrifuged (100,000xg for 30 minutes at 4°C) and re-suspended in fresh cell culture media (RPMI 1640 supplemented with 10% fetal calf serum (FCS), L-glutamine, penicillin/streptomycin, non-essential amino acids, sodium pyruvate, 2-mercaptoethanol (ME)) or saline prior to use.

3.3.3. Bone Marrow-Derived Dendritic Cells and Co-culture with CD4+ T cells

Bone marrow was collected by flushing the femur and tibia of hind legs with RPMI 1640 supplemented with 10% fetal calf serum (FCS), L-glutamine, penicillin/streptomycin, non-essential amino acids, sodium pyruvate, 2-mercaptoethanol (ME). BMDCs were grown in RPMI 1640 supplemented with 10% FCS, L-glutamine, penicillin/streptomycin, non-essential amino acids, sodium pyruvate, 2-mercaptoethanol (ME) and 10 ng/ml of recombinant murine granulocyte macrophage-colony stimulating factor (GM-CSF; R&D Systems, Minneapolis, MN, USA). For studies using recombinant TSLP (rTSLP), 20 ng/mL of rTSLP (R&D Systems, Minneapolis, MN, USA) was added on Day 0 in addition to GM-CSF. Cells were fed on Days 3 and 5 with fresh

GM-CSF. On Day 6, cells were cultured with RSV (MOI = 1). At 24 hours, cells were collected in TRIzol reagent and mRNA was extracted using TRIzol reagent (Invitrogen, Carlsbad, CA) for quantitative RT-PCR. For some experiments, CD4$^+$ T cells were isolated from the lymph nodes of RSV-infected Balb/c mice or spleens from naïve DO-11 mice using the T cell isolation II kit (Miltenyi Biotec). Cells were then cultured with the treated BMDCs. For DO-11 cells, co-culture was performed in the presence of ovalbumin peptide 323-339 (10 µg/mL; Invivo Gen, San Diego, CA). At 48 hours, the supernatant was collected and protein levels were measured with a Bio-Plex cytokine assay (Bio-Rad Laboratories, Hercules, CA).

3.3.4. Quantitative RT-PCR

cDNA from BMDC mRNA (described above) was synthesized using murine leukemia virus reverse transcriptase (Applied Biosystems, Foster City, CA) by incubation at 37℃ for one hour, followed by incubation at 95℃ for 10 min to stop the reaction. Real-time quantitative PCR (qPCR) was measured using Taqman primers, with a FAM-conjugated probe to measure transcription of *Cd80, Cd86, Ox40l, Il6, Ccl2, Ccl3, Ccl5, Kdm5b, Kdm6a, Kdm6b, Tslp, Ccl17, Mid1, Cxcl1, Cxcl2, Irf4, Irf8, Rela, Relb, Stat3, 18s*. Fold change was quantified using the $2^{-\Delta\Delta}$ cycle threshold (CT) method. All reactions were run on a 7500 Real-Time PCR System (Applied Biosystems, Foster City, CA).

3.3.5. ATAC-seq

ATAC-seq was performed as previously described[173]. In brief, 25,000 primary bone-marrow derived dendritic cells were washed in cold PBS and resuspended in cytoplasmic lysis buffer (CER-I from the NE-PER kit, Invitrogen, cat. no. 78833 + 0.1mg/ml digitonin + protease and phosphatase inhibitor, Cat no. 78440). This single-cell suspension was incubated on ice for 15 min with gentle mixing by pipetting at every 2 min. The lysate was centrifuged at 1,300g for 5

min at 4 °C. Nuclei were resuspended in 2× TD buffer, then incubated with Tn5 enzyme (0.5ul) for 30 min at 37 °C (Nextera DNA Library Preparation Kit; cat. no. FC-121-1031). Samples were immediately purified by Qiagen minElute column and PCR-amplified for 12 cycles with the NEBNext High-Fidelity 2X PCR Master Mix (NEB; cat. no. M0541L). qPCR was used to determine the optimal PCR cycles to prevent over-amplification. The amplified library was further purified by Qiagen minElute column and SPRI beads (Beckman Coulter; cat. no. A63881). ATAC-seq libraries were sequenced on the Illumina HiSeq 2500 (125-nucleotide read length).

Paired-end.fastq files were uniquely aligned to the mm10 mouse genome assembly using Novoalign (Novocraft) (with the parameters -r None -k -q 13 -k -t 60 -o sam –a CTGTCTCTTATACACATCT), and converted to .bam files using SAMtools (version 1.3.1). Reads mapped to mitochondrial or duplicated reads were removed by SAMtools and PICARD MarkDuplicates (version 2.9.0), respectively. Filtered .bam files from replicates were merged for downstream analysis. MACS2 (2.1.1.20160309) was used to call ATAC-seq peaks. The coverage tracks were generated using the program bam2wig (http://search.cpan.org/dist/Bio-ToolBox/) with the following parameters:–pe–rpm–span–bw. Bigwig files were then visualized using the IGV (Broad Institute) open source genome browser.

DiffBind analysis was used to identify significant Differentially Accessible Regions (DARs) at an FDR of < 0.1 for all pairwise comparisons between conditions. Finally, BART analysis was used to identify transcription factors associated with the DAR regions[174].

3.3.6. Statistical analysis

Data were analyzed by Prism 7 (GraphPad Software). Data presented are mean values ± SEM. Comparison of two groups was performed with an unpaired, two-tailed Student t-test. Comparison

of three or more groups was analyzed by one-way ANOVA, followed by two-tailed Student t-test for individual comparisons. A p-value <0.05 was considered significant.

3.4. Results

3.4.1. Early-life RSV infection leads to long-term systemic immune alterations in BMDC of male mice

To evaluate long-term immune system alterations following early-life RSV infection, male and female neonatal mice were infected intranasally with RSV (A2/L19-F (3 x10^5 pfu)) at 7 days of age. Bone marrow was collected at 4 weeks post-infection and cultured for 6 days in the presence of GM-SCF to differentiate myeloid-type inflammatory bone-marrow-derived dendritic cells (BMDC). Phenotypic characteristics were then compared to naïve age/sex-matched control mice. BMDC isolated from early-life RSV-infected male mice showed differences in upregulation of maturation/co-stimulatory markers, such as *Cd80/86* as well as *Ox40l* (*Tnfsf4*), a co-stimulatory molecule that is critical for DC-driven Th2 responses[41,175] (**Figure 3-1A**). Differences in gene expression of cytokines related to the pro-inflammatory immune response, specifically *Il6* and inflammatory chemokines *Ccl3* and *Ccl5* were observed in BMDC from both male and female early-life RSV-infected mice compared to naïve mice (**Figure 3-1B**). Studies from our lab have previously shown that epigenetic enzyme demethylases, *Kdm5b* and *Kdm6b* are upregulated following RSV-infection of BMDC and that KDM5B leads to RSV-induced immunopathology[37]. Furthermore, KDM6 family of enzymes have been strongly linked to the inflammatory response[134,137]. We evaluated if these enzymes remain upregulated in BMDC following early-life RSV infection and found that *Kdm6b* continues to be expressed as far out as 4 weeks post-infection in BMDC isolated from male mice but not female mice (**Figure 3-1C**). Additional studies from our lab show that TSLP has a role in leading to enhanced allergic reactions later in life in male

55

mice following early-life RSV-infection[169] and TSLP has been linked to OX-40L upregulation on DC, leading to Th2 responses[41]. Interestingly, we also see increased expression of *Tslp* and its related chemokine, *Ccl17* in BMDC isolated from early-life RSV-infected male mice only (**Figure 3-1D**). Upon *in vitro* RSV infection, significant differences were observed between BMDC isolated from early-life RSV-infected male mice (RSV/Male) and naive mice as well as early-life RSV-infected female mice (RSV/Female), with RSV/Male mice showing significantly increased activation and pro-inflammatory cytokine production compared to the other groups (**Figure 3-1E,F**). Interestingly, the RSV/Female BMDC response is similar to naïve BMDC following *in vitro* RSV infection (**Figure 3-1E,F**). These results indicate differential long-term alterations of BMDC from early-life RSV infected mice, dependent upon sex. Specifically, early-life RSV infected male mice have BMDC that retain signs of activation (upregulation of maturation markers), show differential pro-inflammatory responses compared to naïve mice, and continue to express the epigenetic enzyme, *Kdm6b* as well as *Tslp* that may predispose them to exacerbated responses later in life.
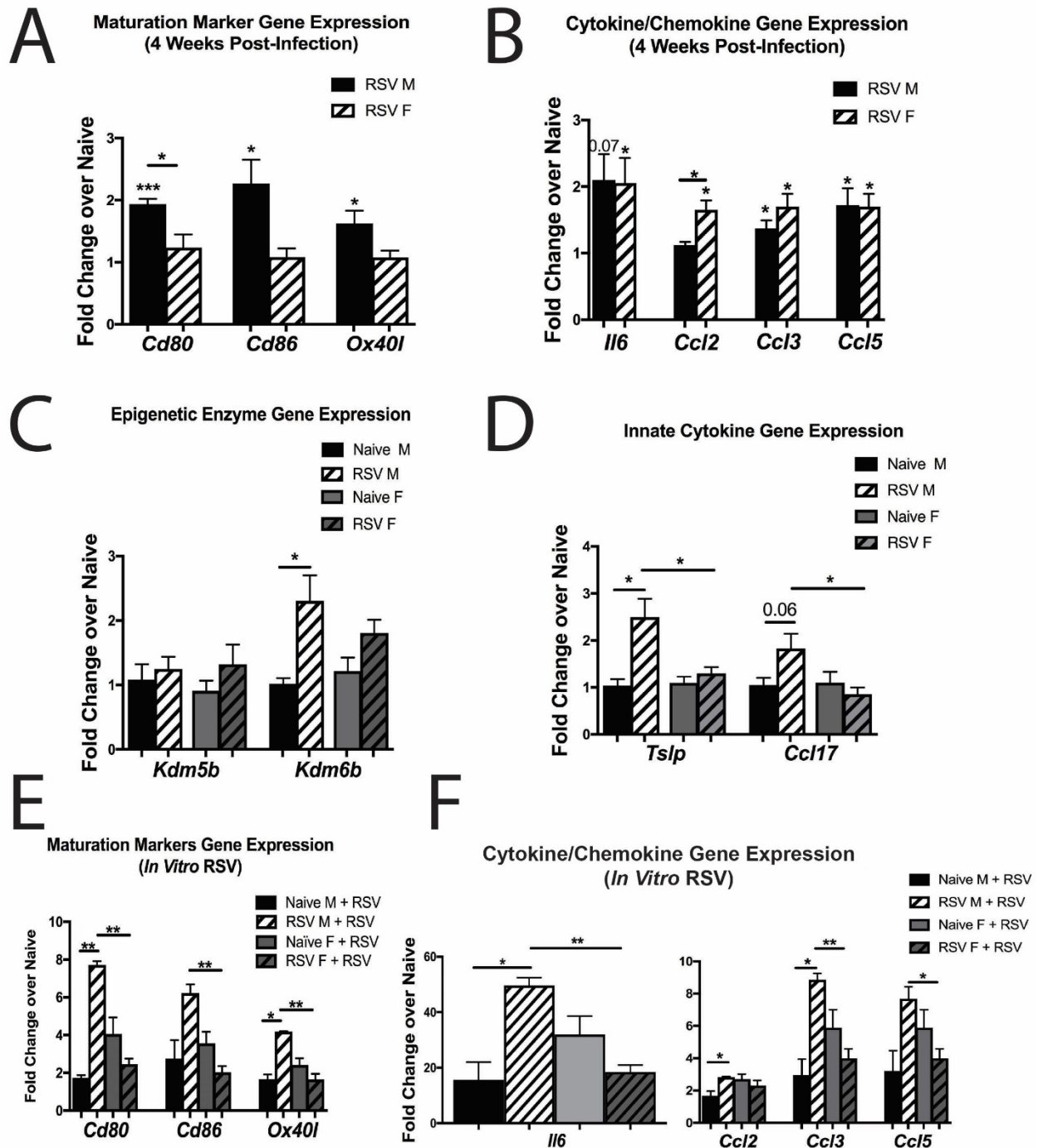
Figure 3- 1. Early-life RSV infection leads to long-term systemic immune alterations in BMDC of male mice.
Male and female Balb/c mice were infected neonatally with RSV (3 x 10⁵ pfu) at 7 days of age and bone marrow collected 4 weeks post-infection. BMDC were cultured in the presence of GM-CSF for 6 days. Naïve age/sex-matched animals were used as controls. BMDC were then plated on cell culture plates overnight, cells collected in trizol and mRNA extracted for qPCR analysis. **A.** Maturation marker expression **B.** Cytokine/chemokine gene expression **C.** Epigenetic enzyme expression **D.** Innate cytokine expression. **E,F**. BMDC were infected with RSV (MOI = 1) overnight, cells collected in trizol and mRNA extracted for qPCR analysis. Data represent Mean ± SEM (N ≥ 3; Representative of at least 2 individual experiments). * = p < 0.05; ** = p < 0.01; *** = p < 0.001.

3.4.2. TSLP during BMDC differentiation leads to Activated DC phenotype

Since we observed persistent expression of *Tslp* at 4 weeks post-infection in BMDC isolated from early-life RSV-infected male mice, we next sought to determine if the presence of TSLP during differentiation into myeloid-type DC is capable of driving the activated DC as shown above. BMDC were isolated from early-life RSV-infected male mice at 4 weeks post-infection as well as naïve age-matched controls and cultured for 6 days in the presence of GM-CSF. Additionally, separate age-matched naïve BMDC cultures were exposed to recombinant TSLP starting on Day 0, along with GM-CSF. BMDC were then infected with RSV (MOI = 1) for 24 hours. The addition of recombinant TSLP to naïve WT BMDC culture (TSLP/WT) lead to increased gene expression of maturation markers, such as *Cd80/86* and *Ox40l* (**Figure 3-2A**) as well as increased *Il6, Ccl2, Ccl3* and *Ccl5* at the mRNA level compared to naïve WT BMDC (**Figure 3-2B,C**). Furthermore, TSLP/WT DC expressed these activation markers and cytokines to a similar extent as BMDC isolated from early-life RSV-infected mice (**Figure 3-2A-C**). Finally, the addition of recombinant TSLP also increased gene expression of key epigenetic enzymes, *Kdm6a/b* (**Figure 3-2D**). These data suggest that the presence of TSLP during differentiation, such as that seen in BMDC following early-life RSV-infection of male mice, directly leads to enhanced/persistent activation and pro-inflammatory cytokine production.
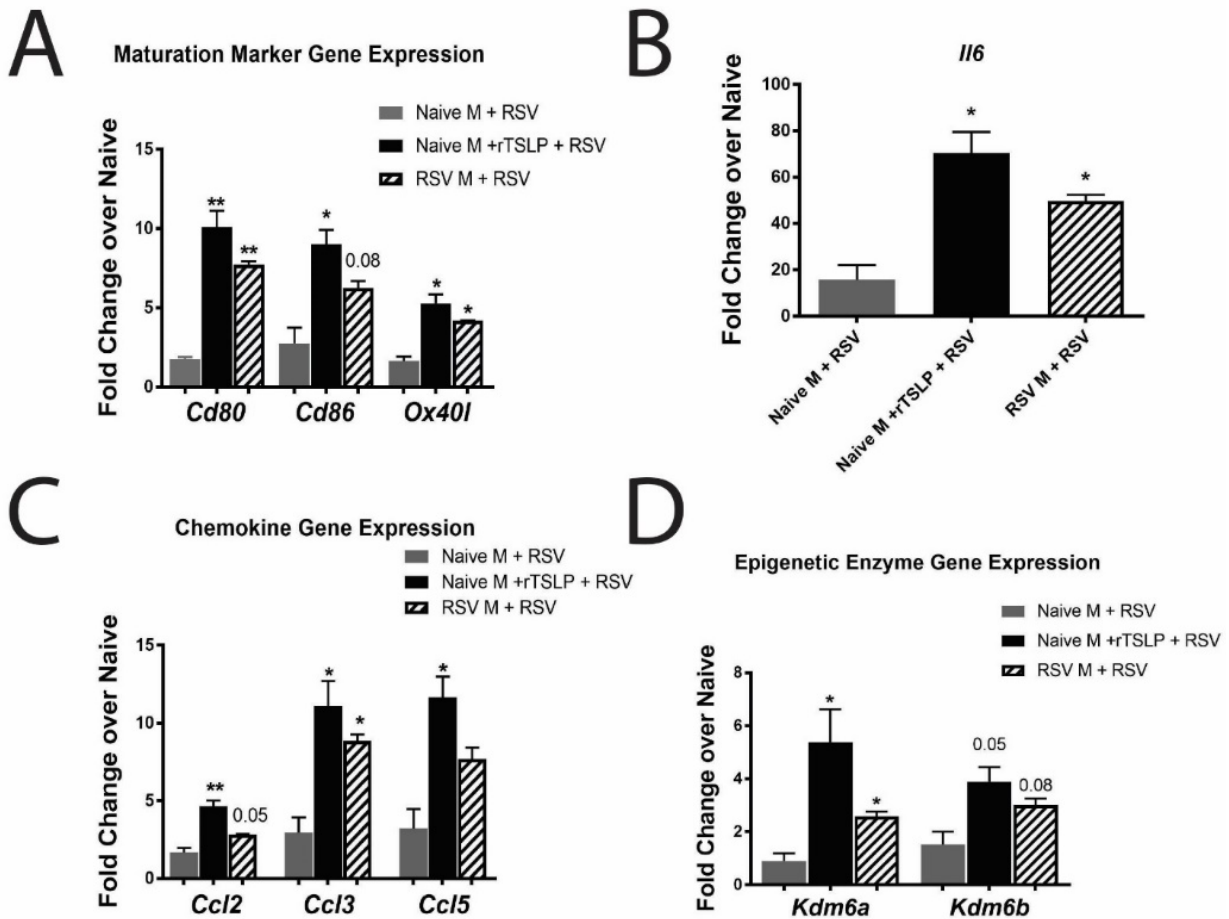
Figure 3- 2. TSLP during BMDC differentiation leads to activated DC phenotype.
Male WT Balb/c mice were infected neonatally with RSV (3×10^5 pfu) at 7 days of age and bone marrow collected 4 weeks post-infection and BMDC cultured in the presence of GM-CSF for 6 days. Naïve age-matched animals were used as controls. BMDC were then infected in vitro with RSV (MOI = 1) overnight, cells collected in trizol and mRNA extracted for qPCR analysis. **A.** Maturation marker expression **B.** *Il6* expression **C.** Chemokine gene expression **D.** Epigenetic enzyme expression. Data represent Mean ± SEM (N ≥ 3; Representative of at least 2 individual experiments). * = p < 0.05; ** = p < 0.01. Naïve M + rTSLP = BMDC collected from age-matched naïve male animals cultured in the presence of GM-CSF + rTSLP.

3.4.3. Knockdown of TSLP signaling abrogates inflammatory phenotype of BMDC from early-life RSV-infected male mice

Due to correlation of TSLP with the persistent phenotypic alterations of BMDC from early-life RSV-infected mice shown above, we further evaluated the role of TSLP using TSLPR knockout (TSLPR-/-) mice. Since a more severe phenotype was observed in BMDC from early-life RSV-infected male mice (**Figure 3-1**) and it has previously been shown that male mice infected neonatally with RSV have persistent expression of TSLP that leads to enhanced allergic

59

response[169], we focused the remaining studies on male mice only. We sought to determine if BMDC isolated from TSLPR-/- male mice have a decreased inflammatory phenotype compared to WT mice following early-life RSV-infection. Male Balb/c WT or TSLPR-/- mice were infected neonatally with RSV at 7 days of age and BMDC were collected at 4 weeks post-infection as described above. Here we show that the expression of the co-stimulatory marker, *Cd80* is decreased in BMDC isolated from TSLPR-/- early-life RSV-infected mice compared to WT mice and while not significant, a trend towards a decrease in *Cd86* and *Ox40l* (**Figure 3-3A**). Additionally, pro-inflammatory cytokines and chemokines associated with RSV-driven immunopathology are decreased in BMDC from TSLPR-/- mice (**Figure 3-3B**) with no significant differences in epigenetic enzymes (**Figure 3-3C**). These results indicate that loss of TSLP signaling protects the BMDC population from a sustained pro-inflammatory phenotype, associated with immunopathology following early-life RSV-infection.
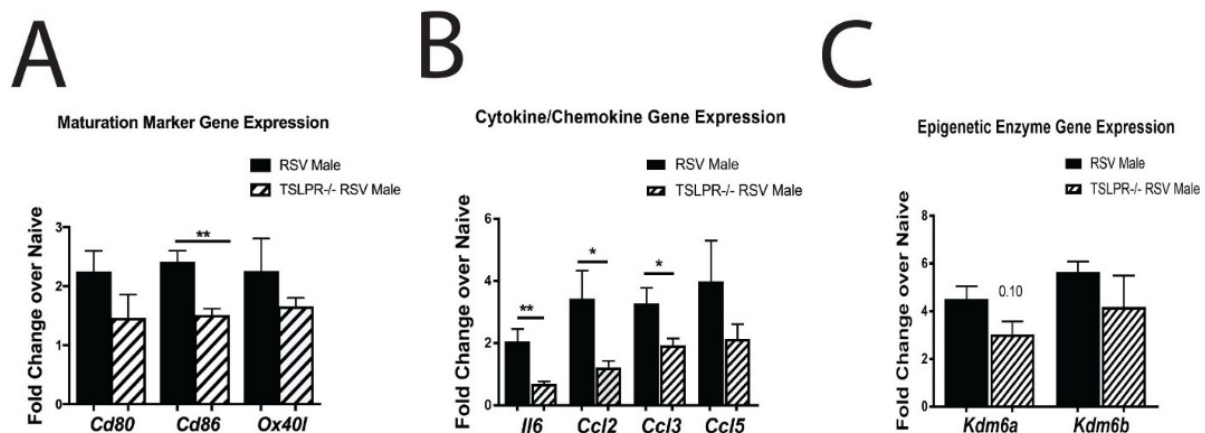
Figure 3- 3. Knockdown of TSLP signaling abrogates inflammatory phenotype of BMDC from early-life RSV-infected male mice.
Male WT Balb/c or TSLPR-/- mice were infected neonatally with RSV (3 x 10^5 pfu) at 7 days of age and bone marrow collected 4 weeks post-infection and BMDC cultured in the presence of GM-CSF for 6 days. BMDC were then plated on cell culture plates overnight, cells collected in trizol and mRNA extracted for qPCR analysis. **A**. Maturation marker expression **B**. Cytokine/chemokine gene expression **C**. Epigenetic enzyme expression. Data represent Mean ± SEM (N ≥ 3; Representative of at least 2 individual experiments). * = p < 0.05; ** = p < 0.01.

3.4.4. Lack of TSLP signaling in BMDC alters cytokine response of CD4+ T-helper cells

Since significant phenotypic differences were observed between WT and TSLPR-/- BMDC, we examined if the activity in these DC resulted in an altered ability to activate T cells. Previous studies have shown that *in vitro* infection of DC followed by co-culture with T cells leads to altered T cell cytokine production [37,176]. WT BMDC or TSLPR-/- BMDC were infected with RSV (MOI = 1.0) for 24 hours and then co-cultured with T cells (1:10) for 48 hours and cytokine production examined. Co-culture of RSV infected TSLPR-/- BMDC with T cells isolated from RSV-infected animals led to significantly increased IFN-γ production compared to WT BMDC (**Appendix 2; Figure A2-1**) as well as a significant shift in the ratio of Th1:Th2 cytokine production (**Figure 3-4A**). A similar trend was observed when naïve TSLPR-/- BMDC were co-cultured with T cells isolated from RSV-infected animals (**Figure 3-4B**), indicating an inherent difference in the ability to activate T cells between WT and TSLPR-/-. Finally, an increase in IFN-γ production was also observed when TSLPR-/- BMDC infected with RSV were co-cultured with ovalbumin peptide specific DO-11 T cells[177,178], following exposure to ova peptide (**Figure 3-4C**). These data indicate that DC-specific TSLP expression has a role in skewing the development of the T cell response following RSV infection towards Th2 by decreasing the ratio of Th1:Th2.
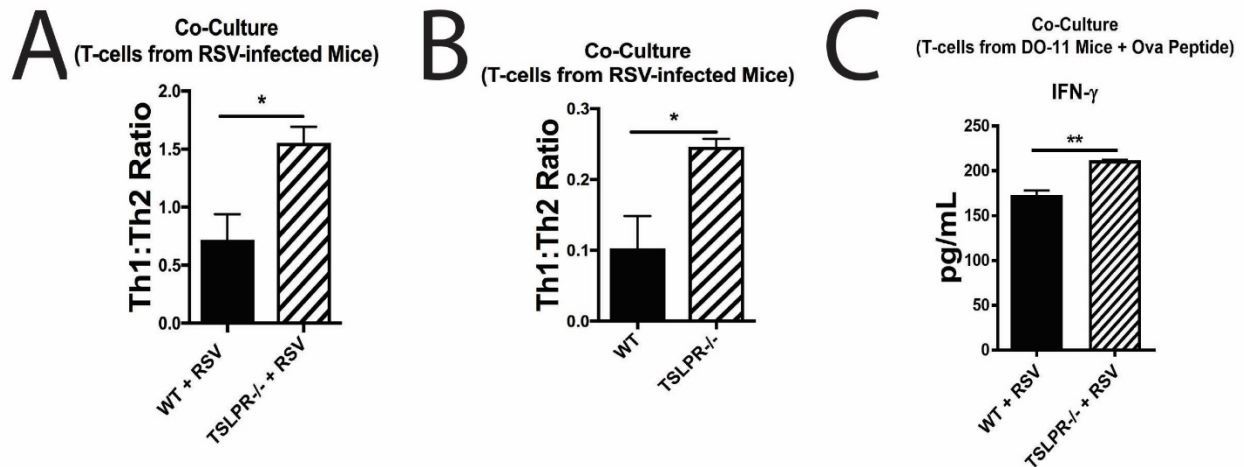
Figure 3- 4. Lack of TSLP signaling in BMDC alters cytokine response of CD4+ T-helper cells.
A. RSV-infected DC co-cultured with CD4+ T cells isolated from the lymph nodes of RSV-infected mice at 8 days post-infection. Supernatant collected and protein concentration analyzed using Bio-Plex assay and Th1:Th2 ratio calculated from these data **B**. Naive DC co-cultured with CD4+ T cells isolated from the lymph nodes of RSV-infected mice at 8 days post-infection. Supernatant collected and protein concentration analyzed using Bio-Plex assay; followed by Th1:Th2 ratio calculation **C**. RSV-infected DC co-cultured with CD4+ T cells isolated from the spleens of naïve DO-11 mice exposed to ovalbumin peptide. Supernatant collected and protein concentration analyzed using Bio-Plex assay. Data represent Mean ± SEM (N = 3). * = p < 0.05; ** = p < 0.01.

3.4.5. Differential chromatin landscape between wild-type and TSLPR-/- BMDC

Since BMDC appeared to have differential activation profiles, we next sought to determine if differences could be observed between WT and TSLPR-/- BMDC at the chromatin level using ATAC-seq evaluation to assess the transcription accessibility. BMDC were isolated from WT and TSLPR-/- early-life RSV-infected male mice at 4 weeks post-infection. BMDC were also isolated from uninfected naïve age-matched WT and TSLPR-/- male mice to be used as controls. Here, using hierarchical, unbiased clustering, we observed no differences between uninfected and infected animals within each group (**Figure 3-5A**). However, significant differences were observed between the WT and TSLPR-/- BMDC (**Figure 3-5A**), indicating an inherent difference in chromatin accessibility at baseline between WT BMDC and those isolated from BMDC lacking TSLP signaling. Next, focusing on BMDC from RSV-infected groups only, due to striking phenotypic differences shown above at the mRNA level compared to naïve BMDC, we performed DiffBind analysis (differential read density analysis) to identify if there are sites that are differentially accessible between WT and TSLPR-/- at 4 weeks post-early-life RSV infection. Here, we found approximately 1000 differentially accessible regions (DARs) between WT and TSLPR-/- BMDC following early-life RSV-infection (**Figure 3-5B and Appendix 2; Table A1**). To verify these regions, we performed additional hierarchical clustering using only the ~1000 DARs and observed very distinct clustering between the WT and TSLPR-/- groups (**Figure 3-5C**). Gene ontology (GO) cluster analysis which overlaps predicted genes with genes within GO annotated pathways to determine pathways that have significant overlap, indicated that many of

these differences corresponded to toll-like receptor pathways (**Figure 3-5D**), crucial for anti-viral and inflammatory responses. It is of interest to note that many of the genes predicted in this pathway include those linked to activated TLR4 and IL-1β (i.e. PIK3, IRAK4, Ly96 (MD-2), IKB) (**Figure 3-5D**); known to lead to persistent immune responses and enhanced inflammatory diseases[179–181182,183]. Further evaluation of genes linked to the DAR regions (**Appendix 2; Table A1**), showed that more open chromatin in TSLPR-/- BMDC were associated with type-1 IFN pathway, in regions such as those near the *Mid1* gene, which may be crucial for viral clearance[184–187] as well as *Spp1* and *Cxcl11*, both strong enhancers of type-1 immunity[188–190] (**Figure 3-5E**). In contrast, more open regions of chromatin in WT BMDC were demonstrated near genes related to RSV-driven immunopathology, such as *Irf4*, *Cxcl1* (KC), *Cxcl2, and Areg*[120,191–193] (**Figure 3-5F**). These data indicate striking differences in the chromatin landscape between WT and TSLPR-/- male mice, with WT BMDC showing more accessible regions near genes linked with Th2 immunity whereas TSLPR-/- BMDC show more accessibility near genes linked with type-1 immunity and a more appropriate anti-viral response.

D

Pathway	p.value	ATAC-seq gene prediction
GO_DEVELOPMENTAL_GROWTH_INVOLVED_IN_MORPHOGENESIS	0.0010	SALL1,RDH10,FLRT3,TGFBR2,TNC,ESR1,DCLK1,S1PR1,AREG, APP,NRP2,TIAM1
GO_INTEGRIN_MEDIATED_SIGNALING_PATHWAY	0.0016	ITGB3,ITGB2,TSPAN32,ITGAV,CDH17,DAB2,TEC,ITGA4,FUT8, ITGB8
GO_ACTIN_FILAMENT	0.0019	LCP1,GAS2,FERMT1,IQGAP2,ACTN2,CD2AP,RCSD1,GNG12, WIPF1
GO_TOLL_LIKE_RECEPTOR_SIGNALING_PATHWAY	**0.0022**	**PIK3R4,RFTN1,IRAK4,LY96,BIRC3,COLEC12,RIPK2,PIK3C3, ITGB2,IKBKB**
GO_REGULATION_OF_CHONDROCYTE_DIFFERENTIATION	0.0023	SOX5,GLI3,SOX6,RARB,SCIN,TRPS1,MAF
GO_POSITIVE_REGULATION_OF_POTASSIUM_ION_TRANSPORT	0.0038	KIF5B,ACTN2,STK39,ADRB2,DPP6,ATP1B3
GO_NEURON_PROJECTION_GUIDANCE	0.0039	TNR,NRP2,FEZ2,DPYSL2,KIF5B,SPTBN1,CDH4,GLI3,APP, EFNB2,ETV1,PLXNA2,EPHA4,GATA3,PLXNA4,EXT1,FLRT3
GO_PATTERN_RECOGNITION_RECEPTOR_SIGNALING_PATHWAY	0.0045	BIRC3,COLEC12,PIK3R4,LY96,RFTN1,IRAK4,MAP2K6,IKBKB, ITGB2,RIPK2,PIK3C3
GO_SOLUTE_CATION_ANTIPORTER_ACTIVITY	0.0085	SLC24A5,SLC24A3,SLC9A9,SLC24A2,SLC8A1
GO_REGULATION_OF_ALPHA_BETA_T_CELL_DIFFERENTIATION	0.0099	GATA3,TGFBR2,IRF4,GLI3,TNFSF18,RIPK2

E

TSLPR-/- Accessible

Gene	p Value	Immune Role
Mid1	9.8E-14	Innate/type-1 immunity: inhibits PP2A (a type-1 IFN inhibitor)
Spp1	1.2E-14	Inhibits Th2/Enhances Th1
Cxcl11	3.1E-09	Type 1 Interferon pathway/Recruitment/Activation of Th1 cells

F

WT Accessible

Gene	p Value	Immune Role
Cxcl1/KC	2.9E-06	Neutrophil recruitment/Th2 response during RSV
Irf4	7.5E-05	Dendritic cell driven Th2 response
Cxcl2	3.5E-05	Mucus production/Airway Hyperreactivity following RSV
Areg	2.1E-04	Inhibits IRF1/IFNλ during RSV/Enhances Th2

Figure 3- 5. Differential chromatin landscape between wild-type and TSLPR-/- BMDC.
Male WT Balb/c or TSLPR-/- mice were infected neonatally with RSV (3 x 10^5 pfu) at 7 days of age and bone marrow collected 4 weeks post-infection. BMDC were cultured in the presence of GM-CSF for 6 days and collected for ATAC-seq evaluation. Naïve age-matched animals were used as controls. **A**. Hierarchical, unbiased clustering was performed to evaluate the overall chromatin landscape of WT vs TSLPR-/- BMDC +/- early-life RSV infection. **B**. DiffBind analysis or differential read analysis was performed to determine differentially accessibly regions (DARs) between WT and TSLPR-/- BMDC at 4 weeks post-early-life RSV-infection. Samples were analyzed in duplicate (N = 8 WT; N = 6 TSLPR-/-); Representative plots of each biological replicate shown. Regions indicated in orange represent those regions more accessible in WT; top 250 predictions shown; Regions indicated in blue represent those regions more accessible in TSLPR-/-; all predictions shown. **C**. Biased clustering was performed focusing on only the regions associated with the DARs discovered during DiffBind analysis. **D**. Top 10 pathways associated with DARs using GO Term Analysis. **E,F**. Selected DARs related to RSV immune response. WT = Wild Type; KO = TSLPR-/-; Uni = Uninfected age-matched control; RSV = mice infected at 7 days of age and BMDC isolated 4 weeks post-infection.

3.4.6. Differential chromatin landscape between wild-type and TSLPR-/- BMDC is related to TSLP-linked transcription factors

We next performed BART analysis which examines a compendia of ChIP data to determine which transcription factors have the highest physical overlap with the predicted DARs and gives an odds ratio of prevalence for binding in order to identify possible transcription factors associated with the specific DARs between WT and TSLPR-/-. Here, we identified IRF4 and STAT3 which have been linked to development of type 2 conventional DC (cDC2) populations, TSLP signaling, and Th2 immunity[170,171,194–196] as well as IRF8, a strong driver of type-1 immunity that has been shown to be inhibited by TSLP[113] (**Figure 3-6A,B**). The probability of an involvement of these transcription factors is corroborated by the data presented in **Figures 3-1-3-3** showing persistent expression of key genes following early-life RSV infection of WT male mice: *Il6, ccl3,* and *ccl5* are known targets of IRF4 and STAT3; *Kdm6b* is a known target of STAT3 and *Irf4* is a target gene of KDM6B[137] and RELA leads to transcriptional activation of *Ox40l*[112]. Interestingly, IRF4 binding sites were also predicted through DAR to have more accessibility in WT BMDC chromatin (**Figure 3-5F**). Expression analysis by qPCR correlated with this prediction, showing that *Irf4* is persistently expressed at 4 weeks post-infection in BMDC isolated from WT but not TSLPR-/- mice (**Figure 3-6C**). TSLP has previously been shown to lead to the expression of *Irf4*[170]; therefore, this increase is likely due to the persistence of TSLP in the WT BMDC and suggests that along with IRF4-related target genes being more accessible at the chromatin level, more IRF4 is available to bind to these regions. We also performed qPCR analysis of *Irf8, Rela/b* and *Stat3* and show that their expression is not significantly altered at 4 weeks post-infection (**Figure 3-6C**). However, while not significant, there does appear to be persistent expression of IRF8 in the WT BMDC at 4 weeks post-infection (**Figure 3-6C**) suggesting possible alterations related to IRF8,

which has known shared functions with IRF4, including upregulation of chemokines (i.e. *Ccl3, Ccl5*)[197,198]. These data indicate that TSLP is able to persistently alter the systemic BMDC population through alteration of transcriptional programs related to Th2 immunity, especially IRF4, that is further enhanced by chromatin accessibility.
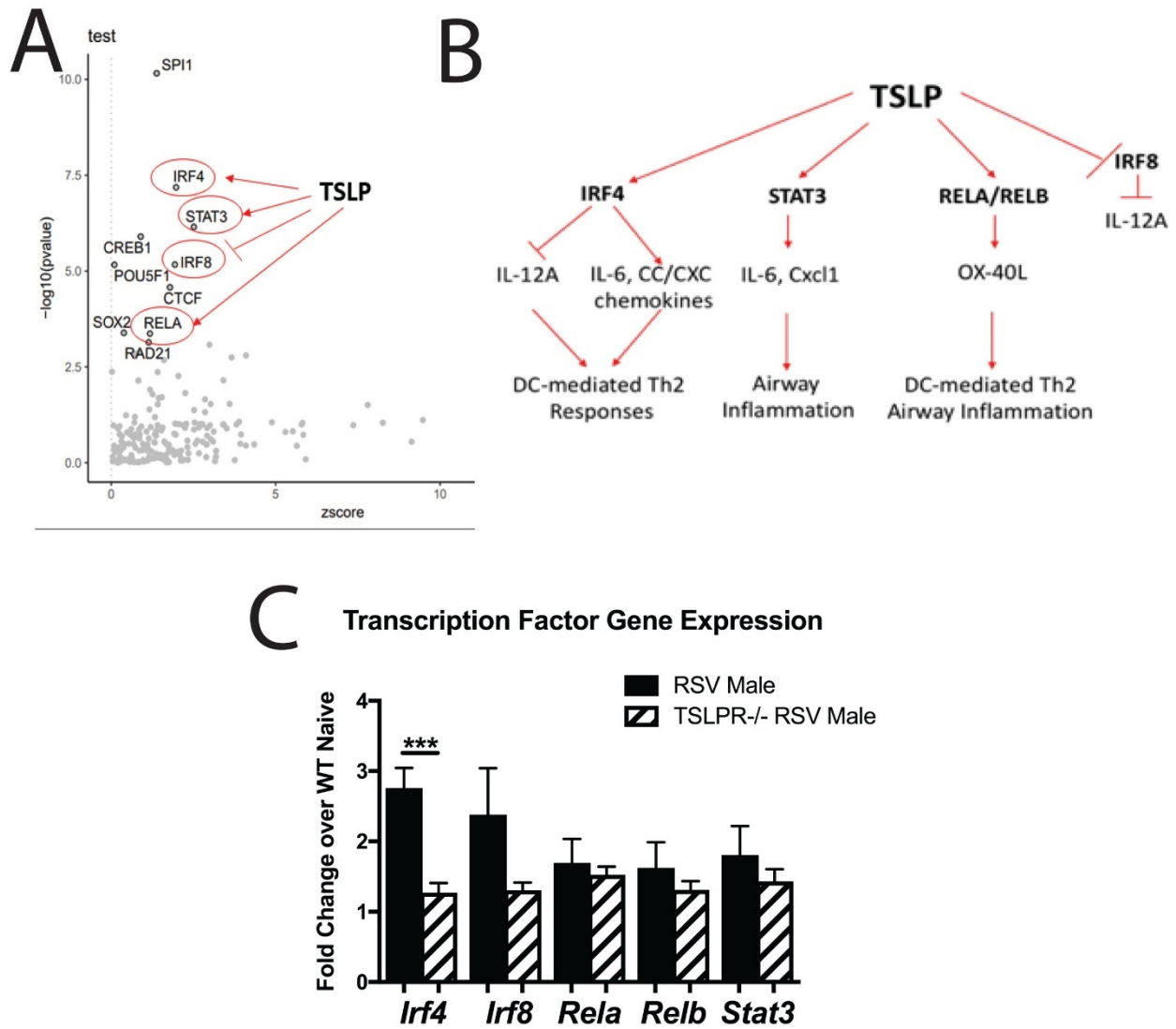
Figure 3- 6. Differential chromatin landscape between wild-type and TSLPR-/- BMDC is related to TSLP-linked transcription factors.
A. BART analysis determined transcription factors likely to bind to DAR predicted genes **B**. Schematic of TSLP linked pathways **C**. Male WT Balb/c or TSLPR-/- mice were infected neonatally with RSV (3 x 10⁵ pfu) at 7 days of age and bone marrow collected 4 weeks post-infection and BMDC cultured in the presence of GM-CSF for 6 days. BMDC were then plated on cell culture plates overnight, cells collected in trizol and mRNA extracted for qPCR analysis for gene expression. Data represent Mean ± SEM (N ≥ 3; Representative of at least 2 individual experiments). *** = p < 0.001.

3.4.7. BMDC isolated from TSLPR-/- male mice have a more appropriate Th1-type anti-viral phenotype

Next, we focused on *Mid1*, a gene associated with type-1 interferon pathway and viral clearance[185,186,199] as it was one of the top predicted genes in the DAR analysis (**Figure 3-5E**), Upon visualization of the DAR plot for this gene, there appears to be a de novo accessible region in *Mid1* of the TSLPR-/- that is not present in WT BMDC (**Figure 3-7A**). This is in direct opposition to the DAR plot of the chromatin region associated with the TSLP receptor gene (*Crlf2*), which clearly shows a loss of accessibility in the TSLPR-/- BMDC (**Figure 3-7B**), supporting visual identification of accessible vs non-accessible regions of chromatin. To further explore this target, BMDC were isolated from early-life RSV-infected WT and TSLPR-/- male mice at 4 weeks post-infection as well as naïve age-matched controls and cultured for 6 days in the presence of GM-CSF. We first performed qPCR to correlate the DAR prediction and verified that *Mid1* is increased in BMDC isolated from early-life RSV-infected TSLPR-/- mice at 4 weeks post-infection (**Figure 3-7C**). To further characterize the role of TSLP in the BMDC response, we evaluated baseline levels of *Ifnb*, which functions downstream of MID1 and is crucial for viral clearance[15], as well as *Il12a*, another type-1 cytokine[200,201]. Here, we see that at baseline, TSLPR-/- BMDC express increased levels of *Mid1*, *Ifnb, and Il12a* compared to WT (**Figure 3-7D**) suggesting an improved type-1 response. Next, we performed *in vitro* RSV infection of WT and TSLPR-/- BMDC to determine kinetics of the anti-viral/immune response. Interestingly, both *Mid1* and *Ifnb* increased very rapidly upon infection in TSLPR-/- BMDC (**Figure 3-7E,F**) and *Il12a* was increased over WT by 24 hours post-infection (**Figure 3-7G**). Overall, these data indicate that TSLPR-/- BMDC have an accelerated more appropriate type-1 immune response upon RSV infection. Furthermore, the increased expression of *Ifnb* and *Il12a* may support the

increased expression of IFN-γ shown above in **Figure 3-4**. These results indicate that loss of TSLP

signaling enhances the production of protective type-1 cytokines, possibly allowing for better viral

protection and faster resolution of the inflammatory response to decrease the persistent production

of cytokines associated with immunopathology.
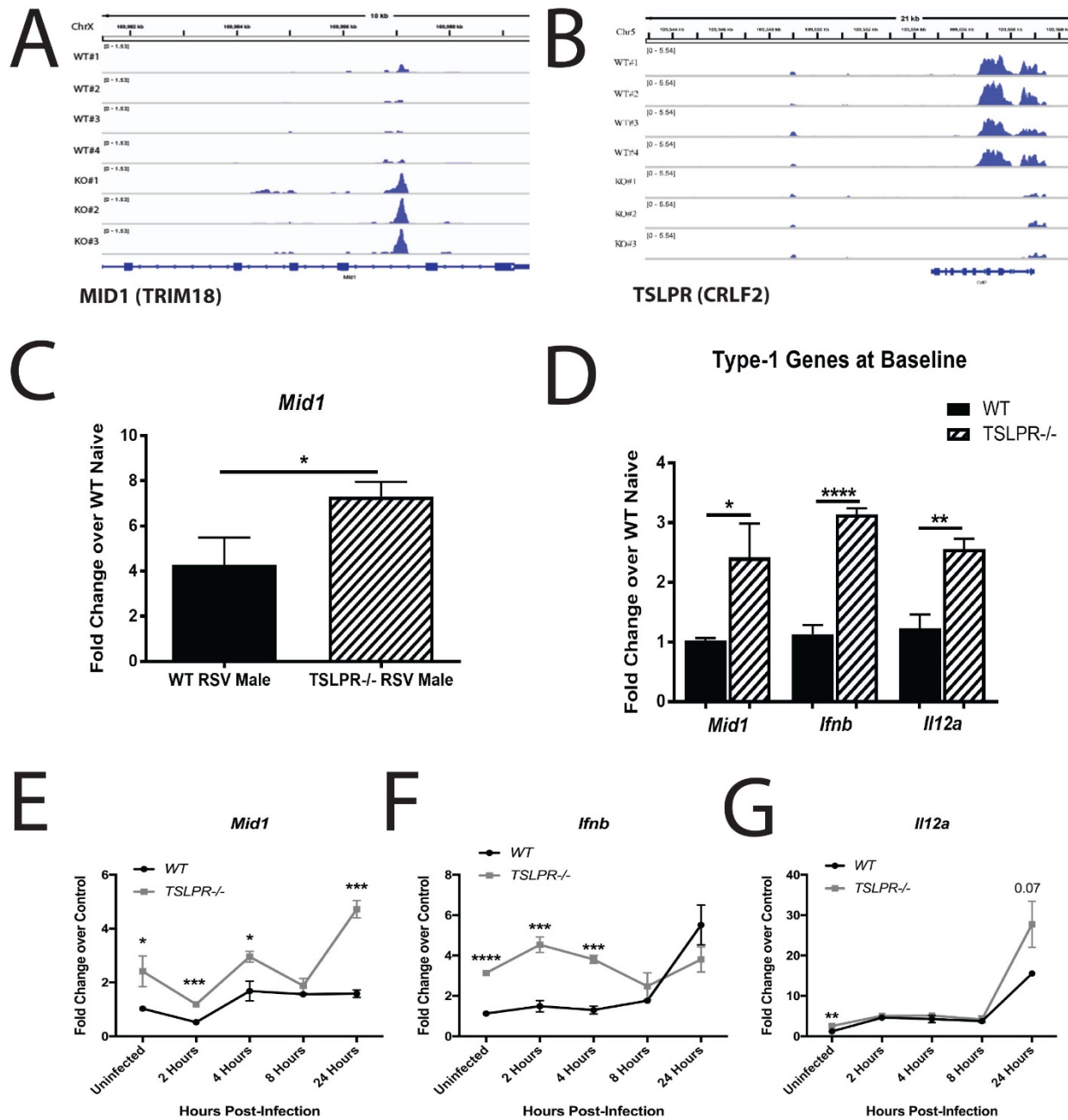
Figure 3- 7. BMDC isolated from TSLPR-/- male mice have a more appropriate Th1-type anti-viral phenotype.

A,B. ATAC-seq DAR plots **C**. Male WT Balb/c or TSLPR-/- mice were infected neonatally with RSV (3 x 10^5 pfu) at 7 days of age and bone marrow collected 4 weeks post-infection and BMDC cultured in the presence of GM-CSF for 6 days. BMDC were then plated on cell culture plates overnight, cells collected in trizol and mRNA extracted for qPCR analysis for gene expression. **D**. BMDC from naïve age-matched control mice were analyzed for mRNA expression of type-1 cytokines. **E-G.** BMDC from naïve age-matched control mice were cultured for 6 days in the presence of GM-CSF and then infected with RSV (MOI = 1) overnight and cells collected in trizol for mRNA analysis. Data represent Mean ± SEM (N ≥ 3; Representative of at least 2 individual experiments). * = p < 0.05; ** = p < 0.01; *** = p < 0.001; **** = p < 0.0001.

3.5. Discussion

RSV is a significant health care burden and cause of pediatric morbidity and mortality. Approximately 50% of all children will become infected with RSV in the first year of life and almost all children by the age of two, with 3-5% of infections resulting in hospitalization due to severe disease[24]. RSV is characterized by a dysregulated immune response that leads to poor immunologic recall that allows re-infection throughout life as well as enhanced likelihood of asthma development[7,20,22,93,154]. Therefore, elucidation of mechanisms that drive disease is crucial for protection from both primary infection and exacerbated diseases later in life. To expand our observations that TSLP is involved in persistently altering the local lung environment following early-life RSV infection in male mice[169], we sought to examine the role of TSLP on DC-specific systemic immune alterations following early-life RSV-infection. Here we show that male mice infected neonatally with RSV have persistently activated BMDC populations at 4 weeks post-early-life RSV-infection compared to both naïve age-matched mice as well as females infected with RSV at the same age. A lack of TSLP signaling in TSLPR-/- BMDC abrogates this phenotype and interestingly, the genomic profile of WT vs TSLPR-/- BMDC are significantly different, specifically in regions associated with anti-viral response. These studies outline 2 important concepts: 1) early-life RSV-infection results in a persistently altered systemic immune phenotype that can be elucidated in the BMDC and 2) the persistence of the early innate cytokine, TSLP, has a role in the altered immune environment by inhibiting Th1 immunity, favoring a Th2 response. Thus, an early viral response in the presence of TSLP may persistently alter or "train" innate

immune cells leading to long-term phenotypes, indicating TSLP as a clinically relevant target early in life.

TSLP has a wide range of immune cell targets, including ILC2, DC and T cells. The initial biologic function of TSLP demonstrated that it interacted with DC to promote Th2 cell differentiation and thus promoted allergic disease[113,114]. TSLP stimulation of CD11b+ DC upregulates OX-40L that interacts with OX-40 on CD4+ T cells to promote a Th2 response[151,152]. In response to TSLP, DCs will themselves produce TSLP that further interacts with DCs and ILC2, creating a feedback loop that is independent of epithelial cell-derived TSLP[115,116]. TSLP interacts with the transcription factor, IRF4, to lead to strong Th2-type responses and the production of cDC2-type cytokines and chemokines[112,170,194]. The TSLP/IRF4 pathway has been implicated in ILC2-driven Th2-immunity through Th9 cells[172]. Additionally, TSLP is responsible for maturation of DC and upregulation of CD80/86 as well as OX-40L[41,202,202]. The data provided in our current studies using BMDC isolated from WT or TSLPR-/- male mice corroborate these findings, indicating TSLP signaling is responsible for the increased activation state of BMDC long-term following early-life RSV-infection related to IRF4 signaling, including upregulation of maturation markers and persistent expression of pro-inflammatory cytokines and chemokines. Thus, TSLP may be central to the development of chronic type-2 immune responses following an early-life RSV-infection by promoting an altered systemic immune environment that trains innate immune cells toward the development of allergic disease.

The reduction of anti-viral responses as well as skewing towards dysregulated Th2/Th17 has been correlated with severe RSV-related disease[20,31,168] as well as exacerbated allergic responses later in life[93]. An important feature of anti-viral immunity is the ability to upregulate Type-1 IFNs leading to enhanced IFN-γ production for optimal viral clearance[15,16] and to

inhibit/reduce Th2 responses. Additionally, IFN-γ has been shown to protect against asthma pathogenesis[203,204]. Studies presented here show a novel role for TSLP in the regulation of Type-1 immunity leading to the inhibition of IFN-γ. ATAC-seq data indicated more accessibility in regions associated with type-1 IFN activation, specifically Midline 1 (*Mid1*). *Mid1* is a member of the TRIM (tripartite motif-containing) family of proteins, which are important anti-viral mediators, involved directly in viral clearance as well as stimulation of IFN-related downstream targets[184–186,199]. While *Mid1* has not previously been directly linked with RSV disease, the TRIM family of proteins has been shown to be protective against RSV pathogenesis[13,205]. Furthermore, MID1 is a known inhibitor of PP2A, which downregulates type-1 IFN production, a pathway many viruses, including RNA viruses, highjack to evade the anti-viral immune response[206–208]. Correlating with the ATAC-seq data, qPCR data showed that following early-life RSV-infection, TSLPR-/- BMDC were able to persistently express *Mid1*. Additionally, increased baseline levels of *Mid1* and *Ifnb* were observed in naïve TSLPR-/- BMDC that may enhance Th1 responses in the absence of TSLP-signaling. In support of this finding, when TSLPR-/- BMDC were infected with RSV *in vitro* followed by co-culture with RSV-responsive T cells, enhanced T cell production of IFN-γ was observed. These data collectively show that BMDC-derived TSLP is capable of inhibiting the anti-viral response by downregulating type-1 signaling to limit T cell production of IFN-γ.

Previous studies have shown long-term alteration of innate immune cells, such as monocytes and macrophages following pathogenic stimuli. For example, LPS-induced tolerance is observed in macrophages where gene-specific chromatin modifications are associated with silencing of genes related to inflammatory molecules while priming for antimicrobial genes suggesting that macrophages could be primed by LPS to become more or less responsive to

subsequent activation signals[126]. Additional studies demonstrate that exposure of monocytes/macrophages to *C. albicans* or β-glucan enhanced their subsequent response to stimulation with unrelated pathogens, leading to the term trained immunity[122,127]. Trained immunity was demonstrated to be accompanied by significant reprogramming of chromatin marks. Long-term persistence of altered responses in myeloid cells after removal of the initial stimulus may reflect either stability of these marks or the sustained activation of the upstream signaling pathways and transcription factors that control their deposition. Our data showing persistent expression of the epigenetic enzyme, *Kdm6b*, an H3K27 histone demethylase known to enhance the inflammatory response[134,137], reinforces the idea that upstream signaling pathways may lead to persistent alteration of systemic innate immune cell populations, such as BMDC. Furthermore, ATAC-seq studies showing links to many transcription factors associated with Th2 immune responses, especially IRF4, in WT BMDC as well as a persistent increase in IRF4 expression following early-life RSV-infection compared to TSLPR-/- BMDC, supports the concept of epigenetic alterations post-RSV-infection.

These studies demonstrate a novel pathway whereby RSV infection leads to upregulation of TSLP as well as the epigenetic enzyme KDM6B and a transcription factor, IRF4, in BMDC that together can modify multiple DC functions (Figure 3-8). These include costimulatory molecule expression as well as activation of defined chemokines and cytokines responsible for RSV-driven immunopathology, which may lead to an enhanced response upon secondary exposures. Knockdown of TSLP signaling leads to abrogation of this activated phenotype and restoration of an appropriately responding BMDC population able to drive Th1 T cell responses. These are the first studies, to our knowledge, that indicate a direct link to TSLP-inhibition of IFN-β as well interrogation of MID1 during the RSV response. Thus, TSLP may be a therapeutic target that

could alter the progression of pathogenic immune responses of the BMDC following early-life RSV-infection and modify the long-term systemic immune environment.
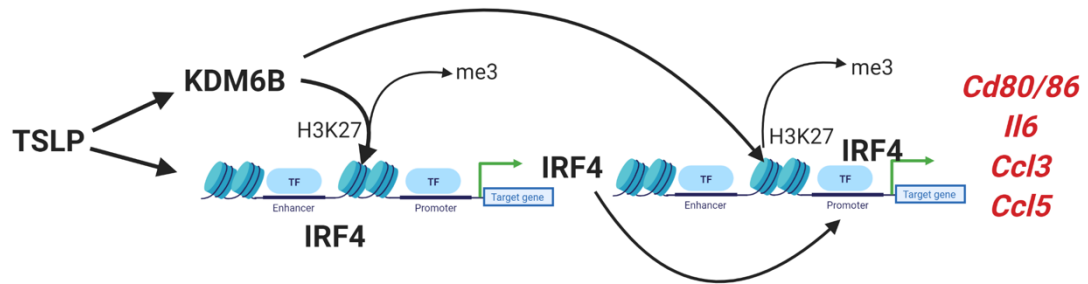
Figure 3- 8. Proposed mechanism of TSLP interactions with KDM6B and IRF4 to persistently activate BMDC. *Figure created with BioRendor.com*

Chapter 4: Upregulation of H3K27 Demethylase KDM6 During RSV Infection Enhances Pro-Inflammatory Responses and Immunopathology

4.1. Abstract

Severe disease following RSV infection has been linked to enhanced pro-inflammatory cytokine production that promotes a Th2-type immune environment. Epigenetic regulation in immune cells following viral infection plays a role in the inflammatory response and may result from upregulation of key epigenetic modifiers. Here we show that RSV-infected bone marrow-derived dendritic cells (BMDC) as well as pulmonary DC from RSV-infected mice upregulated expression of *Kdm6b/Jmjd3* and *Kdm6a/Utx,* H3K27 demethylases. *KDM6*-specific chemical inhibition (GSK J4) in BMDC led to decreased production of chemokines and cytokines associated with the inflammatory response during RSV infection (i.e. CCL-2, CCL-3, CCL-5, IL-6) as well as decreased MHC II and co-stimulatory marker (CD80/86) expression. RSV-infected BMDC treated with GSK J4 altered co-activation of T cell cytokine production to RSV as well as a primary ovalbumin response. Airway sensitization of naïve mice with RSV-infected BMDCs exacerbate a live challenge with RSV infection but was inhibited when BMDCs were treated with GSK J4 prior to sensitization. Finally, *in vivo* treatment with the KDM6 inhibitor, GSK J4, during RSV infection reduced inflammatory DC in the lungs along with IL-13 levels and overall inflammation. These results suggest that KDM6 expression in DC enhances pro-inflammatory innate cytokine production to promote an altered Th2 immune response following RSV infection that leads to more severe immunopathology.

4.2. Introduction

Respiratory syncytial virus (RSV) infects nearly all infants by age two and is the leading cause of bronchiolitis in children worldwide[1,2]. The CDC estimates that up to 125,000 pediatric hospitalizations in the United States each year are due to RSV, at an annual cost of over $300,000,000[2,20,167]. In the late 1960s, attempts to vaccinate children with formalin-inactivated RSV vaccine caused severe exacerbated disease upon re-infection with live RSV due to enhanced inflammatory disease and mucus production[25–27]. Furthermore, several epidemiological studies link severe RSV infection with the later development of hyper-reactive airway disease, including asthma, that persists even years after the initial viral infection has resolved[1,3,20]. RSV likely initiates and reinforces the immune environment by further altering pathogenic immune responses.

During a viral infection, the immune response is regulated by dendritic cells (DC) as they instruct T cells toward distinct T helper type responses[44]. RSV can skew the immune response away from anti-viral and towards a Th2-type response by inhibiting the production of IFN-β and subsequently decreasing the less pathogenic anti-viral Th1 response[45]. The reduction of anti-viral responses as well as skewing towards dysregulated Th2/Th17 has been correlated with severe disease[20,31,168], leading to airway alterations linked to exacerbated allergic responses later in life[93]. RSV-exposed DC are sufficient to promote a more severe and accelerated disease environment when exposed to secondary RSV challenge[89,176] or allergens[89]. Understanding whether and how RSV infection influences DC function to alter the immune environment leading to exacerbation or initiation of a pathogenic environment will be crucial for modifying pulmonary pathologies.

Immune regulation by epigenetic mechanisms, an intense area of research, alters DNA transcription via histone proteins that comprise nucleosomes[209,210]. Lysine residues in the histone tail are often modified to allow an open (active) or closed (silenced) configuration of the gene. For

example, the addition of methyl groups on lysine (K) 4 of histone (H) 3 (i.e. H3K4) leads to activation of gene transcription, whereas H3K27 methylation is a repressive mark[130,211,212]. H3K4 methylation is crucial for active gene transcription, while H3K27 methylation appears to regulate and fine-tune gene transcription[130,134]. This process is controlled by methyltransferases that add methyl groups and demethylases that remove them, such as the lysine demethylase family of enzymes, including KDM5 and KDM6. Removal of the H3K4 methylation mark by KDM5 leads to repressed gene transcription while KDM6, an H3K27 demethylase that removes the methylation mark from H3K27, leads to more active gene transcription. In addition to the canonical role of H3K27 demethylation, KDM6 also contributes to gene activation by modulation of H3K4 methylation through stabilization of the MLL complex[135,136] and guides gene transcription by binding POLII to enhance its movement along genes[137,138]. There is already evidence that KDM6 is involved in the inflammatory response[134,137,213]. Additionally, our lab has previously shown that KDM5B and KDM6B are upregulated during RSV infection and identified that KDM5B enhances RSV-driven immunopathology by inhibiting key cytokines, especially IFN-β[37]. The specific role of KDM6 during RSV infection has not previously been explored.

In the present study, we examined the KDM6 family of histone lysine demethylases (KDM6A/B). Specifically, we demonstrate that RSV infection leads to upregulation of KDM6A/B in BMDC and that inhibition of its enzymatic activity depresses multiple cytokines and chemokines associated with RSV-driven inflammatory responses as well as antigen presentation/co-stimulation of DC. Furthermore, *in vivo* inhibition of KDM6 activity leads to decreased inflammatory DC infiltration into the lungs, reduced immunopathology and decreased Th2-skewing, indicating that KDM6 upregulation during RSV-infection enhances immunopathology, partially through alteration of APC function. These results indicate that

targeting epigenetic pathways and overall DC function may be crucial for limiting long-term RSV-driven disease pathologies.

4.3. Materials and Methods

4.3.1. Animals

All experiments involving the use of animals were approved by the University of Michigan animal care and use committee (protocol PRO0000888, exp. 02/14/2022). Male/female C57BL/6, female OT-II and male/female BALB/c mice, 6 to 8 weeks of age, were purchased from The Jackson Laboratory (Bar Harbor, ME).

4.3.2. RSV-infection and *in vivo* GSK J4 Treatment

A chimeric RSV A2 strain with recombinant Line19 fusion protein (A2/L19-F) was used for all experiments as previously described[145]. This strain was used due to its ability to enhance viral infection, mucus hypersecretion and airway hyperreactivity in mouse models due to Line 19-derived F protein, including pathogenic IL-13 and IL-17 responses[31,145]. Male Balb/c mice were infected intratracheally with 2.0×10^5 pfu of RSV A2/L19-F and tissues harvested at 8 days post-infection. Viral stocks were grown in Hep-2 cells and concentrations determined by plaque assay. Virus was ultra-centrifuged (100,000xg for 30 minutes at 4°C) and re-suspended in fresh cell culture media (RPMI 1640 supplemented with 10% fetal calf serum (FCS), L-glutamine, penicillin/streptomycin, non-essential amino acids, sodium pyruvate, 2-mercaptoethanol (ME)) or 1X DPBS prior to use. In some experiments, cultured dendritic cells were infected with RSV for 24 hours, thoroughly washed, and 2.5×10^5 cells were transferred intratracheally into naïve male mice. Ultraviolet (UV)-inactivated virus was prepared by exposure to UV light to inactivate RSV as previously described [120,214]. For *in vivo* GSK J4 treatment, GSK J4 (Millipore-Sigma, St. Louis, MO, USA) was reconstituted in DMSO and further diluted in PBS without Ca/Mg (final

concentration 2 mg/mL; 2.5% DMSO); 200 µL was given intraperitoneally per animal for a final dosing concentration of 20 mg/kg per animal per dose, given once daily over 7 days.

4.3.3. Bone Marrow-Derived Dendritic Cells and Co-culture with CD4+ T cells

Bone marrow from C57BL/6 or Balb/c mice was collected by flushing the femur and tibia of hind legs with RPMI 1640 supplemented with 10% fetal calf serum (FCS), L-glutamine, penicillin/streptomycin, non-essential amino acids, sodium pyruvate, 2-mercaptoethanol (ME). BMDCs were grown in RPMI 1640 supplemented with 10% FCS, L-glutamine, penicillin/streptomycin, non-essential amino acids, sodium pyruvate, 2-mercaptoethanol (ME) and 10 ng/ml of recombinant murine granulocyte macrophage-colony stimulating factor (GM-CSF; R&D Systems, Minneapolis, MN, USA). Cells were fed on Days 3 and 5 with fresh GM-CSF. On Day 6, cells were cultured with RSV (MOI = 2.5). For some experiments, cells were concurrently treated with 10 µM GSK J4 (Sigma, St. Louis, MO, USA), a chemical inhibitor of KDM6A/B [215], 10 µM inactive isomer control, GSK J5 (abcam), or with ethanol (0.1%) as a control. At 24 hours, supernatant was collected for protein analysis using Bio-Plex cytokine assay (Bio-Rad Laboratories, Hercules, CA). Cells were collected in TRIzol reagent and mRNA was extracted using TRIzol reagent (Invitrogen, Carlsbad, CA) for quantitative RT-PCR or resuspended in PBS for flow cytometry. For some experiments, CD4^{+} T cells were isolated from the lymph nodes of RSV-infected Balb/c mice or spleens from naïve OT-II mice using the T cell isolation II kit (Miltenyi Biotec). Cells were then cultured with the treated BMDCs. For OT-II cells, co-culture was performed in the presence of ovalbumin peptide 323-339 (10 µg/mL; Invivo Gen, San Diego, CA). At 48 hours, the supernatant was collected and protein levels were measured with a Bio-Plex cytokine assay (Bio-Rad Laboratories, Hercules, CA).

4.3.4. Quantitative RT-PCR

Lung tissue was homogenized in TRIzol reagent, and mRNA was subsequently extracted using TRIzol reagent (Invitrogen, Carlsbad, CA). cDNA from lung or BMDC mRNA (described above) was synthesized using murine leukemia virus reverse transcriptase (Applied Biosystems, Foster City, CA) by incubation at 37℃ for one hour, followed by incubation at 95℃ for 10 min to stop the reaction. Real-time quantitative PCR (qPCR) was measured using Taqman primers, with a FAM-conjugated probe to measure transcription of *Kdm6a, Kdm6b, Il4, Il5, Il13, 18s*. Fold change was quantified using the $2^{-\Delta\Delta}$ cycle threshold (CT) method. All reactions were run on a 7500 Real-Time PCR System (Applied Biosystems, Foster City, CA).

4.3.5. Flow Cytometry

BMDC were collected and resuspended in PBS. Live cells were identified using LIVE/DEAD Fixable Yellow Dead Cell Stain kit (Thermo Fisher Scientific, Waltham, MA), incubated at 4°C for 20 minutes then washed and resuspended in PBS with 1% FCS. Fc receptors were blocked with purified anti-CD16/ 32 (clone 93; BioLegend, San Diego, CA). Surface markers were identified using Abs (clones) against the following antigens, all from BioLegend: anti-CD11c (N418), MHC II (M5/114.15.2), CD11b (M1/70), CD80 (16-10/A1), CD86 (GL-1). The lungs were removed, and single cells were isolated by enzymatic digestion with 1 mg/mL collagenase (Roche) and 20 U/mL DNaseI (Sigma, St. Louis, MO) in RPMI 1640 + 10% FCS for 60 min at 37°C. Tissues were further dispersed through an 18-gauge needle (5-mL syringe), red blood cells (RBCs) were lysed and samples were filtered twice through 100-μm nylon mesh. Cells were resuspended in PBS. Live cells were identified using LIVE/DEAD Fixable Yellow Dead Cell Stain kit (Thermo Fisher Scientific, Waltham, MA), then washed and resuspended in PBS with 1% FCS. Fc receptors were blocked with purified anti-CD16/ 32 (clone 93; BioLegend, San

Diego, CA). Surface markers were identified using Abs (clones) against the following antigens, all from BioLegend: anti-CD11c (N418), MHC II (M5/114.15.2), CD11b (M1/70), CD80 (16-10/A1), CD86 (GL-1), F4/80 (BM8), Ly6C (HK1.4), CD3 (145-2C11), CD4 (GK1.5), CD8 (53-6.7), CD69 (H1.2F3). Data were collected using a NovoCyte flow cytometer (ACEA Bioscience, Inc. San Diego, California). Data analysis was performed using FlowJo software (Tree Star, Oregon, USA). All populations were gated as: cells/singlets (doublet discrimination)/live cells. Distinct populations were then gated as follows: CD11c+ dendritic cells: CD11b+/CD80+; CD11b+/CD86+; CD11b+/MHCII+; F4/80 macrophages: CD11c-/CD11b+/F4/80+; inflammatory monocytes: CD11c-/CD11b+/Ly6C+; inflammatory dendritic cells: CD11c+/CD11b+/Ly6C+; T cells: CD3+/CD4+, CD3+/CD8+; activated CD4+ T cells: CD3+/CD4+/CD69+; eosinophils: CD11b+/side scatter (SS)^{hi}/SiglecF+; neutrophils: CD11b+/SS$^{hi/}$Gr-1+.

4.3.6. Chromatin immunoprecipitation

Chromatin immunoprecipitation (ChIP) was performed as previously described[216]. Briefly, cells (1 x 10^6 total cells) were fixed in 18.5% paraformaldehyde (PFA). Glycine (10X) was added to quench extra PFA. Cells were washed using ice-cold PBS and lysed in SDS buffer. Cells were then sonicated using a Branson Digital Sonifier 450 (VWR, West Chester, PA, USA) to create 200–1000 bp fragments. The lysate was clarified by centrifugation, and 5% of the supernatant was saved to measure the input DNA. The remaining chromatin was incubated with 1 μg of anti-H3K27me3 antibody (Active Motif), H3K4me3 antibody (Abcam) or control IgG (Millipore) and incubated at 4°C with rotation overnight. Immune complexes were precipitated with salmon sperm DNA/protein A agarose beads. The bead complexes were washed with a series of buffers (low-salt immune complex buffer, high-salt immune complex buffer, LiCl immune complex buffer, and

Tris/EDTA buffer). Protein-DNA complexes and input DNA were eluted using elution buffer. Crosslinking was reversed by incubation at 65°C, and samples were treated with proteinase K. DNA was purified by phenol:chloroform:isoamyl alcohol separation and ethanol precipitation. Primers for the promoter regions of CD80 (Forward: CACCCCCGCAAGCAGAATCC; Reverse: GGCAACTCAAAGGTCCCCAGAAC) and CD86 (Forward1: AAGAAAAAGTCAACCACCAGGG; Reverse1: TTCAAGTCCGTGCTGCCTAC; Forward1: AAGAAAAAGTCAACCACCAGGG; Reverse2: CGTGGGTGCTTCCGTAAGTT) were designed using Lasergene software and DNA was amplified by qPCR using SYBR Green buffer (Applied Biosystems, Foster City, CA).

4.3.7. Lung Histology

The middle and inferior lobes of the right lung were perfused with 10% formalin for fixation and embedded in paraffin. Five-micrometer lung sections were stained with periodic acid-Schiff (PAS) to detect mucus production, and inflammatory infiltrates. Photomicrographs were captured using a Zeiss Axio Imager Z1 and AxioVision 4.8 software (Zeiss, Munich, Germany).

4.3.8. Lung draining lymph node in vitro re-infection and cytokine production assay

Lung draining lymph nodes (LDLN) were enzymatically digested using 1 mg/mL collagenase A (Roche) and 20 U/mL DNaseI (Sigma-Aldrich) in RPMI 1640 with 10% FCS for 45 min at 37°C. Tissues were further dispersed through an 18-gauge needle (1-mL syringe). RBCs were lysed, and samples were filtered through 100-μm nylon mesh. Cells (5×10^5) from LDLN were plated in 96-well plates and re-infected with 1.5-3.0 x 10^5 pfu of RSV. IL-4, IL-5, IL-13, Il-17A and IFN-γ levels in supernatants were measured with a Bio-Plex cytokine assay (Bio-Rad Laboratories, Hercules, CA).

4.3.9. Statistical analysis

Data were analyzed by Prism 7 (GraphPad Software). Data presented are mean values ± SEM. Comparison of two groups was performed with an unpaired, two-tailed Student *t*-test. Comparison of three or more groups was analyzed by one-way ANOVA, followed by two-tailed Student *t*-test for individual comparisons. A *p*-value <0.05 was considered significant.

4.4. Results

4.4.1. Histone lysine demethylases *Kdm6a* and *Kdm6b* are upregulated following RSV infection

Epigenetic enzymes have been implicated in regulating immune gene transcription during inflammatory responses[217–219]. Previous studies have shown that histone lysine demethylases are upregulated during RSV infection, especially in CD11c+ populations that control the immune response to RSV[37]. In the current studies, male C57BL/6 and Balb/c mice were infected intratracheally with RSV and at 8 days post-infection, we collected the CD11c+ cell population from the lungs and verified RSV infection by evaluation of viral gene expression (**Appendix 3; Figure A3-1A,B**). We then evaluated the epigenetic enzyme expression in the CD11c+ cell population and showed upregulated gene expression of *Kdm6a* and *Kdm6b* H3K27 demethylases in both strains of mice (**Figure 4-1A,B**). Next, we evaluated the upregulation of *Kdm6* demethylases in CD11c+ bone marrow-derived dendritic cells (BMDC) since a significant source of inflammatory CD11c+ cells recruited to the lungs during infection are bone marrow-derived and furthermore, epigenetic alteration of inflammatory DC regulates RSV-driven immunopathology[37]. BMDC were infected with live RSV (MOI = 2.5) for 4, 8, 12, or 24 hours and infection verified by RSV gene expression (**Appendix 3; Figure A3-1C**) and cells were then evaluated for *Kdm6a/b* mRNA expression (**Figure 4-1C**). Significant upregulation of both *Kdm6a*

and *Kdm6b* was observed at 4-12 hours post-infection in the BMDC (**Figure 4-1D,E**). The use of

UV-inactivated RSV did not lead to upregulation of *Kdm6a* or *Kdm6b* (**Appendix 3; Figure A3-**

1D), demonstrating a direct effect of RSV on the expression of these gene regulatory chromatin

modifiers.
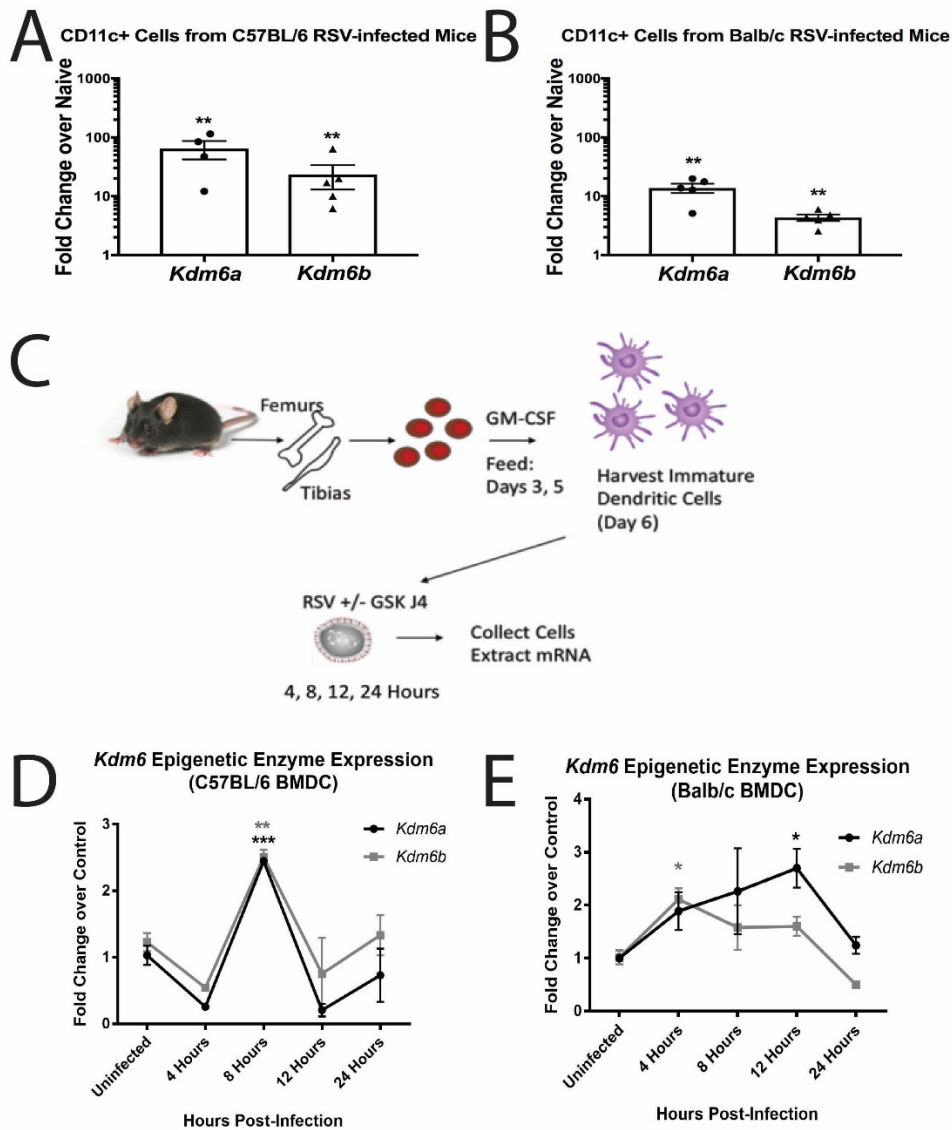
Figure 4- 1. Histone lysine demethylases *Kdm6a* and *Kdm6b* are upregulated following RSV infection.
A, B. Male C57BL/6 or Balb/c mice were infected with RSV (2×10^5 pfu) and lungs collected 8 days post-infection and compared to naïve control animals. Lungs were harvested and the CD11c+ cell population isolated using MACS bead separation, mRNA extracted and qPCR performed to determine epigenetic enzyme expression ($N \geq 3$). **C.** Experimental design for BMDC culture **D, E**. BMDC isolated from C57BL/6 or Balb/c mice were infected *in vitro* with RSV and cells collected at the indicated timepoints, mRNA extracted and qPCR performed to determine epigenetic enzyme expression ($N = 3$). Data represent Mean ± SEM (Representative of 2 individual experiments). * = $p < 0.05$; ** = $p < 0.01$; *** = $p < 0.001$.

4.4.2. Inhibition of KDM6 reduces DC cytokine and co-stimulatory molecule expression

To examine the role of KDM6 enzymes, GSK J4 (10 µM), a competitive inhibitor that blocks KDM6 demethylase activity was used[215]. Based on time-course studies, to determine optimal cytokine and chemokine gene expression, (**Appendix 3; Figure A3-2A**) and to allow for epigenetic modification of these genes following epigenetic enzyme upregulation, BMDC were treated with GSK J4 or vehicle and concurrently infected with RSV for 24 hours. RSV infectivity of BMDC treated with vehicle or GSK J4 was similar, as indicated by the levels of RSV gene expression (**Figure 4-2A**). Additionally, we analyzed the live cell populations using flow cytometry and observed no difference in cell viability compared to vehicle-treated controls (**Figure 4-2B**). Treatment with GSK J4 during RSV-infection led to a significant reduction in CCL-2, CCL-3, CCL-5, and IL-6 (**Figure 4-2C**) indicating a decrease in inflammatory chemokines and cytokines in response to RSV-infection. An inactive isomer of GSK J4 (GSK J5) was also used as a control and showed no reduction in these specific cytokines (**Appendix 3; Figure A3-2B**), confirming specificity of this response to GSK J4. Additionally, correlating with previous studies from our laboratory[120,214], no upregulation of the inflammatory response (i.e. *Il6* or chemokines) was observed using UV-inactivated RSV (**Appendix 3; Figure A3-2C,D**), indicating that active viral infection is necessary for this response. In order to examine DC activation, co-stimulatory and maturation markers were examined and indicated a reduction in CD80 and CD86 as well as MHC II expression (**Figure 4-2D**) and this reduction was confirmed using siRNA to knockdown gene expression of *Kdm6b* (**Appendix 3; Figure A3-2E**). Treatment with GSK J4 demonstrated increased H3K27 methylation status (**Figure 4-2E**), as well as a significant reduction in H3K4 methylation (**Figure 4-2F**), correlating with the reduced expression of key APC associated molecules. Thus, during RSV-infection, KDM6 enzymatic activity led to upregulation

of cytokines and chemokines associated with RSV-driven inflammation and the activation of

molecules necessary for optimal APC function.
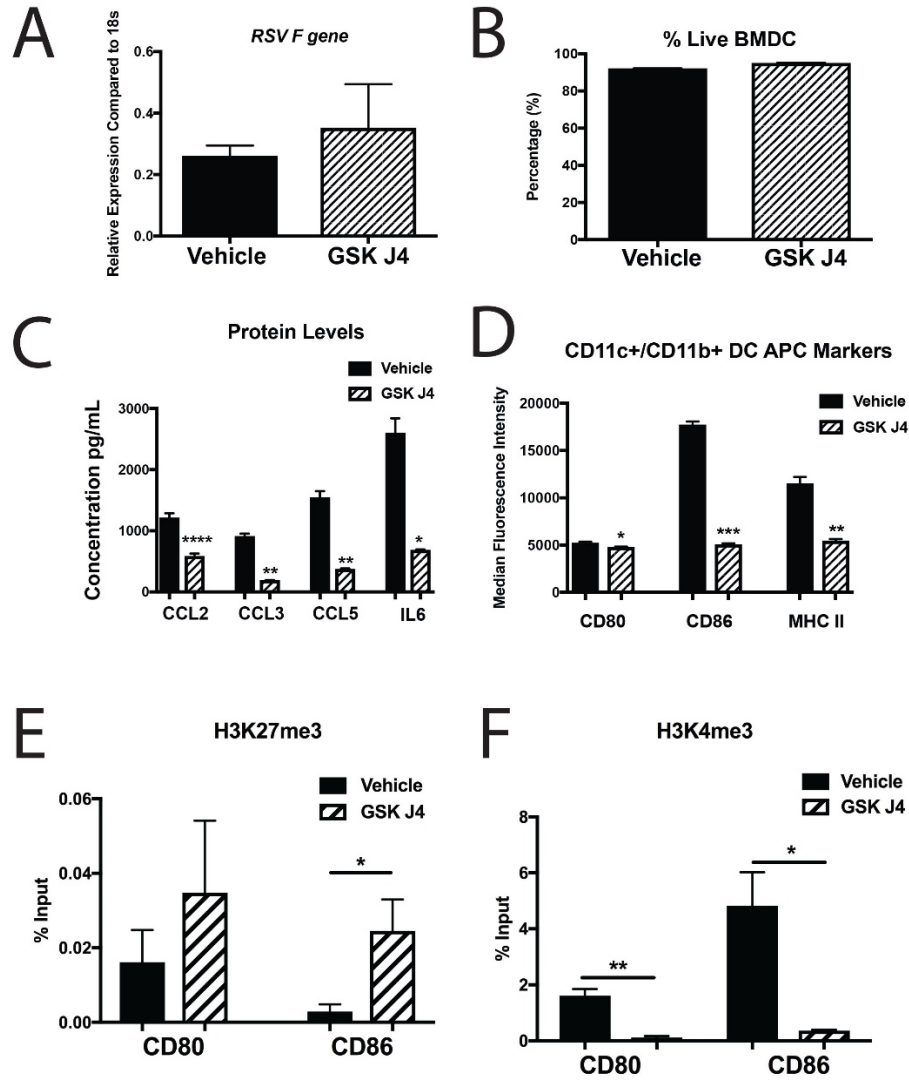
Figure 4- 2. Inhibition of KDM6 reduces DC cytokine and co-stimulatory molecule expression.
BMDC were isolated from C57BL/6 mice, cultured for 6 days in the presence of GM-CSF and infected with RSV + GSK J4 or vehicle control *in vitro* for 24 hours. **A**. mRNA was extracted and qPCR performed to determine RSV F gene expression (N = 3). **B.** Cells were collected, processed and stained for flow cytometry analysis of live cell populations (N = 3). **C**. Supernatant was collected and protein evaluated using Bio-Plex assay (N = 3). **D.** Cells were collected, processed and stained for flow cytometry analysis of APC markers (N = 3). **E, F.** Cells were collected and DNA extracted for ChIP analysis (N ≥ 3). Data represent Mean ± SEM (Representative of at least 2 individual experiments). * = p < 0.05; ** = p < 0.01; *** = p < 0.001; **** = p < 0.0001.

4.4.3. Inhibition of KDM6 in BMDC alters cytokine response of CD4+ T-helper cells

Since both cytokine and co-stimulatory molecules were altered by KDM6 inhibition, we examined

if altering KDM6 activity in DC resulted in an altered ability to activate T cells. Previous studies

have shown that *in vitro* infection of DC, followed by co-culture with T cells leads to altered T cell cytokine production[37,176]. BMDC were infected with RSV (MOI = 2.5) and treated with GSK J4 (10 μM) for 24 hours and then co-cultured with T cells (1:10) for 48 hours and cytokine production examined (**Figure 4-3A**). Co-culture of RSV infected BMDC with T cells isolated from the lymph nodes of RSV-infected Balb/c mice led to significantly reduced IL-17A and IFN-γ production upon inhibition of KDM6 in BMDC (**Figure 4-3B**). Additionally, when BMDC from C57BL/6 mice were infected with RSV +/- GSK J4 and co-cultured with ovalbumin peptide specific OT-II CD4+ T cells[177,178], decreased production of IL-5 and IL-13 following exposure to ova peptide was observed (**Figure 4-3C**). These data indicate that DC-specific KDM6 expression has a role in regulating the development of the T cell response following RSV infection as well as to unrelated primary immune responses linked to Th cell mediated disease.
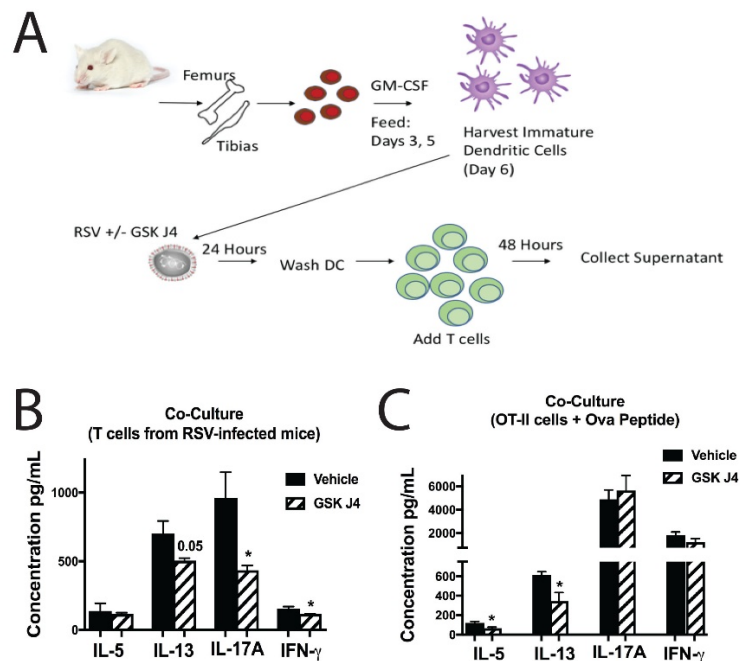
Figure 4- 3. Inhibition of KDM6 in BMDC alters cytokine response of CD4+ T-helper cells.
A. DC/T cell co-culture experimental design **B.** RSV-infected DC (Balb/c) co-cultured with CD4+ T cells isolated from the lymph nodes of RSV-infected female Balb/c mice at 8 days post-infection. Supernatant collected and protein concentration analyzed using Bio-Plex assay (N ≥ 4). **C**. RSV-infected DC (C57BL/6) co-cultured with CD4+ T cells isolated from the spleens of naïve female OT-II mice exposed to ovalbumin peptide. Supernatant collected and protein concentration analyzed using Bio-Plex assay (N = 3). Data represent Mean ± SEM (Representative of 2 individual experiments). * = p < 0.05.

4.4.4. BMDC-induced RSV sensitization is altered by KDM6 inhibition in RSV challenge

To further examine the role of KDM6 enzymatic function, RSV infected BMDC (24 hour) with or without inhibition of KDM6 were transferred intratracheally into naïve Balb/c mice and at 7 days post-DC transfer, BMDC sensitized mice were challenged with RSV (**Figure 4-4A**). Our lab has previously demonstrated that this sensitization protocol with DC elicits a pathogenic immune environment upon RSV re-infection[37,89]. Instillation of RSV-infected BMDC led to enhanced inflammation and mucus within the lungs compared to RSV only (**Figure 4-4B**) at 8 days post-infection. However, KDM6-inhibited BMDC sensitization resulted in reduced inflammation and mucus production compared to vehicle control (**Figure 4-4B**) with a correlative decrease in the expression of pathologic Th2 genes (*Il4, Il5, Il13*) (**Figure 4-4C**). We also observed a decrease in inflammatory innate immune cells (**Figure 4-4D**) as well as neutrophils (**Figure 4-4E**) and activated CD8+ T cells (**Figure 4-4F**) within the lungs of animals given KDM6-inhibited BMDC, correlating with the decreased production of chemokines shown above. These data indicate that BMDC-specific KDM6 activity leads to RSV-driven immunopathology within the lungs consistent with those observed following secondary RSV infections.
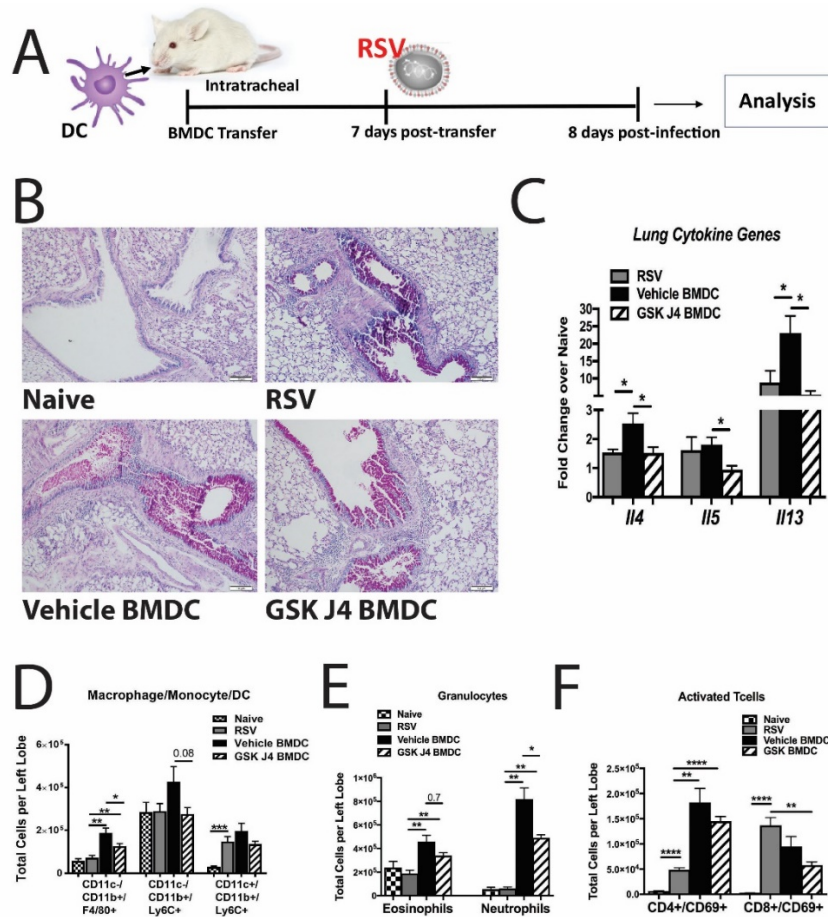
Figure 4- 4. BMDC-induced RSV sensitization is altered by KDM6 inhibition in RSV challenge.
A. DC transfer experimental design **B.** Lungs were embedded in paraffin and Periodic acid-Schiff stain (PAS) was performed to visualize inflammation and mucus (bright pink staining). Representative photos shown. **C.** Lungs were homogenized and mRNA extracted to determine cytokine gene expression compared to naïve controls (N = 5). **D-F**. Lungs were processed into single-cell suspension and stained for flow cytometry analysis. (N = 5). Data represent Mean ± SEM (N = 5 male Balb/c mice/group). * = p < 0.05; ** = p < 0.01; *** = p < 0.001; **** = p < 0.0001.

4.4.5. *In vivo* inhibition of KDM6 alters the immune response to RSV infection

To determine if KDM6 has an immunopathologic role during a primary RSV infection in vivo, Balb/c mice were treated systemically (IP) with GSK J4 (20 mg/kg) daily for 7 days to inhibit KDM6 enzymatic activity (**Figure 4-5A**). Tissues were collected at 8 days post-infection and evaluated for RSV-driven immunopathology. This time point has previously been described in mouse models comparing live viral infection to UV-inactivated RSV control, showing that live RSV is required for activation of the immune response leading to immunopathology, peaking at 8

days post-infection[120,214]. Lung histology showed that KDM6 inhibition resulted in decreased mucus production and inflammation as well as a reduction of bronchus-associated lymphoid tissue (BALT) in the lungs (**Figure 4-5B,C**) with a correlative decrease in mucus score (**Figure 4-5D**) and mucus genes, *gob5* and *muc5ac* (**Figure 4-5E**). Additionally, we observed a decrease in inflammatory CD11c+ DC (CD11b+/MHCII+ and CD11b+/CD86+) and F4/80+ macrophages in the lungs of KDM6-inhibited animals (**Figure 4-5F,G**) with no alteration in eosinophil or neutrophil cell infiltration (**Figure 4-5H**). Furthermore, *in vivo* treatment with GSK J4 led to fewer activated CD4+ T cells within the lungs (**Figure 4-5I**), suggesting a role for KDM6 in the adaptive immune response, likely through altered APC function. Analysis of the cytokine production from RSV re-infected isolated lymph node cells showed reduced IL-13 and IFN-γ in GSK J4-treated mice compared to vehicle control mice (**Figure 4-5J**). Overall, these data show decreased inflammatory responses by inhibiting KDM6 activity, demonstrating a direct link between KDM6 activity and RSV-driven immunopathology.
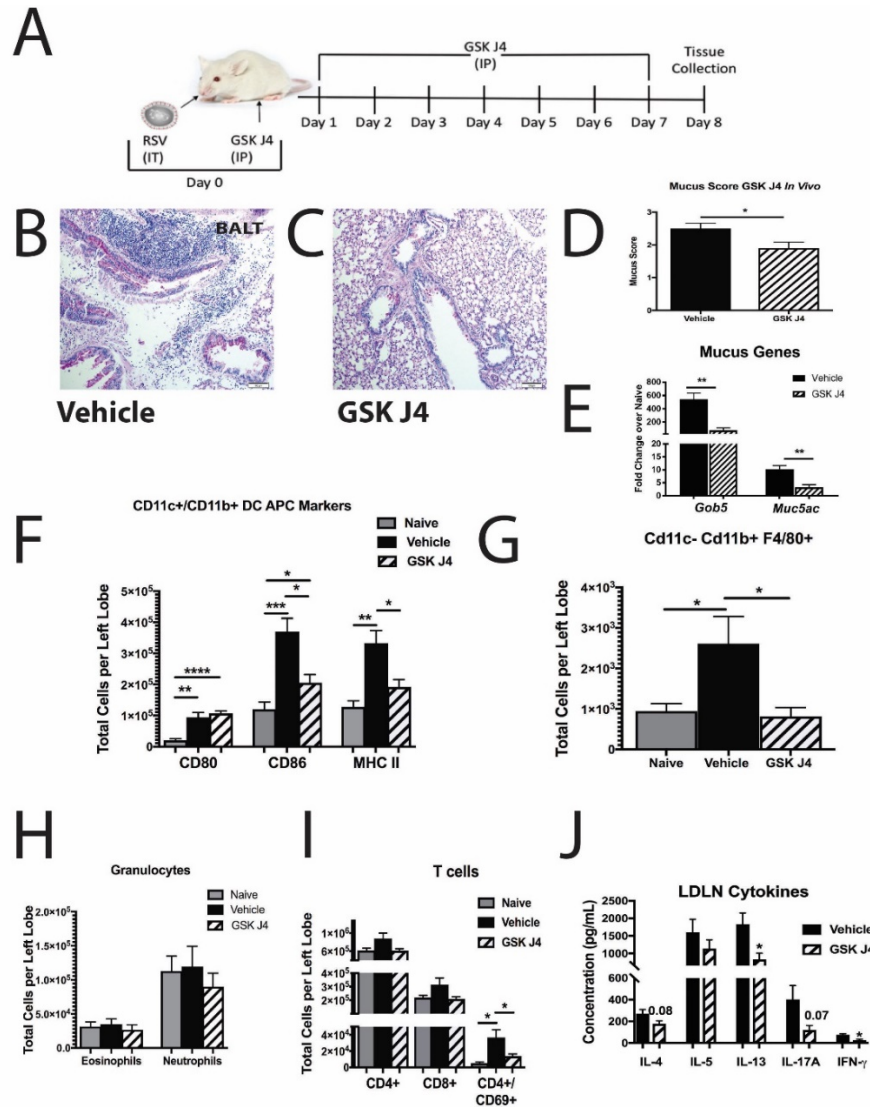
Figure 4- 5. *In vivo* inhibition of KDM6 alters the immune response to RSV infection.
Male Balb/c mice were infected with RSV (2 x 10^5 pfu) and concurrently treated with GSK J4 to inhibit KDM6 enzymatic activity and tissues were harvested at 8 days post-infection. **A**. Experimental design **B,C.** Lungs were embedded in paraffin and Periodic acid-Schiff stain (PAS) was performed to visualize mucus (bright pink staining) and inflammatory infiltrates (blue). Representative photos shown. **D**. Subjective mucus scoring was performed on blinded histological slides on a scale of 1-4 for mucus production (N = 5) **E**. Lungs were homogenized and mRNA extracted to determine mucus gene expression compared to naïve controls (N = 5) **F-I**. Lungs were processed into single-cell suspension and stained for flow cytometry analysis. (N = 5). **J**. Lung draining lymph nodes (LDLN) were processed into single cell suspension and re-infected with RSV *in vitro* for 48 hours to determine cytokine protein levels (N = 5). Data represent Mean ± SEM. Representative of at least 2 independent experiments. * = p < 0.05; ** = p < 0.01; *** = p < 0.001; **** = p < 0.0001.

4.5. Discussion

RSV is an ubiquitous pathogen, infecting nearly all children by the age of two[1,2] and is the second most likely cause of death by a pathogen in infants under the age of one[24]. RSV is characterized by a dysregulated immune response that leads to poor immunologic recall that allows

90

re-infection throughout life. Additionally, clinical data support a link between early life severe RSV infection and the development of airway disease later in life, including asthma[1,3,58,94]. Therefore, elucidation of mechanisms that drive disease is crucial for protection from both primary infection and exacerbated diseases later in life. While epigenetic alterations of DC have been described that change their overall function, including DNA methylation and chromatin modifications, the specific changes during different diseases will require individual investigation. To extend our earlier observations in DC[37,89], we sought to examine the role of specific epigenetic effects on DC-driven mechanisms following RSV infection. These altered innate immune responses are impactful as *in vivo* inhibition of KDM6 enzymes leads to decreased RSV-driven immunopathology. These studies indicate the following novel findings: 1) Upregulation of key epigenetic enzymes, such as KDM6 demethylases, following RSV infection leads to altered APC function, increased pro-inflammatory responses, and immunopathology and 2) targeting specific epigenetic mechanisms that alter inflammatory DC responses may be pivotal for limiting long-term RSV-driven disease pathologies. Thus, an early viral response may specifically "train" innate immune cells leading to long-term phenotypes.

Previous studies have shown that epigenetic modulation directs the differentiation and maturation of immune cells. A key epigenetic gene modifier is H3K27 tri-methylation, which represses gene transcription, and removal of this mark by KDM6 demethylases leads to active gene transcription. Studies have shown that KDM6B can enhance both pro-inflammatory and anti-inflammatory responses by targeting distinct transcription factors, such as NF-kB[137,220,221] in a context-dependent manner in gene promoters[137]. KDM6B can drive M2 polarization via STAT6 activation[222], Th1 cell differentiation via Tbet interaction[223], and support EMT pathways via TGF-β and SMAD3[224]. Additionally, a role has been shown for KDM6A/B in autoimmunity in the

experimental autoimmune encephalomyelitis (EAE) model of multiple sclerosis, with chemical inhibition leading to a tolerogenic DC phenotype and decreased Th1 and Th17 responses[139]. Importantly, the KDM6 family of enzymes has been shown to regulate not only H3K27me3 but also H3K4me deposition through stabilization of the MLL complex[135,136], an H3K4 methyltransferase that deposits activating methylation marks on the histone tail. Studies have shown that the overexpression of KDM6B leads to increased H3K4me3 while leaving H3K27me relatively unchanged[225] similar to our observations of H3K4me3 on CD80/86. Overall our data expand on the inflammatory role for KDM6 in driving pathologic diseases, linking innate cytokine production by inflammatory DC and induction of Th2 cytokines leading to lung immunopathology in RSV infection.

The myeloid/inflammatory DC has been linked to chronic disease that is enhanced and/or exacerbated by RSV[29,89,226]. Our lab has previously observed an upregulation of KDM5B, an H3K4 demethylase, following RSV infection of DCs[37] that contributes to a pathogenic T cell-mediated immune response due to the regulation of critical innate cytokines, especially Type I IFN. While KDM6A/B are upregulated following RSV infection, PolyI:C, a double stranded RNA and TLR3 agonist did not induce KDM6 expression[37]. Interestingly, KDM5B and KDM6 do not appear to regulate the same genes. To evaluate KDM6 targets, inhibition of KDM6 enzymatic activity was accomplished using GSK J4, which has previously been shown to be specific for KDM6 activity[215]. While a study determined minor GSK J4 activity against KDM5 enzymes as well[227], no increase in the level of H3K4me3 on the CD80/86 promoter regions was observed in our data, an expected enzymatic activity if KDM5, a H3K4 demethylase, was inhibited. Furthermore, RSV-infected BMDC with inhibited KDM6 enzymatic function led to decreased APC maturation marker expression (CD80/86 and MHCII) as well as decreased IL-6 along with

chemokines; whereas our previous studies with KDM5B inhibition showed an increase in IL-6 as well as IFN-β with no alteration of APC markers[37]. Importantly, decreased infiltration of inflammatory DC/macrophages into the lung, as well as decreased activation of T cells were observed following inhibition of KDM6 during *in vivo* RSV infection. These latter studies demonstrated that inhibition of KDM6 demethylation led to a reduction of Th2 induced pathology, including development of mucus hypersecretion. These data indicate that the effect of KDM6 activity alters both the innate as well as adaptive immune responses in a related but different mechanism from KDM5B, largely through alteration of APC function. Thus, there appears to be an epigenetic program that controls multiple chromatin modifying enzymes that alters the ability of the immune response to function appropriately during RSV infection.

These studies demonstrate a novel pathway whereby RSV infection leads to upregulation of epigenetic enzymes KDM6A and KDM6B that modify multiple DC functions. These include maturation of APC including costimulatory molecule expression as well as activation of defined chemokines and cytokines responsible for RSV-driven immunopathology (**Figure 4-6**). Inhibition of this activity leads to protection from Th2-driven lung pathogenesis that has been linked both to the exacerbated response following RSV vaccination[228–230] and the enhanced likelihood of asthma development later in life[1,3,58,94]. While these studies focused on DC-driven T cell adaptive responses due to their role in immunopathology, it is likely that the *in vivo* use of GSK J4 blocked multiple responses, including directly modifying macrophages and T cells. Thus, KDM6 may be a therapeutic target that could alter the progression of pathogenic immune responses in the lung during RSV infection and modify the long-term immune environment.
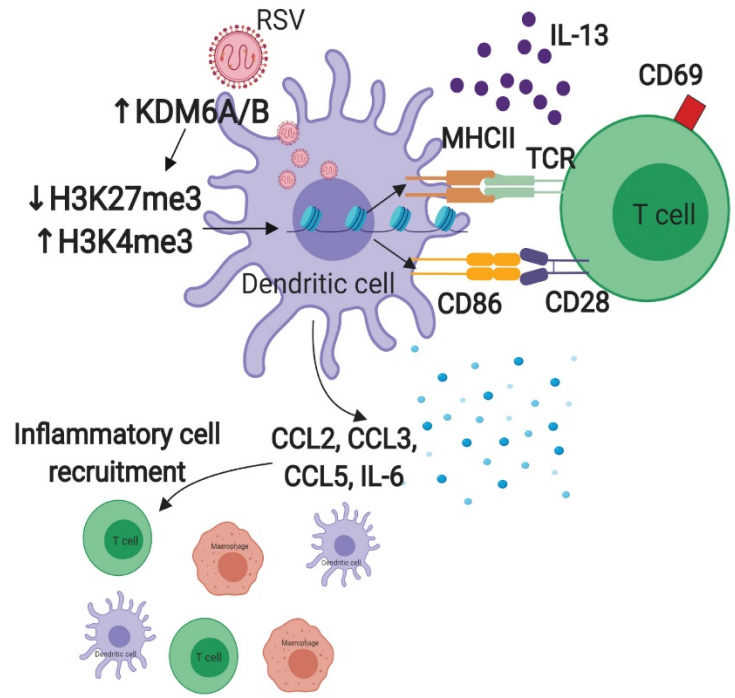
Figure 4- 6. RSV infection leads to upregulation of epigenetic enzymes KDM6A and KDM6B to enhance immunopathology.
Figure created with BioRendor.com

Chapter 5: Discussion and Future Directions

5.1. Sex-Associated Long-term Local Alterations Following Early-life RSV-infection

The studies presented in this dissertation provide novel evidence that correlates with clinical data indicating: 1) Boys are more susceptible to severe RSV than girls and 2) Boys are more likely to develop childhood allergy and asthma than girls. In addition to these findings, we have shown novel results indicating that TSLP has a sex-associated role in RSV-driven allergic exacerbation in males. This expands on data already suggesting that TSLP leads to asthma pathogenesis and correlates with GWAS studies indicating that specific SNPs in TSLP lead to different responses in males vs females; specifically SNP1837253 leads to protection from asthma in boys whereas SNP2289276 leads to enhanced likelihood of asthma development in girls[157]. Collectively, these data indicate clear sex differences in TSLP responses to asthma.

We have shown that upon primary infection with RSV, neonatal female mice are able to clear RSV viral infection faster than males with a correlative increase in IFN-β expression. We also show that males have protracted resolution of the immune response and evidence of persistent inflammation. These data suggest that not only are males more susceptible to the initial viral infection with difficulty clearing the virus but they may also be susceptible to severe disease later in life due to the persistent inflammatory response priming for Th2 responses later in life.

Studies have previously shown that long-term alterations in the lung occur following RSV that include continued mucus expression and inflammatory cell infiltration into the lungs[46,47]. Our data at 4 weeks post-early-life RSV-infection expand upon these findings, with visible mucus within the lungs of male mice, skewing towards Th2, and infiltration of innate immune cells (DC,

ILC2). While we see no significant differences in the number of T cells within the lungs, we do observe strong increases in antigen presenting cells-CD11b+ and CD103+ dendritic cells (DC). The sheer number of inflammatory CD11b+ DC have previously been indicated in leading to severe disease[29,89] as well as exacerbation upon secondary exposures when transferred to the lungs of naïve animals prior to live RSV-infection[37,89]. Additionally, CD103+ DC have been shown to produce strong Th2 responses during RSV and asthma[89,231]. We also see increases in OX-40L+ DC as well as total OX-40L positive cells. TSLP, which is persistently expressed in male mice at 4 weeks post-infection, is responsible for upregulation of OX-40L on DC populations that promote Th2 cell responses[41,112,151]. Also, of note, ILC2 cells have been shown to upregulate OX-40L to interact with T cells to enhance the Th2 response[232,233]; however, IL-33 (also retained at 4 weeks post-infection) was shown to be the driver of this pathway. Whether or not TSLP has the ability to drive this phenomenon is currently unknown.

We determined that these long-term alterations in male mice leave them susceptible to exacerbated allergic responses later in life; characterized by an increased expression of mucus as well as Th2/Th17-skewing when given an early-life RSV infection followed by cockroach allergen (CRA) exposure at 4 weeks post-early-life RSV. No difference in absolute numbers of T cells compared to female mice was observed, but there are differences in T cell responses as indicated by CRA re-stimulated lymph node cytokine production. This may be due to specificity of the T cells in responding to CRA or it could be due to alterations of the antigen presenting cells as there are increases in the number of macrophages, monocytes and DC in the RSV-exacerbated CRA-challenged male mice. Correlating with the data described above at 4 weeks post-infection, we see that the main population affected is the ILC2 population. These data support previous findings that have documented ILC2 as Th2-inducing cells as well as possible drivers of asthma

96

pathogenesis. The specific role that ILC2 have in this response was not determined in these studies; therefore, further analysis of this population through knockdown or genetic reduction/deletion (ST2-/-, RORa^{flox}/IL7R^{Cre}) studies may be necessary. Of important note, we see a similar exacerbated response only in males when CRA challenge is initiated at 12-weeks post-infection (data not shown), indicating that this phenotype is long-lived and well-established.

When TSLP signaling is knocked down, there is a significant reduction in the male exacerbation response. These data correlate with previous findings showing that when TSLP is inhibited during an early-life RSV infection, exacerbation following a second RSV-infection later in life is abrogated[118]. This study found that if TSLP was inhibited during the latter, secondary infection, exacerbation still occurred suggesting that it is the neonatal period that needs to be altered to prevent secondary exacerbations later in life. In our studies, we saw that simply inhibiting TSLP during the allergen challenge phase of the study (without early-life RSV-infection) was not sufficient to protect against allergy development, similar to these findings as well as others, including granuloma development during parasitic helminth responses[161].

As noted above, female mice are capable of upregulating IFN-β much quicker and to a greater extent than male mice, which indicates faster viral clearance and better resolution of the Th2 response. However, this needs further exploration to determine 1) Why/how females produce more IFN-β than males and 2) Whether IFN-β is capable of inhibiting TSLP or vice versa. Interestingly, we also see that TSLPR-/- male mice show a similar phenotype to female mice following neonatal RSV-infection, producing higher levels of IFN-β and quicker viral clearance than do WT male mice (**Appendix 4; Figure A4-1A,B**). These data support the idea that TSLP is regulating production of IFN-β in male mice; however, why TSLP is increased in males (i.e. epigenetic modification, hormonal signaling) needs to be elucidated in this model to enhance these

findings. Since our RNAscope staining indicated that it is the airway epithelial cells that express increased TSLP in RSV-infected male mice, focus on this subset should be maintained for future experiments.

5.2. Long-term Systemic Alterations of BMDC Following Early-life RSV-infection

These studies determined that there are also persistent systemic alterations of BMDC following early-life RSV-infection linked to TSLP signaling. While this is a novel finding, the concept of persistent systemic alterations has been eluded to for quite some time. A vaccine trial in the 1960s with formalin-inactivated RSV led to enhanced disease, including 2 deaths, when vaccinated infants were exposed to live viral infection[25–27]. The details of this phenomenon have been extensively studied and determined that this was largely due to lack of TLR signaling and improper initial response to viral antigen during the vaccination that led to alterations of the immune system and subsequent enhanced immune response upon live infection[228,234,235]. This has been further studied in other models, such as exposures to LPS and *C. albicans*, and has since been termed trained innate immunity[122,126,127]. The studies detailed here show that 1) BMDC populations are persistently altered to remain in a more activated "DC2" state, possibly skewing the BMDC response towards inflammatory rather than tolerant responses upon exposure to allergen and 2) TSLP is at least partially responsible for the skewed activation state in male mice.

BMDC isolated at 4 weeks post-infection from male mice infected neonatally at 7 days of age show significant signs of persistent activation, including upregulation of maturation markers, (CD80/86, OX-40L). The presence of OX-40L is implicated in DC-driven Th2 responses and the concomitant expression of CD80/86 is necessary for optimal OX-40 responses[41,175,236]. The presence of these maturation markers suggest that DC are primed to lead to strong Th2 responses when encountering pathogens or other stimuli. These DC are also continuing to express

inflammatory cytokines/chemokines, even though antigenic stimulation is no longer present, suggesting a shift in transcriptional activation possibly through stabilization of histone or chromatin marks or the increased expression of upstream modifiers, such as transcription factors or histone/DNA modifiers as has been described during trained innate immunity[122,126]. Interestingly, our analysis shows that the epigenetic enzyme, KDM6B continues to be expressed in the BMDC isolated from early-life RSV-infected male mice. KDM6B is a known enhancer of the inflammatory response[134,213,213,220] and has been linked with M2 macrophage polarization[134]. Additionally, studies also show that KDM6 enzymatic activity is required for upregulation of maturation markers such as CD80/86 and plays a role in the expression of the same group of cytokines and chemokines. These data suggest that the continued expression of KDM6B may be allowing for the activation status of these BMDC. We also show increased expression of TSLP and its downstream target, CCL-17. Importantly, it has been reported that CCL-17 is a direct target for KDM6 activity and that the removal of the H3K27me3 mark by KDM6B is required for activation of CCL-17 transcription[237] suggesting a possible link between TSLP signaling, CCL-17 and KDM6B. Additional studies showed that KDM6B demethylase activity is required for the activation of IRF4 which then leads to the upregulation of CCL-17[238]. Of particular note, this same persistent activation does not occur in BMDC isolated from female mice following an early-life RSV-infection which further supports a sex-specific role for long-term alterations following early-life RSV infection with a link to TSLP; however, male/female differences in the BMDC population should be further evaluated.

The presence of TSLP during differentiation of naïve WT BMDC in cell culture led to similar activation and cytokine/chemokine response as the BMDC isolated from early-life RSV infected male mice. Furthermore, the presence of TSLP also led to increased expression of KDM6

enzymes. Additional evaluation was performed using BMDC from TSLPR-/- mice infected during early-life and we observed abrogation of the "activated" phenotype; however, lack of a significant change in KDM6 expression was observed. Therefore, while we've shown that TSLP induces *Kdm6* expression, a lack of TSLP signaling is not sufficient to abolish its upregulation following RSV-infection, which is not surprising since multiple pathways, including NF-$_\kappa$B and JAK/STAT are known to lead to KDM6 activity[137].

ATAC-seq data show significant differences in chromatin landscape between TSLPR-/- and WT BMDC with inherent differences in regions near genes linked with type 1 immunity (*Mid1, Spp1, Cxcl11*) and Th2 responses (*Cxcl1, Cxcl2, Irf4, Areg*) that could lead to better viral control in TSLPR-/- mice while leading to enhanced Th2 disease in WT. BART analysis of genes in differentially accessible regions (DARs) depicted transcription factors linked to Th2 and TSLP-signaling (IRF4, RELA, STAT3)[41,112,170,194–196] as being significant. IRF4 was both a transcription factor linked to accessible genes in the DARs as well a gene itself within the DAR predictions suggested to have more accessible chromatin in WT BMDC. TSLP is known to increase the expression of IRF4 and to regulate similar genes and Th2 responses[170]. However, these data show a novel role for TSLP regulation of IRF4 at the chromatin level in BMDC which could be linked to KDM6B. IRF4 is a target gene of KDM6B[238] and therefore, TSLP-driven expression of KDM6B may lead to the removal of methylation from H3K27 on IRF4 promoter regions leading to more accessible chromatin. Together, this indicates more accessibility to IRF4 target genes as well as more IRF4 available to bind to these regions which could contribute to an accelerated and more pronounced Th2 response.

Further characterization of *Mid1* showed a very strong association for TSLP regulation of type-1 interferon. The levels of *Mid1, Ifnb, and Il112a* are significantly increased in TSLPR-/-

BMDC compared to WT BMDC and upon *in vitro* RSV-infection, TSLPR-/- BMDC have an accelerated type-1 response. Co-culture studies showed that TSLPR-/- BMDC exposed to reactive T cells allow for stronger IFN-γ production than WT BMDC. Together, these data indicate a more appropriate anti-viral response in the absence of TSLP signaling and further strengthen the argument for TSLP/IFN-β regulation. Knockdown experiments targeting *Mid1* and *Ifnb*, especially in TSLPR-/- BMDC, will help to further elucidate this regulation.

Planned RNA-seq experiments on WT and TSLPR-/- BMDC following *in vitro* RSV infection to evaluate initial RSV-infection will lead to further insights into TSLP-driven RSV responses. Additionally, the data here have shown a striking observation of the ability of TSLP to alter the genomic landscape of BMDC populations; however, it will be beneficial to further expand this knowledge to determine if this phenomenon occurs at the progenitor level. Experiments are planned to perform ATAC-seq on the common myeloid progenitor (CMP) cells isolated from WT and TSLPR-/- mice following early-life RSV infection.

5.3. Role of KDM6 Epigenetic Enzymes in RSV-driven Immunopathology

The next set of findings show a novel role for the H3K27 demethylase, KDM6, in enhancing RSV-driven immunopathology. The KDM6 family of enzymes has previously been indicated as an epigenetic enzyme required for fine-tuning the inflammatory response[137,213,220]. Studies from our lab have specifically identified a role for the histone demethylase, KDM5B, in regulation of the immune response to RSV by inhibiting type-1 IFN. To expand upon this knowledge, we further investigated histone demethylases, focusing on KDM6. Findings from these studies determined that 1) KDM6 epigenetic enzymes are upregulated during RSV-infection 2) Inhibition of their activity leads to protection from immunopathology and 3) Targeting DC activity may protect against disease and secondary exacerbations. Similar to the studies described

above in the previous section, these studies show evidence of innate immune cell "training" following RSV-infection.

In these groups of studies, we discovered that RSV infection led to upregulation of KDM6 enzymes in the inflammatory CD11c+ DC population within the lungs as well as BMDC. We utilized the KDM6 inhibitor GSK J4 to inhibit KDM6 enzymatic activity and show that inhibition of this activity leads to a similar phenotype as that observed in TSLPR-/- BMDC, with decreased maturation marker expression and pro-inflammatory cytokine/chemokine expression. Evaluation of ChIP-PCR determined that the decrease in activation marker upregulation was directly linked with increased H3K27me3 (a repressive mark) as well as a decrease in H3K4me3 (an activating mark). These results are supported by previous studies which indicate that KDM6 activity also alters H3K4 methylation[239,240]. In fact, one study determined that the over expression of KDM6B led to very little change in H3K27me3 but significant increases in H3K4me3 that led to specific gene activation. This is likely due to interactions of KDM6 with ASH2L, a component of the MLL complex which deposits the H3K4 methylation mark[241] or its possible interactions with other epigenetic enzymes.

Additional studies determined that alterations of the T cell response to RSV-infected BMDC are diminished when KDM6-inhbited BMDC are exposed to reactive T cells, including decreased production of IL-5, IL-17A and IFN-γ. These data support a role for KDM6 in the overall inflammatory response and are correlated by data presented by Doñas et al[139] that show that DC-specific inhibition by GSK J4 leads to a more tolerogenic DC phenotype with decreased IL-17A and IFN-γ production in a model of experimental autoimmune encephalomyelitis (EAE)[139]. Inflammatory DC are able to lead to enhanced secondary responses when transferred to naïve animals prior to *in vivo* RSV exposure[37,89]. Here, we have recapitulated these data as well

as show that this enhanced response is decreased in KDM6-inhibited BMDC. Specifically, we see significant decreases in inflammatory cell infiltration that correlates with decreased expression of chemokines as seen in KDM6-inhibited BMDC following *in vitro* RSV infection. These data indicate that KDM6 activity plays a role in enhancing secondary RSV infection similar to that seen in vaccine-linked exacerbation[25–27,228,235].

Importantly, *in vivo* treatment with GSK J4 leads to decreased immunopathology and inflammatory cell infiltration into the lung, suggesting that KDM6 activity is crucial for RSV-driven immunopathology. A decrease in infiltration of activated APC into the lungs was observed with GSK J4 treatment, correlating with the above data of KDM6 alteration of APC function. However, the number of activated T cells are also decreased when KDM6 activity is inhibited indicating a role in the adaptive response, whether through APC function or directly related to KDM6 activity on T cells. Studies have shown that KDM6 specifically targets T cells and is responsible for determining T cell differentiation in a tissue dependent manner[242–245]. For example, it was determined that in the colon and lymph node, knockdown of KDM6B led to increased IFN-γ producing Th1 cells but decreases in the small intestine and spleen, and IL-4 producing Th2 cells were increased in the small intestine and colon but unchanged in the spleen and lymph node in the absence of KDM6B[243]. Finally, IL-17 producing Th17 cells were also increased in the small intestine and colon but unchanged in the lymph node[243]. Furthermore, while our studies described here focused on the DC population, we also see alterations in monocytes and macrophages in *in vivo* studies; hence other innate cells may also be affected either through indirect alteration by DC or directly by KDM6 and may require further exploration.

Collectively, these data suggest that KDM6 expression from BMDC leads to activation of DC and induction of chemokines/cytokines necessary for inflammatory cell infiltration into the

lung that ultimately lead to activation of T cells that drive RSV-driven immunopathology. It

should be noted that the activation and pro-inflammatory response is necessary for proper viral

clearance and activation of the immune response; however, the persistence of this response can be

detrimental and lead to immunopathology[7,246–250]. Elucidation of these mechanisms and how they

lead to persistent alterations will be crucial to balance the two and lead to protection from disease.

It is interesting to note that the studies identifying long-term alterations of BMDC

following early-life RSV-infection (**Chapter 3**) show a similar phenotype to that observed in the

presence of KDM6 activity. The long-term alterations following early-life RSV infection also

include KDM6B expression; therefore, it is not unreasonable to conclude that these may be linked.

TSLP and KDM6 both lead to BMDC phenotype linked to persistent activation and we have shown

that TSLP leads to upregulation of KDM6A/B. However, it is critical to point out that knockdown

of TSLP signaling led to an increase in IFN-γ while inhibition of KDM6 activity led to a decrease.

It is likely that they have overlapping as well as distinct roles in these responses; TSLP may be

limiting the anti-viral response while KDM6 is concomitantly contributing to enhanced/persistent

inflammation. When considering treatment options, TSLP may be a better target during early

infection but epigenetic targeting, such as KDM6, may need to be considered later in life, after

immunopathology has been established. This scenario is supported by literature that indicates that

targeting TSLP later in life, after an RSV-infection or during chronic allergy, has minimal

protection against enhanced disease[118,153], suggesting that the window for treatment with anti-

TSLP is narrow. Additionally, targeting epigenetic enzymes such as KDM6 during strong

persistent inflammatory responses has been suggested in other disease, such as cancer[251–254]. To

test this hypothesis, we plan to perform time-course studies. The use of anti-TSLP monoclonal

antibody will be used at multiple time points in neonatal studies, including prior to early-life RSV-

infection, during peak RSV infection (4 days post-infection) at the time of immunopathology development (8 days post-infection) and prior to allergen challenge. Similar studies will be performed using GSK J4 to inhibit KDM6 enzymatic activity in neonatal mice at the same time points. This will help to elucidate when these key players are contributing to RSV disease and to offer insights to be adopted into the clinic.

5.4. Conclusions and Future Studies

Overall, the studies described in this dissertation have determined a novel role for TSLP in the neonatal response to RSV by altering transcriptional and epigenetic pathways of immune cell populations in a sex-dependent manner to persistently alter the immune system. These studies have helped to elucidate why boys may be more susceptible to severe RSV-infection and have more incidences of childhood asthma than do girls and have **identified TSLP as a possibly relevant clinical target, specifically in boys hospitalized due to severe RSV disease**. Importantly, there is a monoclonal TSLP antibody currently being tested in clinical trials in adult asthmatics that could be used for this target. Our data further suggest that the innate immune system can itself lead to strong immunological memory; indicating that targeting innate immune responses should be considered when determining treatment options as well as vaccine development. While the field has made striking discoveries in RSV biology and mechanisms, much more is left to be discovered and studies beyond what have been presented here need to be considered.

We show strong support for the role of TSLP in male-specific pathologies but it will be crucial to determine what is leading to persistent upregulation of TSLP. We have data to suggest that this may be due to decreased ability of males to produce IFN-β. Without type-1 interferon to inhibit TSLP and Th2/Th17 responses, the immune system may essentially "lock" into a Th2 (or Th17)

phenotype. On the other hand, there may be a direct effect on TSLP expression itself through epigenetic mechanisms that lead to the persistent activation of TSLP, such as remodeling and stability of chromatin activation marks/accessibility or the persistence of epigenetic modifiers and/or transcription factors. Finally, it may be a combination of both of these scenarios.

How or why IFN-β is expressed to a greater extent in females than in males needs to be evaluated. A previous study has shown that plasmacytoid DC (pDC) isolated from females produce more IFN-α than do pDC isolated from males[164]. A similar phenomenon has not yet been reported for IFN-β but there is support for this idea. TLR7 and IRAK-1, both found on the X chromosome, have the ability to escape X-inactivation[255,256], and lead to high levels of IFN-β[257–260]. Furthermore, neonatal female infants have significantly higher levels of IRAK-1 in their cord blood compared to male infants[256]. The TLR7/IRAK pathway has also been implicated in Th1-driven autoimmune disease, which is more common in females than males[260–263]. Therefore, RSV stimulation through TLR7 may lead to a stronger IFN-β response in females. Future studies to examine the role of TLR7 could be performed using TLR7 knockout mice. There are multiple chemical inhibitors of the IRAK proteins, including IRAK-1, which could also be used to interrogate this pathway, specifically in female mice. While females are protected from allergic responses following early-life RSV infection, it would be intriguing to evaluate if there is a link between early-life RSV infection in females and increased incidences of autoimmunity. Our studies here have focused on the expression of only IFN-β and cDC populations; interrogating the role of IFN-α and pDC may further enhance these findings and determine what specific IFN subtypes are involved in this model.

Questions also remain about the role of hormones. During childhood, the levels of female hormones (estrogen, progesterone) are nearly equivalent between males and females until

puberty[264,265]. However, testosterone is known to peak and wane throughout childhood to develop male-specific characteristics and the first testosterone peak occurs between 2-4 months of age[265]. Interestingly, clinical data indicate that the infants with the highest likelihood to develop severe RSV disease resulting in hospitalization during peak RSV season are male AND 3-6 months of age[266–269] correlating with this testosterone peak. It might also be interesting to examine a cohort of males hospitalized with severe RSV disease and observe future viral/allergic exacerbations for correlations with testosterone peaks. Additionally, it is known that TLR3/4 stimulation inhibits testosterone signaling and once testosterone dips to a low enough level, Tyro/Axl/Mer (TAM) proteins are produced to downregulate TLR3/4[270,271]. Low level testosterone, as that observed in neonatal males, indicates that TLR3/4 would likely be shut down rapidly to inhibit this signaling and subsequently type-1 IFN. Since RSV signals through TLR3/4, this pathway in males may be inhibiting production of IFN-β. Interrogation of this pathway would be very difficult as it is likely dose-dependent as the incidence of allergy/asthma switches to more predominantly female after puberty. High levels of androgen have been shown to decrease Th2 response[272] while large spikes in estrogen/progesterone are known to lead to Th2 response as well as TSLP induction[273–275] during puberty in females, which may explain this switch of predominance.

Another pathway to consider is androgen/MID1. Studies in castrate-resistant prostate cancer have determined that androgen is a strong inhibitor of MID1 and in the absence of testosterone, MID1 expression is highly increased[276]. Testosterone in the male may be inhibiting the type-1 pathway through inhibition of MID1. We have observed significant differences in the expression of *Mid1* in WT vs TSLPR-/- BMDC isolated from male mice with TSLPR-/- BMDC having higher expression of *Mid1*, suggesting that testosterone alone is not enough to inhibit MID1. It is possible, however, that TSLP is required for testosterone to inhibit MID1. Studies have shown that

testosterone upregulates HIF-1α[277] and HIF-1α, which is induced during RSV-infection, leads to the expression of TSLP[278,279]. Therefore, a reasonable scenario is that during RSV infection, HIF-1α is expressed to a greater extent in male mice due to the presence of testosterone that leads to increased expression of TSLP and TSLP then targets MID1 for inhibition. HIF-1α also has the ability to increase production of testosterone[280], suggesting that this could lead to a continuous positive feedback loop. Additionally, HIF-1α targets KDM6B, which is also persistently expressed in BMDC from early-life RSV-infected male mice, further supporting a role for its involvement in these responses. HIF-1α inhibitors have been developed as well as HIF-1α flox/Cre mouse systems that could be used to elucidate this pathway which would have an impact on multiple fields of study.

Our data described in these studies as well as the differences in TLR signaling between males and females suggest that sex of the infant should be considered when determining treatment options during RSV infection and vaccine development. For instance, knockdown of TSLP signaling had no additional protection in the early-life RSV-infected female mice when exposed to allergen; therefore, whether this treatment would be beneficial in treating females in not clear. Additionally, since the 1960s vaccine trial failure was attributed to improper TLR signaling following vaccination[228,234,235], TLR-specific adjuvants should be considered for successful RSV vaccine development. However, different TLR adjuvants may be needed dependent on sex of the infant; a TLR7 adjuvant may lead to increased likelihood of autoimmune disease in females while TLR3/4 adjuvant in males be unsuccessful due to increased inhibition by testosterone and/or deleterious effects on testosterone signaling.

In addition to the studies detailed in this dissertation, we have evidence that early-life RSV-infection also leads to lung remodeling that may negatively impact lung function later in life.

Airway remodeling, including fibrotic deposition, is a hallmark symptom of asthma[281] and RSV-infection has previously been suggested to lead to fibrosis and collagen deposition[93]. ILC2 production of amphiregulin (Areg), while necessary for lung repair following epithelial injury, may lead to lung fibrosis[75,282,283] and DC-specific AREG is linked to ILC2-driven inflammation/fibrotic responses[284]. Studies with TSLP have indicated that it is required for initiation/persistence of airway remodeling during chronic allergy[285], that may or may not be directly immune-related. It is interesting to note that we see increased CD45+ cells in lungs isolated at 4 weeks post-infection from early-life RSV-infected male mice (**Appendix 4; Figure 4-2A-C**) that correlates with increased DC and ILC2 shown in **Figure 2-4**, whereas TSLPR-/- mice appear more like naive (**Appendix 4; Figure 4-2A-C**). Furthermore, *Areg* was a predicted DAR gene in WT BMDC suggesting a role for TSLP in this pathway that will be further evaluated. Remodeling is also directly linked to a decrease in lung function during pulmonary function tests (PFT)[286,287]. At 4 weeks post-early-life RSV-infection, we performed PFT and observed significant defects in measured parameters consistent with decreased lung function (**Appendix 4; Figure A4-3A-D**). These data correlate with clinical data as well as that which is seen during bleomycin treatment and the fibrotic response[288–290].

Airway simplification may also occur following RSV-infection and is another hallmark of childhood pulmonary pathologies[291] that leads to either physically larger airways or less elasticity in the airways causing a "floppy" lung or a lung that is unable to inflate/deflate properly. To evaluate airway simplification, we observed the distal airways in histological slides and found that early-life RSV-infected male lungs have a simplified appearance compared to naïve age-matched controls and TSLPR-/- mice (**Appendix 4; Figure A4-4A**). The Wellik lab determined that expression of HOX genes were crucial for proper lung development during the neonatal period

and that knockout of these genes leads to lung simplification[292]. Evaluation of HOX5 genes (*Hox5a/b*) showed that WT early-life RSV-infected male mice have slightly decreased HOX expression (~30%) compared to naïve and that lack of TSLP signaling rescues this expression (**Appendix 4; Figure 4-4B**). While these are exciting preliminary findings, much more work needs to be done to verify these phenotypes and determine the mechanism of how RSV and TSLP could be altering lung development.

In conclusion, the studies described in this dissertation have elucidated novel and exciting aspects of RSV-driven immunopathology and suggest that it is imperative to consider sex differences in neonates as well as the innate immune system during RSV disease. To our knowledge, this is the first time that a sex-specific role for TSLP has been shown as well as a link between TSLP regulation of IFN-β and MID1 pathway during RSV-infection (**Figure 5-1**). These studies have also led to unanswered questions that may be more thoroughly explored to further increase our knowledge and understanding of RSV. Hopefully, together with other published literature, this will ultimately lead to better treatment options and the development of a successful vaccine candidate which will not only decrease RSV burden but will also limit the development of childhood asthma, the number one chronic childhood illness.
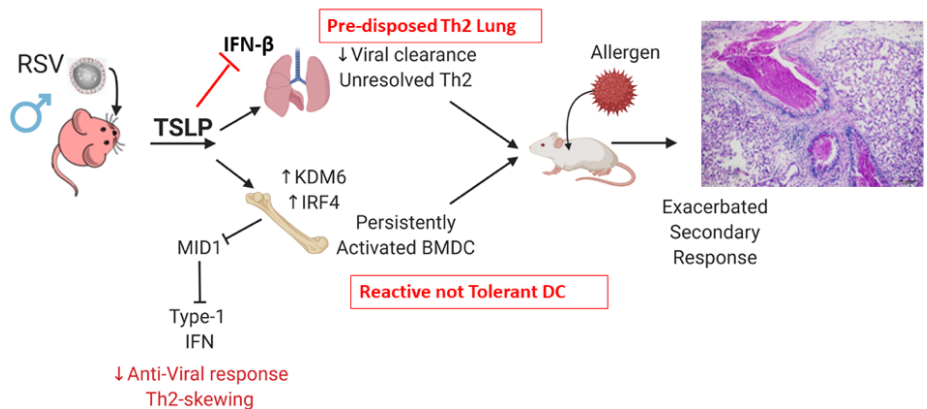
Figure 5- 1. Proposed model of TSLP-driven immune alterations leading to enhanced allergic response in male mice following early-life RSV-infection.
Figure created with BioRendor.com

Appendix 1: Chapter 2 Supplemental Figures
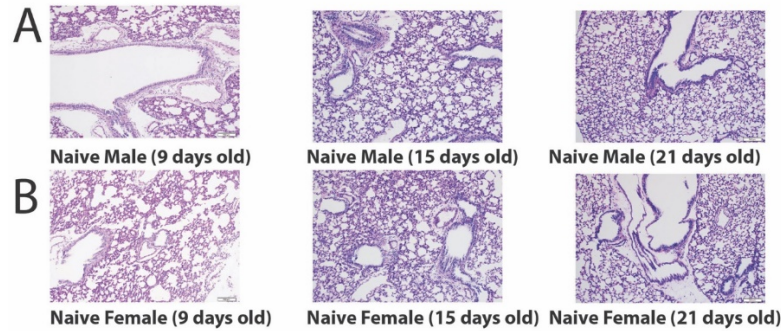
Figure A1- 1. Naïve neonatal male and female mice have similar local lung environment.
Tissues were collected from age-matched male and female uninfected mice at the time of 2 (9 days old), 8 (15 days old), and 14 (21 days old) day post-infection analysis for infected mice. **A,B**. Lungs were embedded in paraffin and Periodic acid-Schiff stain (PAS) was performed. Representative photos shown
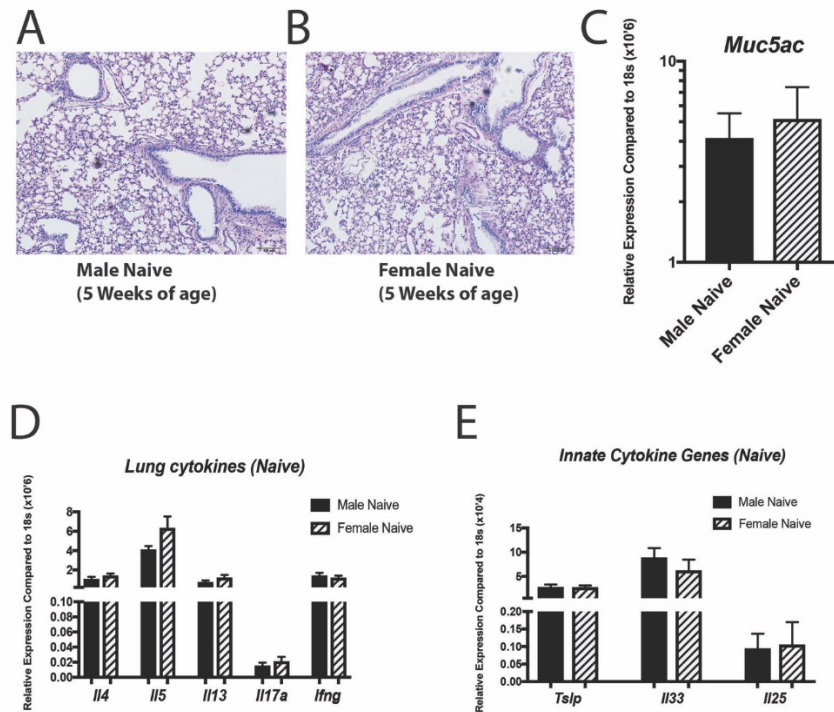
Figure A1- 2. Naïve male and female mice have similar local lung environment at 5 weeks of age.
Tissues were collected from 5 week old male and female uninfected mice at the time of 4 week post-infection analysis for infected mice. **A,B**. Lungs were embedded in paraffin and Periodic acid-Schiff stain (PAS) was performed. Representative photos shown **C-E.** Lungs were homogenized and mRNA extracted to determine relative gene expression compared to 18s housekeeping gene (N = ≥ 3). Data represent Mean ± SEM (2 individual experiments)
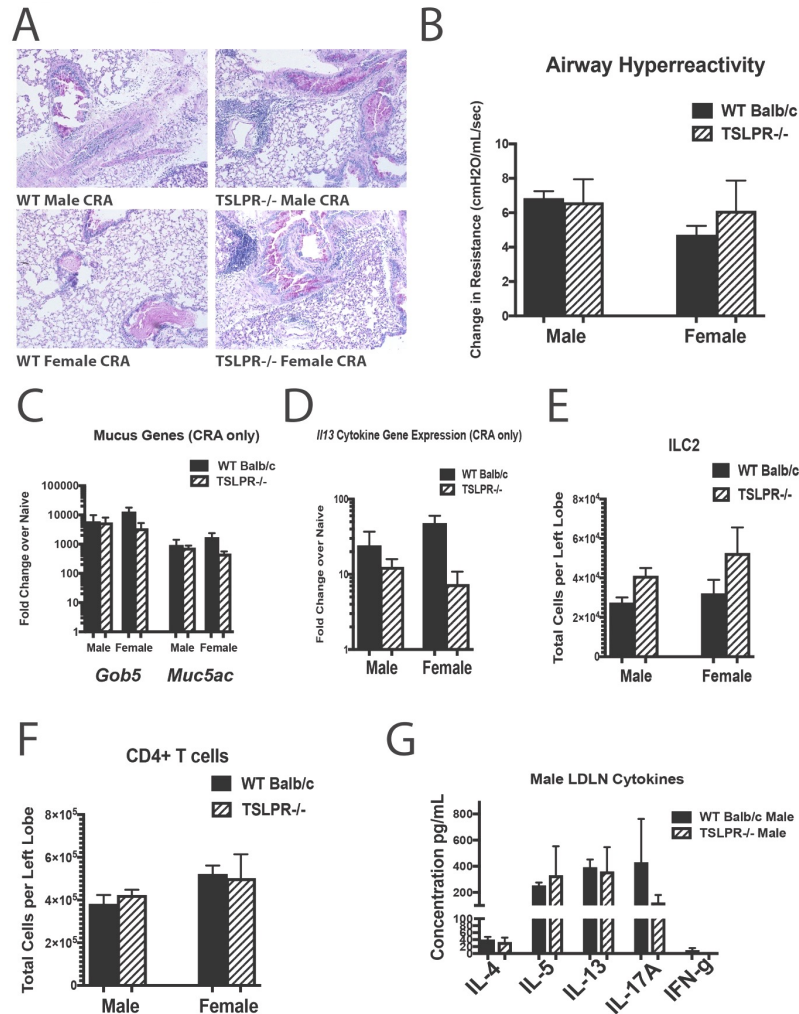
Figure A1- 3. No significant differences are observed in male and female WT or TSLPR-/- mice following CRA challenge alone.

Male and Female WT and TSLPR-/- mice were exposed to CRA allergen challenge at 5 weeks of age (initiated at the time of 4 weeks post-infection for RSV/CRA animals). **A**. Lungs were embedded in paraffin and Periodic acid-Schiff stain (PAS) was performed to visualize mucus (bright pink staining). Representative photos shown **B**. AHR was determined using full-body plethysmography and methacholine challenge (N $\geq$ 3) **C, D**. Lungs were homogenized and mRNA extracted to determine mucus and cytokine gene expression (N $\geq$ 3) **E, F**. Lungs were processed into single-cell suspension and stained for flow cytometry analysis. (N $\geq$ 7) **G**. Lung draining lymph nodes in single cell suspension were re-stimulated with CRA *in vitro* for 48 hours to determine cytokine protein levels (N$\geq$ 3). Data represent Mean $\pm$ SEM (2-3 individual experiments)

Appendix 2: Chapter 3 Supplemental Figures and Tables

Co-Culture
(T-cells from RSV-infected WT Mice)
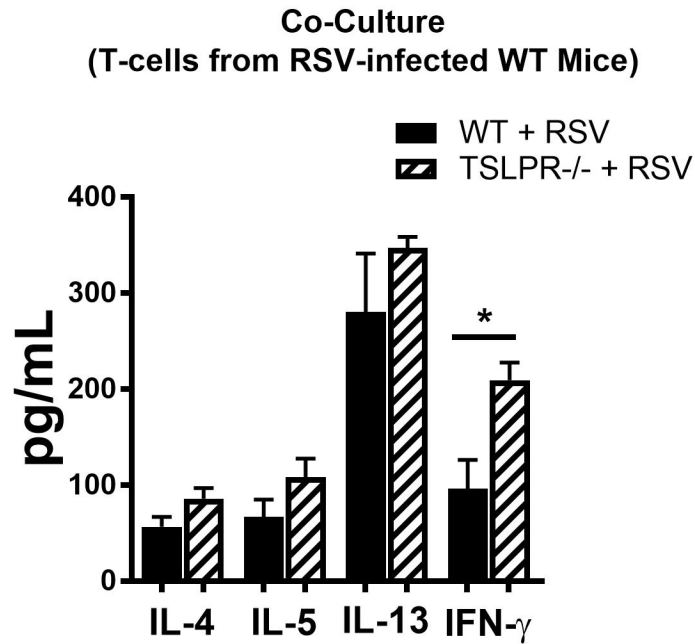
Figure A2- 1. Lack of TSLP signaling in BMDC increases T cell production of IFN-γ.
RSV-infected DC co-cultured with CD4+ T cells isolated from the lymph nodes of RSV-infected mice at 8 days post-infection. Supernatant collected and protein concentration analyzed using Bio-Plex. Data represent Mean ± SEM (N = 3). * = p < 0.05.

Table A 1. DAR predicted gene hits.

seqnames	log2(Fold Change)	p.value	FDR	gene
chr5	7.06	8.4E-118	2.0E-113	Crlf2
chr5	4.95	3.11E-43	3.74E-39	Galnt9
chr5	2.99	6.15E-42	4.94E-38	Arhgap24
chr4	2.78	4.67E-16	9.38E-13	Zfp981
chr5	2.47	6.51E-26	2.24E-22	Pitpnb
chr5	2.09	9.04E-42	5.44E-38	Crlf2
MG4310_MG4311_PATCH	2.05	3.35E-17	8.07E-14	
chr4	1.93	2.65E-10	2.90E-07	Zfp981
chr1	1.67	2.74E-16	6.00E-13	Epha4
chr5	1.64	2.17E-19	5.80E-16	Arhgap24
chr6	1.6	1.33E-10	1.52E-07	Mir7661
chr4	1.57	2.82E-13	4.24E-10	Zfp985
chr5	1.39	2.99E-10	3.13E-07	Aff1
chr4	1.34	4.94E-09	4.25E-06	Zfp985
chr5	1.32	4.44E-13	5.94E-10	Cops4
chr9	1.27	1.29E-07	7.39E-05	Rwdd2a
chr5	1.26	1.02E-09	9.84E-07	Arhgap24
chr15	1.22	3.27E-07	0.000144	Oxr1
chr4	1.22	2.16E-06	0.000592	Ptprd
chr9	1.19	1.33E-08	1.07E-05	Rwdd2a
chr2	1.19	1.69E-07	9.06E-05	Olfr1258
chr2	1.17	8.56E-07	0.000286	Kif16bos
chr4	1.12	2.97E-06	0.000777	Zfp985
chr17	1.11	1.52E-05	0.00265	Kcng3
chr13	1.08	1.50E-08	1.17E-05	1700006H21Rik

chr5	**1.08**	2.04E-06	0.000579	1700028D13Rik
chr8	**1.08**	9.59E-06	0.00192	Gpat4
chr9	**1.08**	1.53E-05	0.00265	Gm4668
chr15	**1.07**	5.55E-08	3.61E-05	2610037D02Rik
chr14	**1.06**	0.000114	0.00989	Tspan14
chr5	**1.04**	9.99E-08	6.01E-05	Galnt9
chr15	**1.04**	1.44E-05	0.00259	4930430F21Rik
chrX	**1.03**	2.85E-09	2.64E-06	Tfe3
chr6	**1.03**	8.56E-07	0.000286	Trpv6
chr18	**1.02**	7.13E-07	0.00026	Mir1901
chr15	**1.02**	5.19E-05	0.00585	Tmem74
chr5	**1.01**	2.86E-06	0.000758	Cxcl1
chr10	**1**	6.43E-09	5.34E-06	Frk
chr6	**1**	1.48E-07	8.13E-05	4930511A08Rik
chr5	**1**	2.28E-05	0.00355	Arhgap24
chr2	**0.99**	8.00E-07	0.000275	Sdcbp2
chrX	**0.99**	3.10E-06	0.000804	Tgif2lx2
chrX	**0.98**	1.17E-13	1.88E-10	Tfe3
chr3	**0.98**	4.60E-07	0.000182	Gm5148
chr12	**0.98**	6.40E-07	0.000245	Vash1
chr10	**0.98**	7.29E-07	0.000261	Rfpl4b
chr3	**0.97**	4.99E-08	3.34E-05	Gm29811
chr5	**0.96**	1.98E-06	0.000568	Tmem60
chr5	**0.96**	6.52E-05	0.00686	Gm10354
chr4	**0.96**	0.000142	0.0114	Zfp985
chr1	**0.94**	2.83E-07	0.000131	Rdh10
chr12	**0.93**	1.01E-05	0.00199	Galc
chr12	**0.93**	3.14E-05	0.00445	Zc3h14

chr5	**0.93**	0.000487	0.0236	Cpeb2
chrX	**0.92**	3.80E-05	0.00485	Nap1l3
chr5	**0.91**	4.21E-08	2.90E-05	Rasgef1b
chr7	**0.91**	1.80E-06	0.000527	Tead1
chr15	**0.91**	9.45E-05	0.00879	Khdrbs3
chr5	**0.91**	0.000125	0.0105	Galnt11
chr2	**0.9**	1.17E-06	0.000376	1700021F07Rik
chr14	**0.9**	4.40E-06	0.00103	Blk
chr18	**0.89**	2.19E-07	0.000108	4930426D05Rik
chr2	**0.89**	2.65E-07	0.000125	Olfr1258
chr8	**0.89**	9.25E-06	0.00189	AW046200
chr6	**0.89**	1.70E-05	0.00284	Pdzrn3
chr1	**0.89**	0.000558	0.0255	Rgs18
chr14	**0.88**	1.02E-07	6.01E-05	Pcca
chr10	**0.88**	3.40E-06	0.00086	Syt1
chr16	**0.88**	4.82E-06	0.00107	Ltn1
chr10	**0.88**	2.46E-05	0.00368	Cabcoco1
chr18	**0.88**	6.53E-05	0.00686	Mir6356
chr9	**0.88**	0.000216	0.0141	Gm32014
chr18	**0.87**	1.48E-07	8.13E-05	Lyzl1
chr5	**0.87**	3.68E-05	0.0048	Lin54
chr4	**0.87**	0.000182	0.0131	Acot7
chr1	**0.87**	0.000284	0.0168	Ercc5
chr5	**0.87**	0.000857	0.0325	Igfbp7
chr5	**0.86**	9.08E-06	0.00187	Cdc7
chrX	**0.86**	9.52E-06	0.00192	Klhl34
chr1	**0.85**	6.28E-07	0.000244	Brinp3
chr18	**0.85**	7.63E-07	0.000266	Arhgap26

116

chr12	**0.85**	6.42E-06	0.00136	Rapgef5
chr2	**0.85**	7.07E-05	0.00724	Trp53rkb
chr6	**0.85**	0.000187	0.0134	Eps8
chr5	**0.84**	1.63E-06	0.000497	Gm7854
chr2	**0.84**	3.46E-06	0.00086	Vapb
chr14	**0.84**	4.70E-06	0.00106	Tbc1d4
chr5	**0.84**	3.57E-05	0.00473	Rasl11b
chrX	**0.84**	4.21E-05	0.00512	Ndp
chr4	**0.84**	5.46E-05	0.00609	Usp24
chr12	**0.83**	2.01E-07	0.000104	Etv1
chr1	**0.83**	4.50E-07	0.000182	Lancl1
chr18	**0.83**	1.71E-06	0.000514	Mir1901
chr10	**0.83**	1.24E-05	0.00238	4921513I03Rik
chr11	**0.83**	5.91E-05	0.0065	Itgb3
chr3	**0.83**	6.39E-05	0.00684	Odf2l
chr6	**0.82**	2.13E-07	0.000107	Bmt2
chr5	**0.82**	6.55E-07	0.000246	9630001P10Rik
chr10	**0.82**	2.62E-06	0.000702	Ccdc59
chr4	**0.82**	3.69E-06	0.000907	Mpdz
chr5	**0.82**	4.12E-06	0.000994	Bmp2k
chr13	**0.82**	1.29E-05	0.00242	Edil3
chr3	**0.82**	3.06E-05	0.00437	Veph1
chr16	**0.82**	1.00E-04	0.00913	Myh15
chr17	**0.82**	0.000325	0.0181	Rftn1
chr13	**0.82**	0.000564	0.0256	Glrx
chr19	**0.81**	7.01E-07	0.00026	Mir3970
chr8	**0.81**	5.07E-06	0.00111	Rasd2
chr2	**0.81**	1.84E-05	0.00299	Bcas1os2

chr2	**0.81**	8.06E-05	0.00783	Dut
chr15	**0.81**	0.000147	0.0116	Dab2
chr5	**0.81**	0.000206	0.0139	Areg
chr5	**0.81**	6.00E-04	0.0267	Tmprss11a
chr8	**0.81**	0.00153	0.0431	4930488L21Rik
chr5	**0.8**	7.66E-08	4.86E-05	Antxr2
chr2	**0.8**	1.09E-05	0.00212	Wipf1
chr14	**0.8**	3.39E-05	0.00463	Tdrd3
chr4	**0.8**	4.06E-05	0.005	Triqk
chr9	**0.8**	0.000145	0.0115	Tmem108
chr6	**0.8**	0.000276	0.0166	4930515G16Rik
chr1	**0.8**	0.000428	0.0215	Mir5126
chr6	**0.8**	0.00147	0.0426	Aebp2
chr13	**0.8**	0.00154	0.0431	Mfsd14b
chr7	**0.79**	1.43E-06	0.000447	Nucb2
chr5	**0.79**	1.90E-06	0.000551	Dthd1
chr3	**0.79**	0.000199	0.0137	Atp1a1
chr11	**0.79**	0.00023	0.0148	4933427E13Rik
chr2	**0.79**	0.000316	0.0178	Taf4
chr6	**0.79**	0.000354	0.019	Suclg1
chr12	**0.79**	0.000393	0.0204	Lrrn3
chr17	**0.79**	0.000721	0.0292	2410021H03Rik
chr18	**0.79**	0.00114	0.0371	Mbp
chr16	**0.78**	2.13E-06	0.000589	Myh15
chr1	**0.78**	2.25E-06	0.000609	Rcsd1
chr3	**0.78**	3.43E-06	0.00086	Gyg
chr4	**0.78**	3.49E-05	0.00469	Slc46a2
chr5	**0.78**	3.54E-05	0.00471	Cxcl2

chr16	**0.78**	0.000176	0.0129	D16Ertd519e
chr9	**0.78**	0.00031	0.0177	Bmper
chr4	**0.78**	0.0012	0.0382	Ttc39b
chr15	**0.77**	9.81E-10	9.84E-07	Tnfrsf11b
chr18	**0.77**	4.28E-06	0.00101	Fam69c
chr2	**0.77**	4.68E-06	0.00106	Arhgap21
chr2	**0.77**	1.36E-05	0.00249	Mir7002
chr6	**0.77**	2.90E-05	0.00423	1700049E22Rik
chr1	**0.77**	3.47E-05	0.00469	Aim2
chr1	**0.77**	5.00E-05	0.00576	Diexf
chr17	**0.77**	5.62E-05	0.00624	Cd2ap
chr18	**0.77**	9.93E-05	0.00908	Zfp608
chr9	**0.77**	0.000253	0.0158	Tmem108
chr14	**0.77**	0.000281	0.0168	Cacna2d3
chr2	**0.77**	0.000376	0.0198	Nmi
chr13	**0.76**	9.92E-06	0.00196	Rala
chr15	**0.76**	1.93E-05	0.00306	Mroh2b
chr3	**0.76**	4.10E-05	0.00501	Gm29811
chr17	**0.76**	7.85E-05	0.00769	Slc8a1
chr9	**0.76**	9.49E-05	0.00879	Slc9a9
chr2	**0.76**	0.000102	0.00916	4921531C22Rik
chr8	**0.76**	0.000135	0.0111	Mir3108
chr1	**0.76**	0.000145	0.0115	Efcab2
chr6	**0.76**	0.000153	0.0118	St8sia1
chr5	**0.76**	0.000165	0.0125	Scarb2
chr17	**0.76**	0.000223	0.0145	Zfp36l2
chr2	**0.76**	0.000349	0.0188	Ttc17
chr12	**0.76**	0.000399	0.0206	Ywhaq

chr10	**0.76**	0.00147	0.0426	Ipcef1
chr4	**0.76**	0.00152	0.0431	A530072M11Rik
chr10	**0.76**	0.00193	0.0479	Ncoa7
chr12	**0.75**	1.78E-08	1.30E-05	Gm35725
chr8	**0.75**	4.57E-07	0.000182	AW046200
chr17	**0.75**	2.10E-06	0.000588	Rab5a
chr7	**0.75**	5.82E-05	0.00643	AI987944
chr18	**0.75**	6.27E-05	0.0068	Ppp2r2b
chr18	**0.75**	9.25E-05	0.00864	Fzd8
chr18	**0.75**	0.000131	0.0109	B4galt6
chr2	**0.75**	0.000139	0.0112	Bcas1os2
chr12	**0.75**	0.000271	0.0165	Etv1
chr4	**0.75**	0.000273	0.0165	Osbpl9
chr2	**0.75**	0.000376	0.0198	Stk39
chr16	**0.75**	0.000378	0.0198	Tigit
chr15	**0.75**	0.000412	0.0209	Rpl37
chr3	**0.75**	0.00105	0.0358	Mir466q
chr1	**0.74**	2.33E-07	0.000112	1810006J02Rik
chr10	**0.74**	1.04E-06	0.000339	Esr1
chr14	**0.74**	1.64E-05	0.0028	Abcc4
chr2	**0.74**	2.37E-05	0.00361	Bcas1os2
chr2	**0.74**	2.50E-05	0.00372	Cdh4
chr16	**0.74**	3.51E-05	0.00469	St3gal6
chr18	**0.74**	4.84E-05	0.00569	Chsy3
chr2	**0.74**	5.04E-05	0.00576	Kif16b
chr8	**0.74**	6.27E-05	0.0068	Efnb2
chr18	**0.74**	0.000181	0.0131	Nr3c1
chr5	**0.74**	0.000205	0.0139	Dpp6

chr12	**0.74**	0.000466	0.0227	Gpr65
chr3	**0.73**	1.22E-06	0.000386	Agtr1b
chr18	**0.73**	2.94E-05	0.00424	Mppe1
chr14	**0.73**	5.00E-05	0.00576	Mir6390
chr14	**0.73**	6.55E-05	0.00686	Klf5
chr18	**0.73**	8.47E-05	0.00806	2210409D07Rik
chr4	**0.73**	0.000102	0.00914	Dhrs3
chr3	**0.73**	0.000125	0.0105	Col24a1
chr10	**0.73**	0.000269	0.0165	Gm29685
chr7	**0.73**	0.000292	0.017	Gm4971
chr3	**0.73**	0.000324	0.0181	Il12a
chr2	**0.73**	0.000748	0.0297	Slc24a3
chr13	**0.73**	0.000895	0.033	Actn2
chr7	**0.73**	0.000968	0.0344	Ptpre
chr12	**0.73**	0.00126	0.0394	Fut8
chr3	**0.73**	0.0015	0.0428	Selenof
chr18	**0.73**	0.00159	0.044	Colec12
chr1	**0.73**	0.00181	0.0469	Dock10
chr18	**0.72**	4.62E-06	0.00106	Rab18
chr2	**0.72**	6.06E-06	0.00129	Arhgap21
chrX	**0.72**	1.27E-05	0.0024	Spin4
chr1	**0.72**	1.29E-05	0.00242	Prg4
chr6	**0.72**	1.51E-05	0.00265	Edem1
chr12	**0.72**	1.57E-05	0.0027	Sp8
chr1	**0.72**	3.96E-05	0.005	Irf6
chr12	**0.72**	7.24E-05	0.00739	Lrfn5
chr15	**0.72**	7.74E-05	0.00761	1700084J12Rik
chr17	**0.72**	0.000105	0.0093	Epb41l3

chr5	**0.72**	0.000108	0.00953	Cxcl13
chr5	**0.72**	0.000115	0.00991	Arhgap24
chr18	**0.72**	0.000125	0.0105	Mkx
chr7	**0.72**	0.000185	0.0132	Fam196a
chr3	**0.72**	0.00022	0.0143	Rxfp1
chr5	**0.72**	0.000299	0.0172	Lrrc8d
chr8	**0.72**	0.000326	0.0181	Naf1
chr15	**0.72**	0.000332	0.0182	Trio
chr18	**0.72**	0.000366	0.0194	Dmxl1
chrY	**0.72**	0.000422	0.0213	Gm20871
chr1	**0.72**	0.000703	0.029	Tnfrsf11a
chr16	**0.72**	0.000735	0.0295	Mb21d2
chr7	**0.72**	0.00123	0.0387	Slco3a1
chr15	**0.72**	0.00169	0.0454	Gm20740
chr7	**0.71**	1.57E-06	0.000486	Xylt1
chr18	**0.71**	1.80E-05	0.00295	Setbp1
chr5	**0.71**	2.45E-05	0.00368	Hsd17b13
chr6	**0.71**	2.52E-05	0.00372	Hpgds
chr14	**0.71**	3.69E-05	0.0048	1700100I10Rik
chr12	**0.71**	3.72E-05	0.0048	Dhrs7
chr9	**0.71**	3.74E-05	0.0048	Tpbg
chr12	**0.71**	4.66E-05	0.00554	Eml1
chr14	**0.71**	5.15E-05	0.00585	Ggact
chr3	**0.71**	6.94E-05	0.00718	Cyr61
chr2	**0.71**	7.34E-05	0.00741	Otor
chr13	**0.71**	7.52E-05	0.00749	Irf4
chr1	**0.71**	8.30E-05	0.00798	Khdc1b
chr19	**0.71**	0.000106	0.00939	Sorbs1

chr1	**0.71**	0.000117	0.01	Col19a1
chr3	**0.71**	0.000138	0.0112	4930406D18Rik
chr3	**0.71**	0.000287	0.0168	A830029E22Rik
chr8	**0.71**	0.000314	0.0178	Mir21c
chr2	**0.71**	0.000497	0.0238	Fermt1
chr15	**0.71**	0.000501	0.0239	Npr3
chr5	**0.71**	0.00059	0.0265	Clnk
chrX	**0.71**	0.000631	0.0274	Cysltr1
chr3	**0.71**	0.000806	0.0312	Platr4
chr4	**0.71**	0.00108	0.0361	Adamtsl1
chr5	**0.71**	0.00189	0.0477	Arhgap24
chr18	**0.7**	8.47E-06	0.00176	Setbp1
chr13	**0.7**	3.23E-05	0.0045	Gm3604
chr12	**0.7**	3.75E-05	0.0048	Mir669c
chr18	**0.7**	8.94E-05	0.00845	Chsy3
chr5	**0.7**	0.000104	0.00929	Abcb1b
chr16	**0.7**	0.00015	0.0117	Mir691
chr15	**0.7**	0.000173	0.0128	Tnfrsf11b
chr7	**0.7**	0.000205	0.0139	5830432E09Rik
chr17	**0.7**	0.000215	0.0141	L3mbtl4
chr14	**0.7**	0.00024	0.0152	Slc4a7
chr1	**0.7**	0.000266	0.0164	Rgs18
chr9	**0.7**	0.000285	0.0168	Tgfbr2
chr17	**0.7**	0.000315	0.0178	Ston1
chr7	**0.7**	0.000517	0.0243	Tlnrd1
chr6	**0.7**	0.000544	0.0252	Ccser1
chr11	**0.7**	0.000633	0.0274	F930015N05Rik
chr9	**0.7**	0.00161	0.0442	Stac

chr1	**0.69**	2.02E-07	0.000104	Hhat
chr6	**0.69**	3.25E-07	0.000144	Fam3c
chr10	**0.69**	3.29E-07	0.000144	Nup37
chr17	**0.69**	1.93E-05	0.00306	Xdh
chr1	**0.69**	7.64E-05	0.00754	Nenf
chr15	**0.69**	0.000157	0.012	Trio
chr1	**0.69**	0.000158	0.012	Mir205
chr5	**0.69**	0.000193	0.0135	Mir703
chr6	**0.69**	0.000201	0.0138	Ergic2
chr5	**0.69**	0.000214	0.0141	Tmprss11c
chr18	**0.69**	0.000251	0.0158	Pcdh12
chr18	**0.69**	0.000711	0.0292	AW554918
chr1	**0.69**	0.00118	0.0379	9130227L01Rik
chr17	**0.69**	0.00134	0.0405	Gm9805
chr5	**0.69**	0.00149	0.0428	Speer8-ps1
chr9	**0.69**	0.0015	0.0428	Zc3h12c
chr9	**0.69**	0.00171	0.0456	Tgfbr2
chr16	**0.69**	0.00192	0.0477	Gm15713
chr18	**0.68**	7.37E-07	0.000261	Mir5127
chr18	**0.68**	2.66E-05	0.00391	Ss18
chr18	**0.68**	4.05E-05	0.005	4930445N18Rik
chr16	**0.68**	4.37E-05	0.00529	Ncam2
chr2	**0.68**	4.94E-05	0.00576	9130015L21Rik
chr12	**0.68**	0.000114	0.00989	Wdr25
chr2	**0.68**	0.000129	0.0108	Slc24a5
chr8	**0.68**	0.000137	0.0112	Sall1
chr17	**0.68**	0.000214	0.0141	Gm20491
chr15	**0.68**	0.000324	0.0181	Khdrbs3

chr				
chr5	**0.68**	0.000328	0.0181	Cpeb2
chr18	**0.68**	0.000388	0.0202	Megf10
chr16	**0.68**	0.000445	0.0222	St3gal6
chr14	**0.68**	0.000496	0.0238	Dpysl2
chr13	**0.68**	0.000604	0.0267	Lhfpl2
chrX	**0.68**	0.000685	0.0285	Phex
chr7	**0.68**	0.000878	0.0329	Cfap161
chr8	**0.68**	0.000993	0.0349	Sh2d4a
chr7	**0.68**	0.00106	0.036	1700120G07Rik
chr12	**0.68**	0.00126	0.0394	Mir680-3
chr1	**0.68**	0.00129	0.0398	Rnf152
chr13	**0.68**	0.0014	0.0414	Dapk1
chr9	**0.68**	0.0019	0.0477	Zc3h12c
chr17	**0.67**	3.98E-06	0.000968	Epb41l3
chr6	**0.67**	4.21E-06	0.00101	A430035B10Rik
chr18	**0.67**	6.67E-06	0.0014	Garem1
chr14	**0.67**	1.52E-05	0.00265	Rap2a
chr11	**0.67**	6.74E-05	0.00703	Mir744
chr9	**0.67**	0.000105	0.00929	Pdcd6ip
chr4	**0.67**	0.000116	0.00997	Dhrs3
chr2	**0.67**	0.000119	0.0101	Rtf2
chr9	**0.67**	0.000303	0.0173	Fat3
chr19	**0.67**	0.000336	0.0184	Sgms1
chr5	**0.67**	0.000343	0.0186	Sfswap
chr6	**0.67**	0.000372	0.0196	Tcaf1
chr7	**0.67**	0.000452	0.0223	Atp10a
chr14	**0.67**	0.000598	0.0267	Ear2
chr13	**0.67**	0.000667	0.0281	Tmem171

chr18	**0.67**	0.000677	0.0284	1700044K03Rik
chr2	**0.67**	0.000722	0.0292	Ninl
chr2	**0.67**	0.000913	0.0335	Ube2e3
chr2	**0.67**	0.000959	0.0343	Gpd2
chr13	**0.67**	0.0011	0.0365	Pfkp
chr15	**0.67**	0.00112	0.0367	Wdr70
chr6	**0.67**	0.00114	0.0371	Vopp1
chr7	**0.67**	0.0015	0.0428	Sox6
chr2	**0.66**	3.22E-06	0.000825	Upp2
chr7	**0.66**	1.65E-05	0.0028	Gas2
chr14	**0.66**	2.02E-05	0.00319	Ear10
chr10	**0.66**	7.35E-05	0.00741	Ccdc6
chr16	**0.66**	7.43E-05	0.00746	Tomm70a
chr12	**0.66**	7.93E-05	0.00773	Tmem18
chr12	**0.66**	9.11E-05	0.00857	Itgb8
chr2	**0.66**	0.000152	0.0118	Sdcbp2
chr13	**0.66**	0.000161	0.0122	A530046M15Rik
chr6	**0.66**	0.000183	0.0132	Klra1
chr4	**0.66**	0.000191	0.0134	Gm11413
chr1	**0.66**	0.000228	0.0147	Nrp2
chr12	**0.66**	0.000236	0.015	3200001D21Rik
chr3	**0.66**	0.000256	0.016	Ptger3
chr3	**0.66**	0.000375	0.0197	Ppp3ca
chr13	**0.66**	0.000476	0.0231	A430090L17Rik
chr9	**0.66**	0.000618	0.0272	Birc3
chr5	**0.66**	0.00063	0.0274	Rasgef1b
chr9	**0.66**	0.000735	0.0295	Cpne4
chr13	**0.66**	0.000854	0.0325	Slc28a3

chr3	**0.66**	0.000994	0.0349	Gipc2
chr2	**0.66**	0.00116	0.0376	4933406D12Rik
chr6	**0.66**	0.00129	0.0398	C1galt1
chr14	**0.66**	0.0014	0.0414	Mir6390
chr9	**0.66**	0.0016	0.0441	Stac
chr1	**0.65**	4.09E-07	0.000173	B3galt2
chr4	**0.65**	1.26E-05	0.0024	Tnc
chr11	**0.65**	1.39E-05	0.00253	Map2k6
chr13	**0.65**	3.23E-05	0.0045	Rnf180
chr13	**0.65**	7.46E-05	0.00746	Cwc27
chr9	**0.65**	0.000169	0.0127	Mei4
chr13	**0.65**	0.000171	0.0128	1700029F12Rik
chr3	**0.65**	0.000247	0.0156	Gipc2
chr10	**0.65**	0.000262	0.0162	Gm36595
chr2	**0.65**	0.000296	0.0172	Gm826
chr18	**0.65**	0.000411	0.0209	Prrc1
chr6	**0.65**	0.000638	0.0275	Sox5
chr7	**0.65**	0.000667	0.0281	Syt9
chr13	**0.65**	0.000858	0.0325	Sugct
chr18	**0.65**	0.0013	0.0398	Tubb6
chr1	**0.64**	9.75E-06	0.00194	Plxna2
chr15	**0.64**	3.28E-05	0.00452	Cpq
chr16	**0.64**	5.03E-05	0.00576	Samsn1
chr4	**0.64**	6.53E-05	0.00686	Tle1
chr13	**0.64**	6.54E-05	0.00686	Akr1e1
chr13	**0.64**	8.40E-05	0.00803	1700024I08Rik
chr3	**0.64**	0.000109	0.00955	Gm30173
chr16	**0.64**	0.000123	0.0104	E330011O21Rik

chr1	**0.64**	0.00017	0.0127	D1Ertd622e
chr2	**0.64**	0.00019	0.0134	Sema6d
chr2	**0.64**	0.000227	0.0147	Napb
chr17	**0.64**	0.000301	0.0172	Srbd1
chr11	**0.64**	0.00036	0.0192	Meis1
chr16	**0.64**	0.00042	0.0213	Mir691
chr4	**0.64**	0.000643	0.0276	Ttc39b
chr13	**0.64**	0.000719	0.0292	Pik3r1
chr6	**0.64**	0.000732	0.0295	Fxyd4
chr2	**0.64**	0.000774	0.0306	Mindy3
chr17	**0.64**	0.000809	0.0313	Crim1
chr9	**0.64**	0.00089	0.0329	Bbs9
chr6	**0.64**	0.000899	0.0331	Ppp1r17
chr9	**0.64**	0.000996	0.0349	Grik4
chr4	**0.64**	0.00105	0.0358	BC039966
chr16	**0.64**	0.00113	0.037	App
chr2	**0.64**	0.00117	0.0377	9630028H03Rik
chr16	**0.64**	0.00123	0.0387	Filip1l
chr7	**0.64**	0.00144	0.0424	Tjp1
chr13	**0.64**	0.00168	0.0453	Pfkp
chr17	**0.64**	0.00178	0.0466	Clip4
chrX	**0.64**	0.00179	0.0466	Ap1s2
chr3	**0.64**	0.00189	0.0477	Ctbs
chr5	**0.64**	0.00194	0.0479	Cnot6l
chr9	**0.63**	9.62E-07	0.000317	Cep162
chr18	**0.63**	1.75E-05	0.00289	Zfp608
chr1	**0.63**	4.56E-05	0.00547	Slc39a10
chr12	**0.63**	8.16E-05	0.0079	Prkch

chr10	**0.63**	9.95E-05	0.00908	Itgb2
chr18	**0.63**	0.000201	0.0138	Ss18
chr11	**0.63**	0.000216	0.0141	4933406G16Rik
chr2	**0.63**	0.000236	0.015	Pfkfb3
chr16	**0.63**	0.000271	0.0165	4930529L06Rik
chr10	**0.63**	0.000295	0.0171	Adgrg6
chr10	**0.63**	0.000335	0.0184	Cep85l
chr5	**0.63**	0.000399	0.0206	Cpeb2
chr1	**0.63**	0.00052	0.0244	Traf3ip3
chr4	**0.63**	0.00056	0.0255	Slc24a2
chr18	**0.63**	0.000719	0.0292	Sncaip
chr18	**0.63**	0.000727	0.0293	Cyb5a
chr15	**0.63**	0.000743	0.0297	Dennd3
chr3	**0.63**	0.000766	0.0303	St6galnac5
chr14	**0.63**	0.000844	0.0323	Gpr18
chr13	**0.63**	0.000946	0.0342	Golm1
chr14	**0.63**	0.001	0.0351	Mbnl2
chr5	**0.63**	0.00107	0.0361	Slc15a4
chr6	**0.63**	0.0011	0.0365	Chn2
chr1	**0.63**	0.00115	0.0373	Gm4846
chr3	**0.63**	0.00145	0.0424	Gpr149
chr1	**0.63**	0.00146	0.0425	Rgs1
chr17	**0.63**	0.0019	0.0477	Pabpc6
chr13	**0.63**	0.00191	0.0477	Edil3
chr3	**0.62**	1.44E-05	0.00259	Gm6260
chr1	**0.62**	2.33E-05	0.00357	Gorab
chr14	**0.62**	4.67E-05	0.00554	Dock5
chr13	**0.62**	0.000171	0.0128	Gli3

chr5	**0.62**	0.000204	0.0139	Arpc1a
chr2	**0.62**	0.000235	0.015	Dhx35
chr4	**0.62**	0.000259	0.0161	Kcnab2
chr6	**0.62**	0.000342	0.0186	Uroc1
chr2	**0.62**	0.000533	0.0248	Pfkfb3
chr14	**0.62**	0.000811	0.0313	Flnb
chr8	**0.62**	0.000887	0.0329	Irf2
chr9	**0.62**	0.00101	0.0351	Herpud2
chr4	**0.62**	0.00101	0.0352	Saxo1
chr1	**0.62**	0.00132	0.0402	Sft2d2
chr4	**0.62**	0.00133	0.0403	Ripk2
chr4	**0.62**	0.0014	0.0414	Triqk
chr15	**0.62**	0.00173	0.0459	Ext1
chr17	**0.62**	0.002	0.0488	4930405O22Rik
chr2	**0.61**	4.77E-06	0.00106	Zfp120
chr15	**0.61**	2.33E-05	0.00357	Oxr1
chr13	**0.61**	3.40E-05	0.00463	Cwc27
chr14	**0.61**	6.36E-05	0.00684	Rnf219
chr6	**0.61**	7.29E-05	0.00741	Tspan9
chr15	**0.61**	0.000176	0.0129	Gm19276
chr1	**0.61**	0.000188	0.0134	Htr5b
chr2	**0.61**	0.000211	0.0141	P2rx3
chr2	**0.61**	3.00E-04	0.0172	Ube2e3
chr13	**0.61**	3.00E-04	0.0172	Ipo11
chr10	**0.61**	0.00033	0.0182	Wisp3
chr8	**0.61**	0.000361	0.0192	Efnb2
chr19	**0.61**	0.000443	0.0221	Dkk1
chr6	**0.61**	0.000634	0.0274	1700101I11Rik

chr2	**0.61**	0.000701	0.029	Mafb
chr14	**0.61**	0.000779	0.0306	Lmo7
chr2	**0.61**	0.000798	0.031	Plxdc2
chr18	**0.61**	0.000871	0.0328	Setbp1
chr13	**0.61**	0.000896	0.033	Mir3961
chr11	**0.61**	0.000964	0.0343	4933406G16Rik
chr1	**0.61**	0.00102	0.0353	Map2
chr1	**0.61**	0.00107	0.0361	Dnm3os
chr5	**0.61**	0.00114	0.0372	1700016H13Rik
chr17	**0.61**	0.00124	0.0387	Nudt12
chr6	**0.61**	0.00128	0.0398	Tpk1
chr14	**0.61**	0.00129	0.0398	Fndc3a
chr4	**0.61**	0.00158	0.0439	Nsmaf
chr13	**0.61**	0.00164	0.0447	Marveld2
chr13	**0.61**	0.00164	0.0447	Dip2c
chr1	**0.61**	0.00196	0.0484	Tnfsf18
chr18	**0.6**	3.39E-07	0.000146	Prelid2
chr5	**0.6**	1.35E-05	0.00249	Gm19619
chr2	**0.6**	1.47E-05	0.00261	Pkp4
chr3	**0.6**	7.61E-05	0.00754	Zc2hc1a
chr1	**0.6**	8.87E-05	0.00842	Mir3962
chr4	**0.6**	9.94E-05	0.00908	Zfp462
chr17	**0.6**	0.000102	0.00914	Txndc2
chr18	**0.6**	0.000135	0.0111	Ttc39c
chr13	**0.6**	0.000138	0.0112	Adamts6
chr18	**0.6**	0.00018	0.0131	Pabpc2
chr2	**0.6**	0.000211	0.0141	Sdcbp2
chr3	**0.6**	0.000241	0.0152	Gm6260

chr7	**0.6**	0.000272	0.0165	Swap70
chr5	**0.6**	0.000283	0.0168	Wsb2
chr13	**0.6**	0.000315	0.0178	Emb
chr15	**0.6**	0.000343	0.0186	Ctnnd2
chr15	**0.6**	0.000349	0.0188	Tmem74
chr18	**0.6**	0.000359	0.0192	Gramd3
chr12	**0.6**	0.00041	0.0209	Arl4a
chr9	**0.6**	0.000443	0.0221	Filip1
chr14	**0.6**	0.000471	0.023	Extl3
chr13	**0.6**	0.000473	0.023	Nnt
chr19	**0.6**	0.000492	0.0237	Psat1
chr3	**0.6**	0.000552	0.0254	Dclk1
chr18	**0.6**	0.000561	0.0255	Pabpc2
chr16	**0.6**	0.000653	0.0278	Retnlb
chr17	**0.6**	0.000786	0.0308	4930517M08Rik
chr14	**0.6**	0.000857	0.0325	Rarb
chr5	**0.6**	0.000915	0.0335	Rasgef1b
chr6	**0.6**	0.000932	0.0339	Rpia
chr9	**0.6**	0.00117	0.0377	Ky
chr5	**0.6**	0.00117	0.0378	Rfc5
chr17	**0.6**	0.00138	0.0412	Slc8a1
chr4	**0.6**	0.00148	0.0427	Ripk2
chr18	**0.6**	0.00149	0.0428	Gm10536
chr18	**0.6**	0.0015	0.0428	Map3k8
chr5	**0.6**	0.00152	0.0431	Cdk8
chr19	**0.6**	0.00178	0.0465	Tmem2
chr12	**0.6**	0.0018	0.0467	Immp2l
chr13	**0.6**	0.00181	0.0469	Nr2f1

chr14	**0.6**	0.00189	0.0477	Lcp1
chr2	**0.6**	0.00198	0.0486	Itga4
chr14	**0.59**	5.59E-06	0.00121	Slain1
chr14	**0.59**	0.000109	0.00955	Stk24
chr15	**0.59**	0.000139	0.0112	Fbxo4
chr6	**0.59**	0.000148	0.0117	Adipor2
chr7	**0.59**	0.000171	0.0128	Dbx1
chr12	**0.59**	0.000215	0.0141	Scin
chr7	**0.59**	0.000269	0.0165	4930543N07Rik
chr1	**0.59**	0.000279	0.0167	Fam168b
chr1	**0.59**	0.000464	0.0227	Tnr
chr18	**0.59**	0.000509	0.024	Kctd16
chr5	**0.59**	0.000601	0.0267	Adam22
chr5	**0.59**	0.000633	0.0274	Hgf
chr13	**0.59**	0.000665	0.0281	Mir3961
chr15	**0.59**	0.000695	0.0288	Ndrg1
chr17	**0.59**	0.000727	0.0293	Nudt12
chr14	**0.59**	0.000822	0.0317	Ube2e1
chr16	**0.59**	0.000885	0.0329	Bach1
chr12	**0.59**	0.000928	0.0338	3200001D21Rik
chr12	**0.59**	0.000929	0.0338	Stxbp6
chr17	**0.59**	0.00095	0.0342	Tbc1d5
chr9	**0.59**	0.00098	0.0346	Dopey1
chr18	**0.59**	0.00105	0.0359	Mir122
chr3	**0.59**	0.00108	0.0362	4933417G07Rik
chr3	**0.59**	0.00111	0.0365	Adgrl2
chr8	**0.59**	0.00133	0.0403	Cmtm4
chr6	**0.59**	0.00137	0.041	Gm7457

chrX	**0.59**	0.00171	0.0456	Rnf128
chr15	**0.59**	0.00182	0.047	Slc1a3
chr13	**0.59**	0.0019	0.0477	Iqgap2
chr1	**0.58**	9.16E-05	0.00859	Farsb
chr9	**0.58**	0.00015	0.0117	Vwa5a
chr2	**0.58**	0.000233	0.015	3300002I08Rik
chr2	**0.58**	0.000254	0.0158	Sdcbp2
chr15	**0.58**	4.00E-04	0.0206	Samd12
chr15	**0.58**	0.000637	0.0275	Ago2
chr4	**0.58**	0.000666	0.0281	Plpp3
chr14	**0.58**	0.00071	0.0292	Abcc4
chr18	**0.58**	0.000854	0.0325	Mocos
chr10	**0.58**	0.000858	0.0325	Ipcef1
chr8	**0.58**	0.00095	0.0342	Lyl1
chr7	**0.58**	0.00112	0.0367	Tspan32
chr14	**0.58**	0.0015	0.0428	Msra
chr2	**0.58**	0.00151	0.043	Secisbp2l
chr7	**0.58**	0.00153	0.0431	Stk33
chr19	**0.58**	0.00157	0.0437	Hells
chr8	**0.58**	0.00164	0.0447	1-Mar
chr3	**0.58**	0.00183	0.0471	Lmo4
chr16	**0.58**	0.00187	0.0476	Fbxo40
chr15	**0.57**	5.01E-05	0.00576	Irak4
chr11	**0.57**	8.32E-05	0.00798	Sptbn1
chr5	**0.57**	9.60E-05	0.00886	Medag
chr4	**0.57**	0.000101	0.00914	Ror1
chr17	**0.57**	0.000132	0.0109	Epb41l3
chr6	**0.57**	0.000319	0.0179	Gprin3

134

chr11	**0.57**	0.000409	0.0209	Cacng1
chr3	**0.57**	0.00049	0.0237	Mecom
chr18	**0.57**	0.000547	0.0253	Zfp608
chr3	**0.57**	0.000595	0.0266	Ctso
chr13	**0.57**	0.00064	0.0275	Pfkp
chr18	**0.57**	0.000677	0.0284	Adrb2
chr8	**0.57**	0.000882	0.0329	Tma16
chr6	**0.57**	0.000958	0.0343	Tex52
chr7	**0.57**	0.00103	0.0353	Tead1
chr10	**0.57**	0.00104	0.0357	Rnf217
chr3	**0.57**	0.00108	0.0361	Trim55
chr10	**0.57**	0.0011	0.0365	Sash1
chr6	**0.57**	0.00123	0.0387	6820426E19Rik
chr1	**0.57**	0.00146	0.0425	Prex2
chr8	**0.57**	0.00185	0.0475	Maf
chr3	**0.57**	0.00201	0.049	Gm48909
chr5	**0.56**	1.72E-05	0.00287	Scarb2
chr2	**0.56**	2.93E-05	0.00424	Gm14325
chr3	**0.56**	3.29E-05	0.00452	Map9
chr5	**0.56**	4.04E-05	0.005	Antxr2
chr19	**0.56**	4.41E-05	0.00531	Pfpl
chr3	**0.56**	5.27E-05	0.00591	Depdc1a
chr5	**0.56**	0.000151	0.0117	Steap4
chr12	**0.56**	0.000192	0.0134	Etv1
chr8	**0.56**	0.000299	0.0172	Prag1
chr18	**0.56**	0.00036	0.0192	Zfp608
chr9	**0.56**	0.000387	0.0202	Rsl24d1
chr17	**0.56**	0.000453	0.0223	Fez2

chr17	**0.56**	0.000505	0.0239	Zfp677
chr10	**0.56**	0.000524	0.0245	Gm36595
chr12	**0.56**	0.000554	0.0255	Etv1
chr6	**0.56**	0.000591	0.0265	Plxna4
chr8	**0.56**	7.00E-04	0.029	Lncbate1
chr12	**0.56**	0.000915	0.0335	Lrrn3
chr1	**0.56**	0.000985	0.0347	Gm5523
chr1	**0.56**	0.00112	0.0367	Ly96
chr7	**0.56**	0.00114	0.0371	Klhl25
chr10	**0.56**	0.00121	0.0384	Mmp19
chr5	**0.56**	0.00173	0.0459	Aff1
chr19	**0.56**	0.00176	0.0463	Pcgf5
chr10	**0.56**	0.00177	0.0464	Gm18409
chr13	**0.56**	0.00179	0.0466	Mir713
chr18	**0.56**	0.00182	0.047	Mir122
chr8	**0.56**	0.00206	0.0498	Mir21c
chr18	**0.55**	5.91E-06	0.00127	Stard4
chr17	**0.55**	6.94E-05	0.00718	Dreh
chr1	**0.55**	0.000126	0.0105	Rgs1
chr4	**0.55**	0.000185	0.0132	Trabd2b
chr18	**0.55**	0.000269	0.0165	Pik3c3
chr19	**0.55**	0.000279	0.0167	A1cf
chr16	**0.55**	0.000408	0.0209	Tiam1
chr1	**0.55**	0.000499	0.0238	Pard3b
chr2	**0.55**	0.000542	0.0252	Gm2004
chr15	**0.55**	0.00059	0.0265	Oxr1
chr1	**0.55**	0.000661	0.028	Hhat
chr10	**0.55**	0.000694	0.0288	Platr7

chr6	**0.55**	0.000713	0.0292	
chr6	**0.55**	0.000804	0.0312	Slc2a3
chr9	**0.55**	0.000969	0.0344	Mir6386
chr2	**0.55**	0.00123	0.0387	Bcas1os2
chr5	**0.55**	0.0014	0.0414	Kl
chr5	**0.55**	0.00143	0.0421	Adgra3
chr9	**0.55**	0.00165	0.0447	Smco4
chrX	**0.55**	0.00166	0.0449	Gm6377
chr15	**0.55**	0.00166	0.0449	4930447A16Rik
chr3	**0.55**	0.00178	0.0466	P2ry14
chr10	**0.55**	0.00192	0.0478	Tmem19
chr4	**0.55**	0.00202	0.0492	A530072M11Rik
chr5	**0.55**	0.00206	0.0498	Antxr2
chr3	**0.54**	1.86E-05	0.00301	Fpgt
chr1	**0.54**	0.000116	0.00997	Rnf152
chr17	**0.54**	0.000142	0.0114	Slc8a1
chr13	**0.54**	0.00015	0.0117	Spz1
chr13	**0.54**	0.000184	0.0132	AW209491
chr17	**0.54**	0.000311	0.0177	Capn13
chr9	**0.54**	0.00045	0.0223	Glb1l2
chr5	**0.54**	0.000503	0.0239	Mrpl1
chr1	**0.54**	0.000562	0.0255	Ptgs2os2
chr8	**0.54**	0.000575	0.0259	Msr1
chr2	**0.54**	0.000579	0.0261	Mir5129
chr2	**0.54**	0.000619	0.0272	Gm13315
chr7	**0.54**	0.000654	0.0278	Gm15412
chr18	**0.54**	0.000778	0.0306	Zfp608
chr8	**0.54**	0.000798	0.031	Rnf122

chr3	**0.54**	0.000831	0.0319	4930503B20Rik
chr6	**0.54**	0.000873	0.0328	M6pr
chr9	**0.54**	0.000874	0.0328	Eef1a1
chrX	**0.54**	0.000961	0.0343	Rragb
chr8	**0.54**	0.00101	0.0351	Ikbkb
chr9	**0.54**	0.0011	0.0365	Pxylp1
chr10	**0.54**	0.0011	0.0365	Lss
chr17	**0.54**	0.00112	0.0367	Synj2
chr5	**0.54**	0.00119	0.0379	Antxr2
chr17	**0.54**	0.00123	0.0387	L3mbtl4
chr2	**0.54**	0.00134	0.0403	Itgav
chr4	**0.54**	0.00137	0.041	Rragc
chr9	**0.54**	0.00139	0.0414	Azi2
chr10	**0.54**	0.00145	0.0425	1110002J07Rik
chr13	**0.54**	0.00148	0.0428	Klf6
chr3	**0.54**	0.00153	0.0431	Etnppl
chr6	**0.54**	0.0016	0.0441	Gm7457
chr10	**0.54**	0.00185	0.0475	Ust
chr11	**0.54**	0.00189	0.0477	Tex14
chr14	**0.54**	0.00198	0.0486	Mbnl2
chr18	**0.54**	0.00203	0.0494	Osbpl1a
chr15	**0.53**	1.79E-06	0.000527	Alg10b
chr18	**0.53**	1.91E-05	0.00306	Txnl1
chr2	**0.53**	3.16E-05	0.00446	Ube2e3
chr18	**0.53**	3.61E-05	0.00475	Snx24
chr13	**0.53**	4.06E-05	0.005	Vcan
chr3	**0.53**	7.06E-05	0.00724	Snx7
chr16	**0.53**	0.000135	0.0111	Ccdc50

chr14	**0.53**	0.000645	0.0277	Txndc16
chr19	**0.53**	0.000648	0.0277	Afap1l2
chr3	**0.53**	0.000779	0.0306	Selenof
chr4	**0.53**	0.000962	0.0343	Mknk1
chr17	**0.53**	0.000979	0.0346	Foxn2
chr6	**0.53**	0.0011	0.0365	Aebp2
chr12	**0.53**	0.0011	0.0365	Ptprn2
chr12	**0.53**	0.00117	0.0377	Atxn7l1os2
chr13	**0.53**	0.0012	0.0381	Mrpl36
chr17	**0.53**	0.0013	0.0399	Zfp36l2
chr14	**0.53**	0.00139	0.0414	1700100I10Rik
chr8	**0.53**	0.0016	0.0442	Bean1
chr7	**0.53**	0.00161	0.0442	Ppfibp2
chr18	**0.53**	0.00174	0.046	Kif5b
chr6	**0.53**	0.00187	0.0476	Bicd1
chr4	**0.53**	0.0019	0.0477	Car8
chr17	**0.53**	0.00192	0.0477	Agpat4
chr6	**0.53**	0.00205	0.0495	4930515G16Rik
chr5	**0.52**	4.03E-05	0.005	Dpp6
chr14	**0.52**	5.18E-05	0.00585	Erc2
chr2	**0.52**	0.000141	0.0113	Bcas1
chr6	**0.52**	0.000158	0.012	Moxd2
chr8	**0.52**	0.000208	0.014	Fam149a
chr10	**0.52**	0.000282	0.0168	Zfp873
chr13	**0.52**	0.000337	0.0184	4922502H24Rik
chr2	**0.52**	4.00E-04	0.0206	Rbm45
chr5	**0.52**	0.000452	0.0223	Phtf2
chr6	**0.52**	0.000454	0.0223	Sox5os3

chr18	**0.52**	0.00049	0.0237	Setbp1
chr6	**0.52**	0.000617	0.0272	Smim10l1
chr13	**0.52**	0.000716	0.0292	Lpcat1
chr18	**0.52**	0.000751	0.0298	Abhd3
chr14	**0.52**	0.000795	0.031	Stk24
chr7	**0.52**	0.000796	0.031	Wdr11
chr7	**0.52**	0.000858	0.0325	Mmp21
chr18	**0.52**	0.000883	0.0329	Ldlrad4
chr6	**0.52**	0.000896	0.033	Gng12
chr16	**0.52**	0.000945	0.0342	Pla1a
chr16	**0.52**	0.000947	0.0342	App
chr6	**0.52**	0.000978	0.0346	Tulp3
chr6	**0.52**	0.00105	0.0358	Il12rb2
chr14	**0.52**	0.00117	0.0377	Rarb
chr7	**0.52**	0.00123	0.0387	Atp10a
chr9	**0.52**	0.00134	0.0403	5830418P13Rik
chr5	**0.52**	0.0014	0.0414	Tec
chr12	**0.52**	0.00144	0.0422	Mir6388
chr1	**0.52**	0.00149	0.0428	4-Mar
chr17	**0.52**	0.00155	0.0434	Igf2r
chr8	**0.52**	0.00164	0.0447	Neil3
chr13	**0.52**	0.00165	0.0447	Lyst
chrX	**0.52**	0.00174	0.046	Chm
chr9	**0.52**	0.00179	0.0466	Arhgap32
chr1	**0.52**	0.00185	0.0474	Nrp2
chr11	**0.52**	0.00187	0.0476	Trim25
chr1	**0.52**	0.00192	0.0477	Slc39a10
chr1	**0.52**	0.00193	0.0478	Gpatch2

chr16	**0.52**	0.00198	0.0486	Gpr15
chr2	**0.52**	0.00203	0.0494	Top1
chr4	**0.51**	6.34E-05	0.00684	9530080O11Rik
chr10	**0.51**	0.000189	0.0134	Ncoa7
chr3	**0.51**	0.000194	0.0135	Rapgef2
chr2	**0.51**	0.000267	0.0165	Arhgap15
chr16	**0.51**	0.00034	0.0185	Gm10791
chr15	**0.51**	0.000504	0.0239	Slc38a2
chr4	**0.51**	0.000731	0.0294	Zfp984
chr2	**0.51**	0.000885	0.0329	Top1
chr10	**0.51**	0.000975	0.0345	Adgrg6
chr2	**0.51**	0.000999	0.035	Arpc5l
chr4	**0.51**	0.00101	0.0352	Zfp462
chr18	**0.51**	0.00103	0.0355	Setbp1
chr1	**0.51**	0.00105	0.0358	Fmo9
chr3	**0.51**	0.00106	0.0359	Mir7008
chr9	**0.51**	0.00116	0.0376	Rwdd2a
chr10	**0.51**	0.00119	0.0381	Stxbp5
chr14	**0.51**	0.00134	0.0403	Prss52
chr19	**0.51**	0.00139	0.0414	Pfpl
chr9	**0.51**	0.00151	0.043	Gm15511
chr4	**0.51**	0.00153	0.0431	9530080O11Rik
chr8	**0.51**	0.00155	0.0434	Kifc3
chr2	**0.51**	0.00159	0.0439	Gm14326
chr18	**0.51**	0.00161	0.0442	Pmaip1
chr7	**0.51**	0.00205	0.0497	Slc17a6
chr18	**0.5**	2.38E-05	0.00361	Commd10
chr18	**0.5**	0.000224	0.0145	Adrb2

chr3	**0.5**	0.000323	0.0181	Gm1653
chr2	**0.5**	0.000495	0.0238	Flrt3
chr8	**0.5**	0.000504	0.0239	Cdyl2
chr13	**0.5**	0.000569	0.0257	Ubqln1
chr18	**0.5**	0.00101	0.0352	Mcc
chr4	**0.5**	0.00115	0.0373	Virma
chr17	**0.5**	0.00136	0.0409	Ldhal6b
chr18	**0.5**	0.00137	0.041	Svil
chr1	**0.5**	0.00153	0.0431	Pla2g4a
chr17	**0.5**	0.00157	0.0437	Gm7072
chr9	**0.5**	0.00186	0.0475	Tgfbr2
chr15	**0.5**	0.00189	0.0477	Ext1
chr9	**0.5**	0.00197	0.0486	Ttc21a
chr5	**0.49**	0.000182	0.0131	Hgf
chrX	**0.49**	0.00019	0.0134	Amer1
chr17	**0.49**	0.000252	0.0158	Spaca6
chr10	**0.49**	0.000364	0.0193	4930430F08Rik
chr6	**0.49**	0.000407	0.0209	Asns
chr1	**0.49**	0.000655	0.0278	Rpe
chr7	**0.49**	0.000681	0.0285	Trim6
chr9	**0.49**	0.000889	0.0329	1700057G04Rik
chr18	**0.49**	0.00102	0.0352	Crem
chr3	**0.49**	0.00112	0.0367	S1pr1
chr6	**0.49**	0.00129	0.0398	Gm31520
chr13	**0.49**	0.00132	0.0403	Cdk20
chr1	**0.49**	0.00133	0.0403	Gm19705
chr18	**0.49**	0.00133	0.0403	Ythdc2
chr10	**0.49**	0.0014	0.0414	Ifngas1

chr5	**0.49**	0.00147	0.0426	2900026A02Rik
chr4	**0.49**	0.00149	0.0428	Ifna1
chr10	**0.49**	0.00174	0.046	Themis
chr8	**0.49**	0.00176	0.0463	AI429214
chr18	**0.49**	0.00176	0.0463	Cyb5a
chr15	**0.49**	0.0019	0.0477	Trps1
chr3	**0.49**	0.00192	0.0478	Pde7a
chr3	**0.49**	0.002	0.0488	Camk2d
chr7	**0.49**	0.00207	0.0499	Ceacam16
chr17	**0.48**	6.08E-05	0.00666	Fam98a
chr12	**0.48**	0.000214	0.0141	Fam181a
chr9	**0.48**	0.000547	0.0253	Pik3r4
chr3	**0.48**	0.000624	0.0273	Dclk1
chr7	**0.48**	0.000649	0.0277	Eef2k
chr13	**0.48**	0.000747	0.0297	Vps41
chr2	**0.48**	0.000957	0.0343	Slc38a11
chr16	**0.48**	0.00097	0.0344	Cpox
chr1	**0.48**	0.0011	0.0365	Wdfy1
chr8	**0.48**	0.00118	0.0379	Atp6v1b2
chr13	**0.48**	0.00129	0.0398	Emb
chr8	**0.48**	0.00146	0.0425	Mcm5
chr3	**0.48**	0.00171	0.0456	Pdgfc
chr15	**0.48**	0.00173	0.0459	Med30
chr14	**0.48**	0.00174	0.046	Ang6
chr11	**0.48**	0.00194	0.0479	Prkca
chr9	**0.48**	0.00205	0.0495	Glb1l2
chr10	**0.47**	0.000173	0.0128	Echdc1
chr3	**0.47**	0.000209	0.0141	Tyw3

chr18	**0.47**	0.000286	0.0168	Hdhd2
chr6	**0.47**	0.000682	0.0285	Eps8
chr1	**0.47**	0.000747	0.0297	Aspm
chr10	**0.47**	0.000829	0.0319	Washc3
chr2	**0.47**	0.000868	0.0328	Dph6
chr14	**0.47**	0.000872	0.0328	Mir6239
chr18	**0.47**	0.000948	0.0342	Stard6
chrX	**0.47**	0.00109	0.0364	Pdzd11
chr1	**0.47**	0.00128	0.0398	Pfkfb2
chr2	**0.47**	0.00154	0.0431	Cd93
chr6	**0.47**	0.00161	0.0442	Aebp2
chr1	**0.47**	0.00182	0.047	Aim2
chr17	**0.47**	0.00191	0.0477	Akain1
chr13	**0.47**	0.00194	0.0479	Scgn
chr3	**0.46**	4.04E-05	0.005	Rnpc3
chr3	**0.46**	0.000194	0.0135	Tbck
chr1	**0.46**	0.000274	0.0166	Rhbdd1
chr1	**0.46**	0.00029	0.0169	D230017M19Rik
chr6	**0.46**	0.000328	0.0181	Amn1
chr19	**0.46**	0.000423	0.0213	Ptar1
chr16	**0.46**	0.000559	0.0255	Tigit
chr12	**0.46**	0.000738	0.0295	Ldah
chr2	**0.46**	0.00104	0.0357	Ndufaf5
chr9	**0.46**	0.00123	0.0387	Atp1b3
chr14	**0.46**	0.00125	0.0391	5430440P10Rik
chr9	**0.46**	0.00149	0.0428	Alkbh8
chr13	**0.46**	0.00151	0.043	4833420G17Rik
chr2	**0.46**	0.0016	0.0442	Gm13546

chr4	**0.46**	0.00161	0.0442	Cdh17
chr2	**0.46**	0.00173	0.0459	B230118H07Rik
chr2	**0.46**	0.0018	0.0468	Cdh26
chr16	**0.46**	0.00184	0.0474	4930529L06Rik
chr4	**0.46**	0.00186	0.0475	Rmdn1
chr13	**0.46**	0.00199	0.0488	Akr1e1
chrX	**0.46**	0.002	0.0488	Nap1l2
chr1	**0.46**	0.00201	0.049	Ccdc93
chr2	**0.45**	0.000411	0.0209	Lnpk
chrX	**0.45**	0.000436	0.0219	Fancb
chr13	**0.45**	0.000602	0.0267	Ice1
chr6	**0.45**	0.000683	0.0285	6820426E19Rik
chr2	**0.45**	0.000715	0.0292	Tasp1
chr5	**0.45**	0.00107	0.0361	Antxr2
chr4	**0.45**	0.00121	0.0383	Bach2
chr7	**0.45**	0.00134	0.0403	Trim68
chr1	**0.45**	0.00155	0.0434	Tmem14a
chr1	**0.45**	0.00187	0.0476	Ptgs2os
chr15	**0.45**	0.00202	0.0492	Zdhhc25
chr10	**0.45**	0.00204	0.0495	Atxn7l3b
chr16	**0.44**	0.000173	0.0128	Dcbld2
chr6	**0.44**	0.000197	0.0136	Phf14
chr9	**0.44**	0.000537	0.025	Nudt16
chr7	**0.44**	0.00104	0.0357	Uros
chr10	**0.44**	0.00124	0.0387	Ctgf
chr10	**0.44**	0.00128	0.0398	2610008E11Rik
chr3	**0.44**	0.00131	0.04	Tet2
chr18	**0.44**	0.00157	0.0437	Vaultrc5

chr2	**0.44**	0.00162	0.0444	Depdc7
chr8	**0.44**	0.00164	0.0447	Fbxo8
chr2	**0.44**	0.00179	0.0466	Gata3
chr1	**0.44**	0.0018	0.0468	Vamp4
chr5	**0.44**	0.00182	0.047	Slc4a4
chr10	**0.44**	0.00187	0.0476	Ppp1r12a
chr19	**0.44**	0.00187	0.0476	Mirt1
chr3	**0.44**	0.00207	0.0499	Adgrl2
chr18	**0.43**	0.000571	0.0258	Lars
chr17	**0.43**	0.000605	0.0267	LOC102640673
chr1	**0.43**	0.00106	0.036	B3galt2
chr13	**0.43**	0.00168	0.0452	2210408I21Rik
chr14	**0.43**	0.00183	0.0472	Ndfip2
chr11	**0.43**	0.00191	0.0477	Utp18
chr1	**0.42**	0.000153	0.0118	Cenpf
chr4	**0.42**	2.00E-04	0.0138	Kdm4c
chr17	**0.42**	0.000215	0.0141	Sgo1
chr15	**0.42**	0.000283	0.0168	Eny2
chr2	**0.42**	0.000531	0.0248	Ccdc34
chr14	**0.42**	0.000788	0.0308	Ghitm
chr1	**0.42**	0.0011	0.0365	Exo1
chr11	**0.42**	0.00155	0.0434	Fignl1
chr10	**0.42**	0.00171	0.0456	Rnf217
chr7	**0.41**	0.000622	0.0273	Prcp
chr18	**0.41**	0.00063	0.0274	Dmxl1
chr17	**0.41**	0.000944	0.0342	Arhgap28
chr12	**0.41**	0.00102	0.0352	Rdh14
chr18	**0.41**	0.00147	0.0426	Timm21

chr3	**0.41**	0.00158	0.0439	Cenpe
chr7	**0.4**	0.000286	0.0168	2310057M21Rik
chr18	**0.4**	0.000524	0.0245	Dcp2
chr17	**0.4**	0.000717	0.0292	Ppp2r1a
chr4	**0.4**	0.000833	0.032	Wwp1
chr13	**0.4**	0.000884	0.0329	Mfsd14b
chr6	**0.4**	0.00102	0.0352	Bet1
chr18	**0.4**	0.00119	0.038	Thoc1
chr10	**0.4**	0.00132	0.0402	E2f7
chr13	**0.4**	0.00133	0.0403	Med10
chr9	**0.4**	0.00133	0.0403	Plscr1
chr3	**0.4**	0.00152	0.043	Wars2
chr14	**0.4**	0.00154	0.0431	Stc1
chr7	**0.4**	0.00166	0.0449	Pla2g4c
chr3	**0.4**	0.00166	0.0449	Cpb1
chr10	**0.4**	0.00175	0.0461	Ipmk
chr1	**0.4**	0.00177	0.0464	Ptgs2os2
chr6	**0.4**	0.00191	0.0477	Il12rb2
chr1	**0.39**	0.000156	0.012	Gm16432
chr5	**0.39**	0.000453	0.0223	Lcorl
chr1	**0.39**	0.000923	0.0337	Lypla1
chr13	**0.39**	0.00106	0.036	Cox7c
chr14	**0.39**	0.00118	0.0379	Dnajc3
chr10	**0.39**	0.00141	0.0414	Adgb
chr1	**0.39**	0.00142	0.0418	Sgo2a
chr5	**0.39**	0.00169	0.0454	Mob1b
chr5	**0.39**	0.0017	0.0456	Cdk8
chr17	**0.39**	0.0019	0.0477	Zfp960

147

chr8	**0.38**	0.000397	0.0206	Gm21119
chr17	**0.38**	0.000463	0.0227	Zfp960
chr10	**0.38**	0.00051	0.0241	Tmtc3
chr17	**0.38**	0.000779	0.0306	Mut
chr17	**0.38**	0.00112	0.0367	Tgif1
chr3	**0.38**	0.0012	0.0381	Ttc14
chr8	**0.38**	0.0014	0.0414	1700029J07Rik
chr6	**0.38**	0.00163	0.0444	Tmem106b
chr18	**0.38**	0.00172	0.0458	Fbxo38
chr5	**0.38**	0.00198	0.0486	Rnf6
chr16	**0.37**	0.00186	0.0475	Nsun3
chr2	**0.36**	0.0013	0.0398	Tnks1bp1
chr7	**0.36**	0.0015	0.0428	1700003G18Rik
chr8	**0.35**	0.000887	0.0329	4930467E23Rik
chr8	**0.35**	0.00167	0.045	6820431F20Rik
chr18	**0.35**	0.00172	0.0459	Taf4b
chr6	**0.33**	0.00137	0.041	Recql
chr5	**-0.4**	0.00129	0.0398	Pitpnb
JH584304.1	**-0.44**	0.000443	0.0221	
chr7	**-0.44**	0.00056	0.0255	1600014C10Rik
chr5	**-0.44**	0.00191	0.0477	Rasa4
chr13	**-0.49**	0.000357	0.0191	Zfp346
chr5	**-0.49**	0.00149	0.0428	Pgam5
chr5	**-0.51**	0.000709	0.0292	Snora26
chr15	**-0.51**	0.00124	0.0387	Polr3h
chr10	**-0.51**	0.00147	0.0426	Btbd2
chr11	**-0.53**	0.000918	0.0336	Myh10
chr13	**-0.55**	4.49E-06	0.00104	Tspan17

chr8	**-0.55**	0.000751	0.0298	Polr2c
chr11	**-0.55**	0.00194	0.0479	Vamp2
chr11	**-0.56**	0.000306	0.0175	Fam117a
chr10	**-0.62**	0.000214	0.0141	Mex3d
chr7	**-0.65**	3.05E-05	0.00437	Mki67
chr6	**-0.7**	0.000684	0.0285	Rn4.5s
chr4	**-0.71**	0.000632	0.0274	Fam46b
chr5	**-0.84**	4.82E-05	0.00569	Coq2
chr2	**-0.85**	1.67E-05	0.00281	Cstad
chr5	**-0.91**	8.89E-08	5.49E-05	Lrrc8c
chr4	**-0.92**	2.10E-05	0.00328	Pde4b
chr4	**-0.94**	4.44E-07	0.000182	Pde4b
chr5	**-1.01**	1.72E-08	1.29E-05	BC005561
chr5	**-1.06**	7.66E-11	9.23E-08	Hnrnpd
chr5	**-1.5**	3.09E-09	2.75E-06	Cxcl11
chrY	**-1.54**	1.96E-08	1.39E-05	Mid1/G530011O06Rik
chr11	**-1.56**	1.01E-12	1.28E-09	Sfi1
chr13	**-1.63**	3.93E-13	5.57E-10	Gadd45g
chrX	**-2.02**	9.75E-14	1.68E-10	Mid1/G530011O06Rik
chr5	**-2.33**	1.17E-14	2.17E-11	Spp1
chr5	**-2.36**	2.29E-25	6.90E-22	Lrrc8d
chr5	**-2.73**	5.33E-38	2.14E-34	Zfp33b
chr5	**-2.98**	2.61E-41	1.26E-37	Arhgap24

Appendix 3: Chapter 4 Supplemental Figures
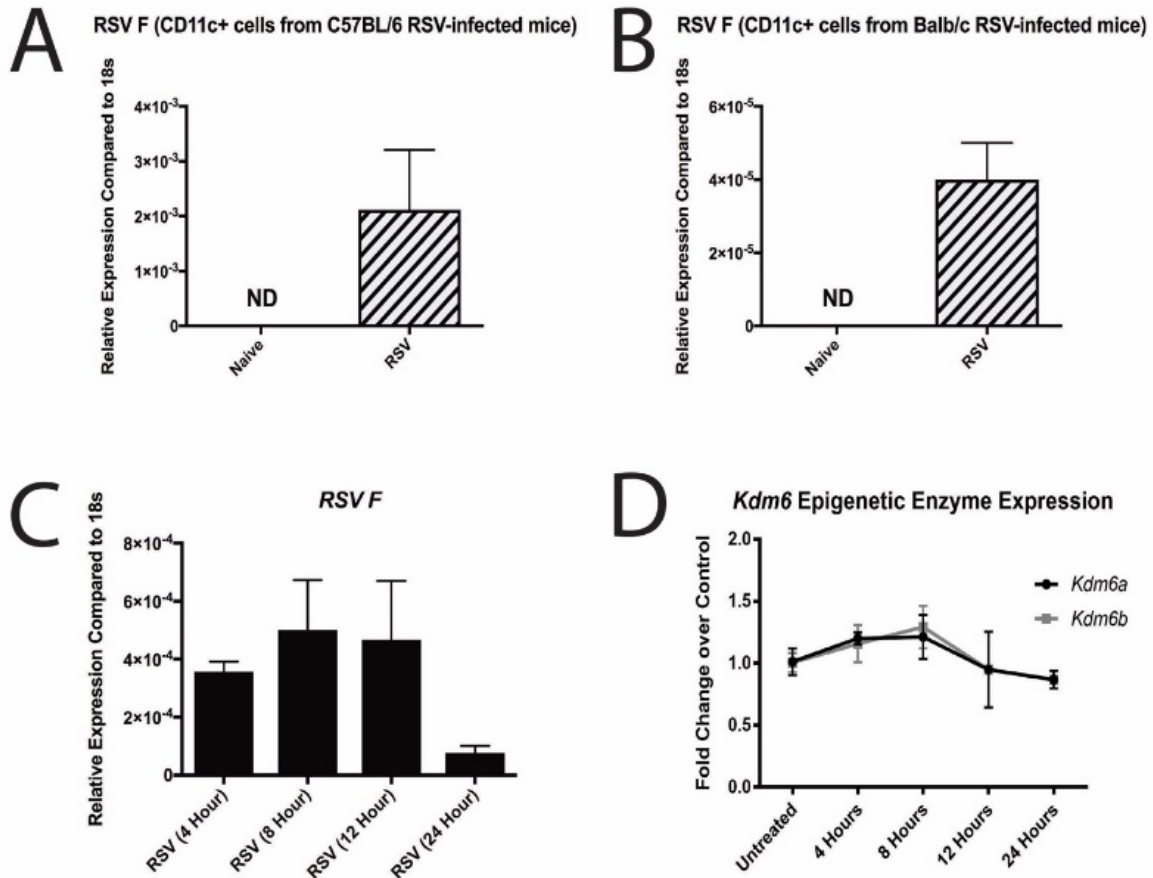
Figure A3- 1. Chapter 4 Supplemental Figure 1.
A, B. Male C57BL/6 or Balb/c mice were infected with RSV (2×10^5 pfu) and lungs collected 8 days post-infection and compared to naïve control animals. Lungs were harvested and the CD11c+ cell population isolated using MACS bead separation, mRNA extracted and qPCR performed to determine RSV F gene expression ($N \geq 3$). **C.** BMDC isolated from Balb/c mice were infected *in vitro* with RSV and cells collected at the indicated timepoints, mRNA extracted and qPCR performed to determine RSV F gene expression ($N = 4$). **D.** BMDC isolated from Balb/c mice were exposed *in vitro* to UV-inactivated RSV and cells collected at the indicated timepoints, mRNA extracted and qPCR performed to determine epigenetic enzyme expression ($N = 3$). Data represent Mean ± SEM (Representative of 2 individual experiments).
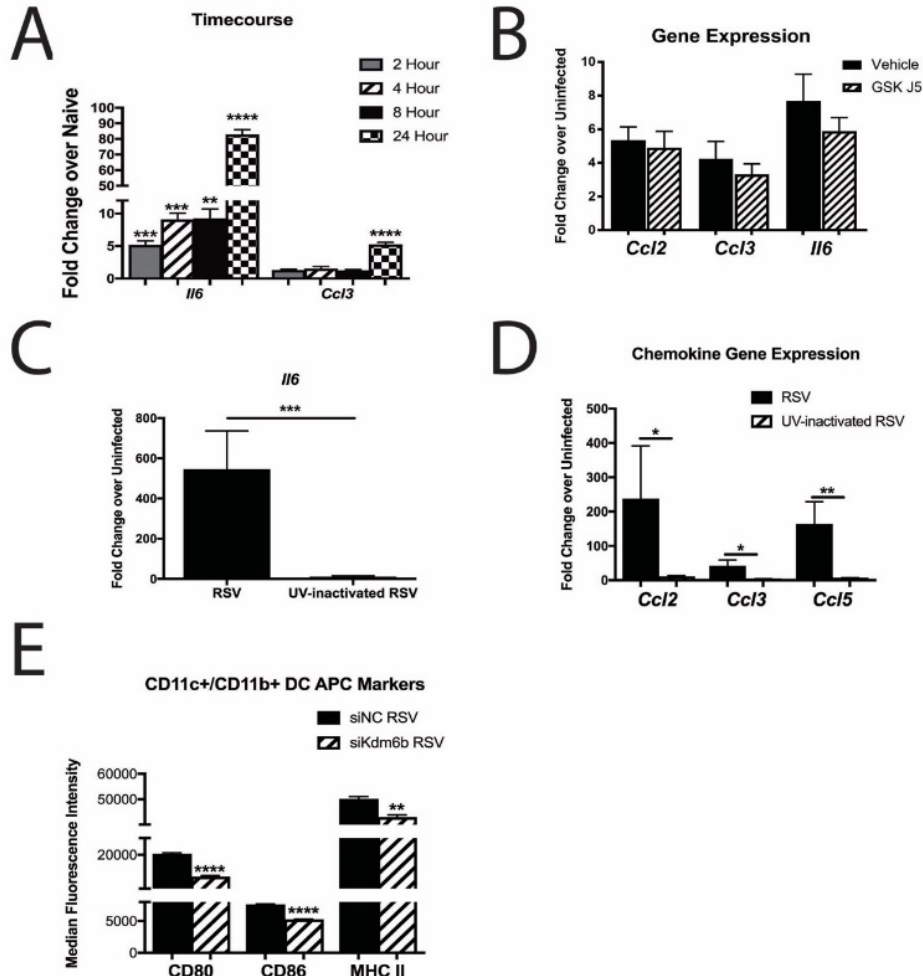
Figure A3- 2. Chapter 4 Supplemental Figure 2.
BMDC were isolated from Balb/c mice, cultured for 6 days in the presence of GM-CSF and infected with RSV *in vitro* for the indicated time points. **A**. mRNA was extracted and qPCR performed to determine cytokine/chemokine gene expression (N = 3). **B.** BMDC were exposed to GSK J5 or vehicle control during RSV-infection for 24 hours, mRNA was extracted and qPCR performed to determine cytokine/chemokine gene expression (N = 3). **C,D**. BMDC were exposed *in vitro* to UV-inactivated RSV and cells collected after 24 hours, mRNA extracted and qPCR performed to determine cytokine/chemokine gene expression (N = 3). **E.** Kdm6b gene was knocked down in BMDC using siRNA (siKdm6b) (non-targeting control (siNC) used for control) for 48 hours, followed by RSV-infection for 24 hours. Cells were collected, processed and stained for flow cytometry analysis of APC markers (N = 3). Data represent Mean ± SEM (Representative of at least 2 individual experiments). * = p < 0.05; ** = p < 0.01; *** = p < 0.001; **** = p < 0.0001.

Appendix 4: Chapter 5 Additional Results
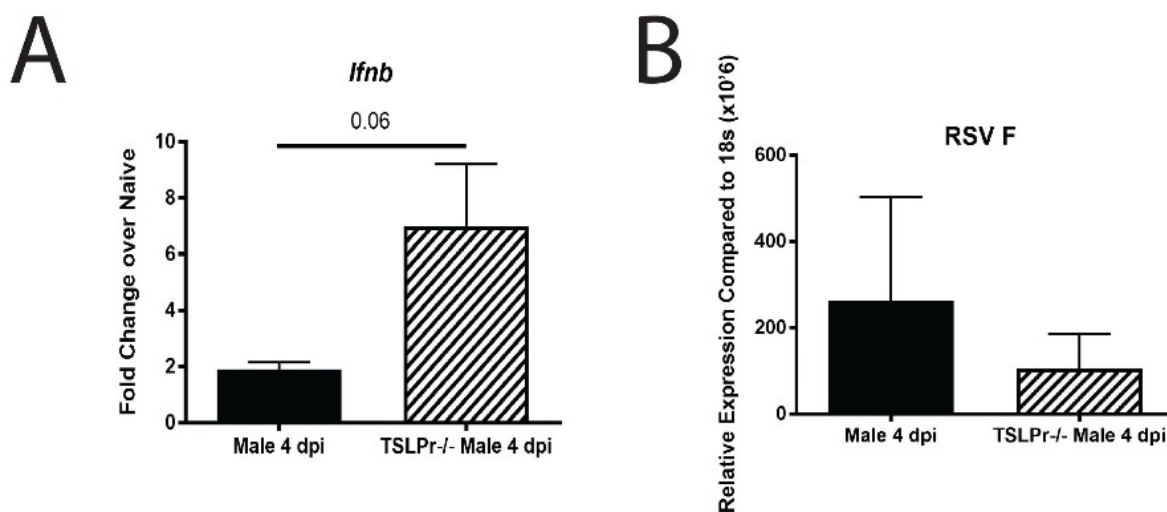
Figure A4- 1. Neonatal RSV infection of TSLPR-/- male mice leads to increased *Ifnb* and faster viral clearance.
Male WT and TSLPR-/- mice were infected with RSV at 7 days of age and tissues collected at 4 days post-infection to evaluate primary response and clearance of RSV gene. **A, B**. Lungs were homogenized and mRNA extracted to determine interferon-β and RSV F gene expression, respectively (N ≥ 3)
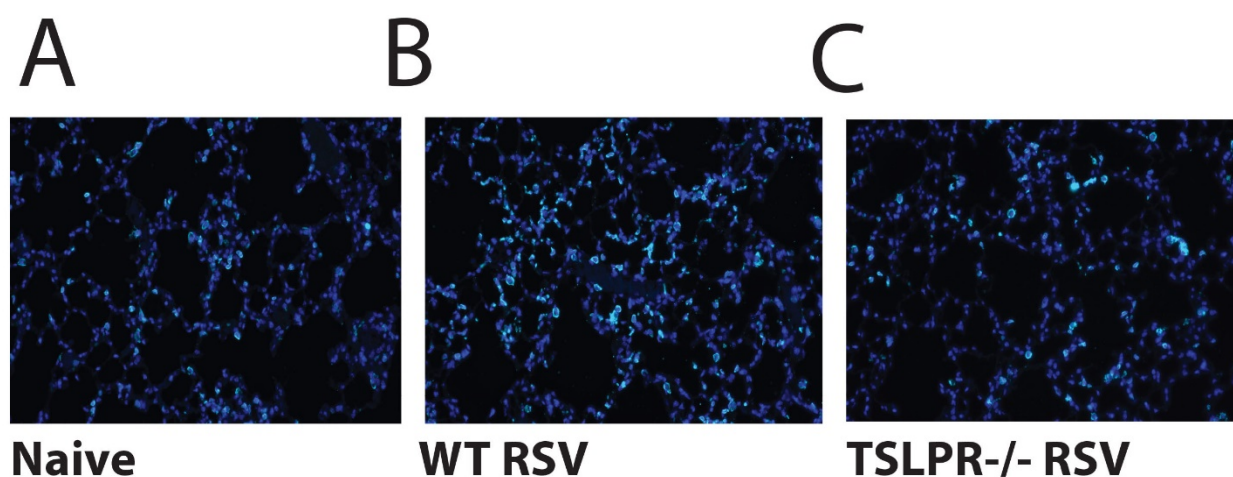

Figure A4- 2. Increased CD45+ cells in lungs of WT mice at 4 weeks post-early-life RSV-infection.
Male WT and TSLPR-/- mice were infected neonatally with RSV at 7 days of age and CD45+ immunofluorescence staining (staining in blue) performed at 4 weeks post-infection. **A**. Naïve age-matched control **B**. WT early-life RSV. **C**. TSLPR-/- early-life RSV. Representative photos shown
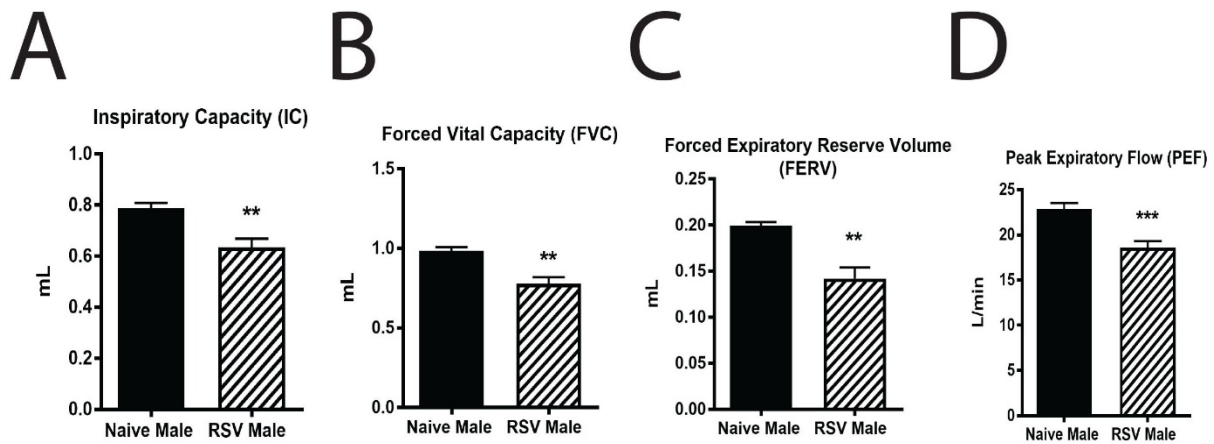
Figure A4- 3. PFT analysis following early-life RSV-infection.
Male WT and TSLPR-/- mice were infected neonatally with RSV at 7 days of age and analyzed for indications of lung remodeling at 4 weeks post-infection **A-D**. Pulmonary Function Test analysis. ± SEM (N ≥ 3). ** = p < 0.01; *** = p < 0.001.
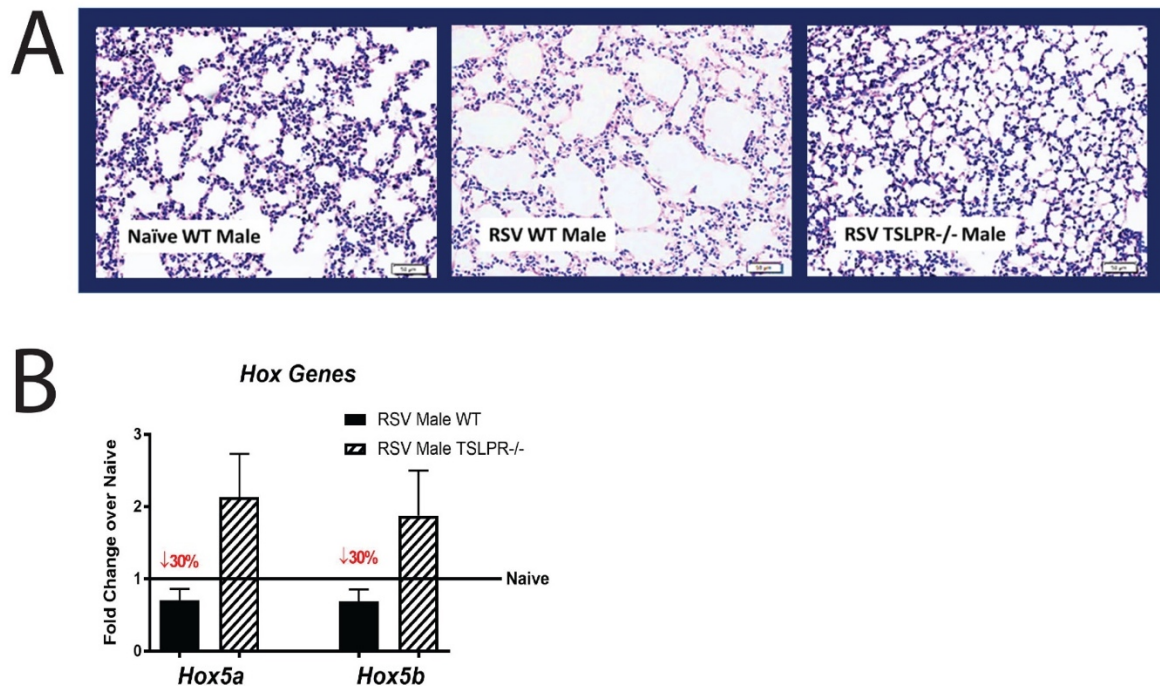

Figure A4- 4. Lung remodeling following early-life RSV-infection.
Male WT and TSLPR-/- mice were infected neonatally with RSV at 7 days of age and analyzed for indications of lung remodeling at 4 weeks post-infection **A**. Lungs were embedded in paraffin and H&E staining was performed to visualize alveolar spaces. Representative photos shown **B**. Lungs were homogenized and mRNA extracted to determine HOX5 gene expression. ± SEM (N ≥ 3).

153

Bibliography

1. Sigurs, N. *et al.* Asthma and allergy patterns over 18 years after severe RSV bronchiolitis in the first year of life. *Thorax* **65**, 1045–1052 (2010).

2. Nair, H. *et al.* Global burden of acute lower respiratory infections due to respiratory syncytial virus in young children: a systematic review and meta-analysis. *Lancet Lond. Engl.* **375**, 1545–1555 (2010).

3. Henderson, J. *et al.* Hospitalization for RSV bronchiolitis before 12 months of age and subsequent asthma, atopy and wheeze: a longitudinal birth cohort study. *Pediatr. Allergy Immunol. Off. Publ. Eur. Soc. Pediatr. Allergy Immunol.* **16**, 386–392 (2005).

4. Chatzis, O. *et al.* Burden of severe RSV disease among immunocompromised children and adults: a 10 year retrospective study. *BMC Infect. Dis.* **18**, (2018).

5. Walsh, E. E. Respiratory Syncytial Virus infection: an illness for all ages. *Clin. Chest Med.* **38**, 29–36 (2017).

6. Griffiths, C., Drews, S. J. & Marchant, D. J. Respiratory Syncytial Virus: Infection, Detection, and New Options for Prevention and Treatment. *Clin. Microbiol. Rev.* **30**, 277–319 (2017).

7. Collins, P. L., Fearns, R. & Graham, B. S. Respiratory Syncytial Virus: Virology, Reverse Genetics, and Pathogenesis of Disease. *Curr. Top. Microbiol. Immunol.* **372**, 3–38 (2013).

8. Sullender, W. M. Respiratory Syncytial Virus Genetic and Antigenic Diversity. *Clin. Microbiol. Rev.* **13**, 1–15 (2000).

9. McLellan, J. S., Ray, W. C. & Peeples, M. E. Structure and Function of RSV Surface Glycoproteins. *Curr. Top. Microbiol. Immunol.* **372**, 83–104 (2013).

10. Low, K.-W., Tan, T., Ng, K., Tan, B.-H. & Sugrue, R. J. The RSV F and G glycoproteins interact to form a complex on the surface of infected cells. *Biochem. Biophys. Res. Commun.* **366**, 308–313 (2008).

11. Collins, P. L. & Graham, B. S. Viral and Host Factors in Human Respiratory Syncytial Virus Pathogenesis. *J. Virol.* **82**, 2040–2055 (2008).

12. Lo, M. S., Brazas, R. M. & Holtzman, M. J. Respiratory Syncytial Virus Nonstructural Proteins NS1 and NS2 Mediate Inhibition of Stat2 Expression and Alpha/Beta Interferon Responsiveness. *J. Virol.* **79**, 9315–9319 (2005).

13. Ling, Z., Tran, K. C. & Teng, M. N. Human Respiratory Syncytial Virus Nonstructural Protein NS2 Antagonizes the Activation of Beta Interferon Transcription by Interacting with RIG-I. *J. Virol.* **83**, 3734–3742 (2009).

14. Nice, T. J., Robinson, B. A. & Van Winkle, J. A. The role of interferon in persistent viral infection: insights from murine norovirus. *Trends Microbiol.* **26**, 510–524 (2018).

15. Stetson, D. B. & Medzhitov, R. Type I interferons in host defense. *Immunity* **25**, 373–381 (2006).

16. Teijaro, J. R. Type I interferons in viral control and immune regulation. *Curr. Opin. Virol.* **16**, 31–40 (2016).

17. Munir, S. *et al.* Nonstructural Proteins 1 and 2 of Respiratory Syncytial Virus Suppress Maturation of Human Dendritic Cells. *J. Virol.* **82**, 8780–8796 (2008).

18. Munir, S. *et al.* Respiratory Syncytial Virus Interferon Antagonist NS1 Protein Suppresses and Skews the Human T Lymphocyte Response. *PLoS Pathog.* **7**, (2011).

19. Bukreyev, A. *et al.* The Secreted Form of Respiratory Syncytial Virus G Glycoprotein Helps the Virus Evade Antibody-Mediated Restriction of Replication by Acting as an Antigen Decoy and through Effects on Fc Receptor-Bearing Leukocytes. *J. Virol.* **82**, 12191–12204 (2008).

20. Lambert, L., Sagfors, A. M., Openshaw, P. J. M. & Culley, F. J. Immunity to RSV in Early-Life. *Front. Immunol.* **5**, (2014).

21. Lanari, M., Vandini, S., Capretti, M. G., Lazzarotto, T. & Faldella, G. Respiratory Syncytial Virus Infections in Infants Affected by Primary Immunodeficiency. *J. Immunol. Res.* **2014**, (2014).

22. Borchers, A. T., Chang, C., Gershwin, M. E. & Gershwin, L. J. Respiratory Syncytial Virus—A Comprehensive Review. *Clin. Rev. Allergy Immunol.* **45**, 331–379 (2013).

23. Zhang, X. *et al.* [Risk factors for acute respiratory syncytial virus infection of lower respiratory tract in hospitalized infants]. *Zhonghua Er Ke Za Zhi Chin. J. Pediatr.* **52**, 373–377 (2014).

24. Ruckwardt, T. J., Morabito, K. M. & Graham, B. S. Determinants of early life immune responses to RSV infection. *Curr. Opin. Virol.* **16**, 151–157 (2016).

25. Fulginiti, V. A. *et al.* Respiratory virus immunization. I. A field trial of two inactivated respiratory virus vaccines; an aqueous trivalent parainfluenza virus vaccine and an alum-precipitated respiratory syncytial virus vaccine. *Am. J. Epidemiol.* **89**, 435–448 (1969).

26. Kapikian, A. Z., Mitchell, R. H., Chanock, R. M., Shvedoff, R. A. & Stewart, C. E. An epidemiologic study of altered clinical reactivity to respiratory syncytial (RS) virus infection in children previously vaccinated with an inactivated RS virus vaccine. *Am. J. Epidemiol.* **89**, 405–421 (1969).

27. Kim, H. W. *et al.* Respiratory syncytial virus disease in infants despite prior administration of antigenic inactivated vaccine. *Am. J. Epidemiol.* **89**, 422–434 (1969).

28. Simoes, E. A. F. *et al.* Palivizumab Prophylaxis, Respiratory Syncytial Virus, and Subsequent Recurrent Wheezing. *J. Pediatr.* **151**, 34-42.e1 (2007).

29. McDermott, D. S., Weiss, K. A., Knudson, C. J. & Varga, S. M. Central role of dendritic cells in shaping the adaptive immune response during respiratory syncytial virus infection. *Future Virol.* **6**, 963–973 (2011).

30. Meng, J., Stobart, C. C., Hotard, A. L. & Moore, M. L. An Overview of Respiratory Syncytial Virus. *PLoS Pathog.* **10**, (2014).

31. Mukherjee, S. *et al.* IL-17-induced pulmonary pathogenesis during respiratory viral infection and exacerbation of allergic disease. *Am. J. Pathol.* **179**, 248–258 (2011).

32. Stoppelenburg, A. J., de Roock, S., Hennus, M. P., Bont, L. & Boes, M. Elevated Th17 response in infants undergoing respiratory viral infection. *Am. J. Pathol.* **184**, 1274–1279 (2014).

33. Lukacs, N. W. *et al.* Respiratory virus-induced TLR7 activation controls IL-17-associated increased mucus via IL-23 regulation. *J. Immunol. Baltim. Md 1950* **185**, 2231–2239 (2010).

34. Hashimoto, K. *et al.* Respiratory syncytial virus infection in the absence of STAT 1 results in airway dysfunction, airway mucus, and augmented IL-17 levels. *J. Allergy Clin. Immunol.* **116**, 550–557 (2005).

35. Lotz, M. T. & Peebles, R. S. Mechanisms of Respiratory Syncytial Virus Modulation of Airway Immune Responses. *Curr. Allergy Asthma Rep.* **12**, 380–387 (2012).

36. Becker, Y. Respiratory syncytial virus (RSV) evades the human adaptive immune system by skewing the Th1/Th2 cytokine balance toward increased levels of Th2 cytokines and IgE, markers of allergy--a review. *Virus Genes* **33**, 235–252 (2006).

37. Ptaschinski, C. *et al.* RSV-Induced H3K4 Demethylase KDM5B Leads to Regulation of Dendritic Cell-Derived Innate Cytokines and Exacerbates Pathogenesis In Vivo. *PLoS Pathog.* **11**, e1004978 (2015).

38. Nagata, D. E. de A. *et al.* Epigenetic control of Foxp3 by SMYD3 H3K4 histone methyltransferase controls iTreg development and regulates pathogenic T-cell responses during pulmonary viral infection. *Mucosal Immunol.* **8**, 1131–1143 (2015).

39. Artis, D. & Spits, H. The biology of innate lymphoid cells. *Nature* **517**, 293–301 (2015).

40. Huang, Y. & Paul, W. E. Inflammatory group 2 innate lymphoid cells. *Int. Immunol.* **28**, 23–28 (2016).

41. Ito, T. *et al.* TSLP-activated dendritic cells induce an inflammatory T helper type 2 cell response through OX40 ligand. *J. Exp. Med.* **202**, 1213–1223 (2005).

42. Wang, Q., Du, J., Zhu, J., Yang, X. & Zhou, B. Thymic stromal lymphopoietin signaling in CD4(+) T cells is required for TH2 memory. *J. Allergy Clin. Immunol.* **135**, 781-791.e3 (2015).

43. Roan, F., Obata-Ninomiya, K. & Ziegler, S. F. Epithelial cell-derived cytokines: more than just signaling the alarm. *J. Clin. Invest.* **129**, 1441–1451 (2019).

44. Freer, G. & Matteucci, D. Influence of dendritic cells on viral pathogenicity. *PLoS Pathog.* **5**, e1000384 (2009).

45. Swedan, S., Andrews, J., Majumdar, T., Musiyenko, A. & Barik, S. Multiple Functional Domains and Complexes of the Two Nonstructural Proteins of Human Respiratory Syncytial Virus Contribute to Interferon Suppression and Cellular Location ▽ . *J. Virol.* **85**, 10090–10100 (2011).

46. Cormier, S. A., You, D. & Honnegowda, S. The use of a neonatal mouse model to study respiratory syncytial virus infections. *Expert Rev. Anti Infect. Ther.* **8**, 1371–1380 (2010).

47. Saravia, J. *et al.* Respiratory Syncytial Virus Disease Is Mediated by Age-Variable IL-33. *PLoS Pathog.* **11**, e1005217 (2015).

48. Miller, J. F. a. P. Events that led to the discovery of T-cell development and function – a personal recollection. *Tissue Antigens* **63**, 509–517 (2004).

49. Mitchell, G. F. & Miller, J. F. Cell to cell interaction in the immune response. II. The source of hemolysin-forming cells in irradiated mice given bone marrow and thymus or thoracic duct lymphocytes. *J. Exp. Med.* **128**, 821–837 (1968).

50. Miller, J. F. & Mitchell, G. F. Cell to cell interaction in the immune response. I. Hemolysin-forming cells in neonatally thymectomized mice reconstituted with thymus or thoracic duct lymphocytes. *J. Exp. Med.* **128**, 801–820 (1968).

51. Mahnke, Y. D., Brodie, T. M., Sallusto, F., Roederer, M. & Lugli, E. The who's who of T-cell differentiation: human memory T-cell subsets. *Eur. J. Immunol.* **43**, 2797–2809 (2013).

52. Mosmann, T. R. & Sad, S. The expanding universe of T-cell subsets: Th1, Th2 and more. *Immunol. Today* **17**, 138–146 (1996).

53. Zhu, J., Yamane, H. & Paul, W. E. Differentiation of Effector CD4 T Cell Populations. *Annu. Rev. Immunol.* **28**, 445–489 (2010).

54. Romagnani, S. Th1/Th2 cells. *Inflamm. Bowel Dis.* **5**, 285–294 (1999).

55. Swain, S. L., McKinstry, K. K. & Strutt, T. M. Expanding roles for CD4+ T cells in immunity to viruses. *Nat. Rev. Immunol.* **12**, 136–148 (2012).

56. Kang, S., Brown, H. M. & Hwang, S. Direct Antiviral Mechanisms of Interferon-Gamma. *Immune Netw.* **18**, (2018).

57. Guglani, L. & Khader, S. A. Th17 cytokines in mucosal immunity and inflammation. *Curr. Opin. HIV AIDS* **5**, 120–127 (2010).

58. Bacharier, L. B. *et al.* Determinants of asthma after severe respiratory syncytial virus bronchiolitis. *J. Allergy Clin. Immunol.* **130**, 91-100.e3 (2012).

59. Nelms, K., Keegan, A. D., Zamorano, J., Ryan, J. J. & Paul, W. E. The IL-4 receptor: signaling mechanisms and biologic functions. *Annu. Rev. Immunol.* **17**, 701–738 (1999).

60. Luzina, I. G. *et al.* Regulation of inflammation by interleukin-4: a review of "alternatives". *J. Leukoc. Biol.* **92**, 753–764 (2012).

61. Deo, S. S., Mistry, K. J., Kakade, A. M. & Niphadkar, P. V. Role played by Th2 type cytokines in IgE mediated allergy and asthma. *Lung India Off. Organ Indian Chest Soc.* **27**, 66–71 (2010).

62. LaPorte, S. L. *et al.* Molecular and structural basis of cytokine receptor pleiotropy in the Interleukin-4/13 system. *Cell* **132**, 259–272 (2008).

63. Andrews, A.-L., Holloway, J. W., Holgate, S. T. & Davies, D. E. IL-4 Receptor α Is an Important Modulator of IL-4 and IL-13 Receptor Binding: Implications for the Development of Therapeutic Targets. *J. Immunol.* **176**, 7456–7461 (2006).

64. Kelly-Welch, A. E., Hanson, E. M., Boothby, M. R. & Keegan, A. D. Interleukin-4 and interleukin-13 signaling connections maps. *Science* **300**, 1527–1528 (2003).

65. Mueller, T. D., Zhang, J.-L., Sebald, W. & Duschl, A. Structure, binding, and antagonists in the IL-4/IL-13 receptor system. *Biochim. Biophys. Acta* **1592**, 237–250 (2002).

66. Hilton, D. J. *et al.* Cloning and characterization of a binding subunit of the interleukin 13 receptor that is also a component of the interleukin 4 receptor. *Proc. Natl. Acad. Sci. U. S. A.* **93**, 497–501 (1996).

67. Aman, M. J. *et al.* cDNA cloning and characterization of the human interleukin 13 receptor alpha chain. *J. Biol. Chem.* **271**, 29265–29270 (1996).

68. Wills-Karp, M. & Finkelman, F. D. Untangling the Complex Web of IL-4– and IL-13–Mediated Signaling Pathways. *Sci. Signal.* **1**, pe55 (2008).

69. Takatsu, K. Interleukin-5 and IL-5 receptor in health and diseases. *Proc. Jpn. Acad. Ser. B Phys. Biol. Sci.* **87**, 463–485 (2011).

70. Possa, S. S., Leick, E. A., Prado, C. M., Martins, M. A. & Tibério, I. F. L. C. Eosinophilic Inflammation in Allergic Asthma. *Front. Pharmacol.* **4**, (2013).

71. Mould, A. W. *et al.* The Effect of IL-5 and Eotaxin Expression in the Lung on Eosinophil Trafficking and Degranulation and the Induction of Bronchial Hyperreactivity. *J. Immunol.* **164**, 2142–2150 (2000).

72. Thai, P., Chen, Y., Dolganov, G. & Wu, R. Differential Regulation of MUC5AC/Muc5ac and hCLCA-1/mGob-5 Expression in Airway Epithelium. *Am. J. Respir. Cell Mol. Biol.* **33**, 523–530 (2005).

73. Stier, M. T. *et al.* Respiratory syncytial virus infection activates IL-13-producing group 2 innate lymphoid cells through thymic stromal lymphopoietin. *J. Allergy Clin. Immunol.* **138**, 814-824.e11 (2016).

74. McKenzie, A. N. J. Type-2 Innate Lymphoid Cells in Asthma and Allergy. *Ann. Am. Thorac. Soc.* **11**, S263–S270 (2014).

75. Mindt, B. C., Fritz, J. H. & Duerr, C. U. Group 2 Innate Lymphoid Cells in Pulmonary Immunity and Tissue Homeostasis. *Front. Immunol.* **9**, 840 (2018).

76. Han, M. *et al.* The Innate Cytokines IL-25, IL-33, and TSLP Cooperate in the Induction of Type 2 Innate Lymphoid Cell Expansion and Mucous Metaplasia in Rhinovirus-Infected Immature Mice. *J. Immunol. Baltim. Md 1950* **199**, 1308–1318 (2017).

77. Rajput, C. *et al.* RORα-dependent type 2 innate lymphoid cells are required and sufficient for mucous metaplasia in immature mice. *Am. J. Physiol. Lung Cell. Mol. Physiol.* **312**, L983–L993 (2017).

78. Schuijs, M. J. & Halim, T. Y. F. Group 2 innate lymphocytes at the interface between innate and adaptive immunity. *Ann. N. Y. Acad. Sci.* **1417**, 87–103 (2018).

79. Halim, T. Y. *et al.* Group 2 innate lymphoid cells license dendritic cells to potentiate memory T helper 2 cell responses. *Nat. Immunol.* **17**, 57–64 (2016).

80. Halim, T. Y. F. *et al.* Group 2 innate lymphoid cells are critical for the initiation of adaptive T helper 2 cell-mediated allergic lung inflammation. *Immunity* **40**, 425–435 (2014).

81. Halwani, R., Al-Muhsen, S. & Hamid, Q. T helper 17 cells in airway diseases: from laboratory bench to bedside. *Chest* **143**, 494–501 (2013).

82. Flannigan, K. L. *et al.* IL-17A-mediated neutrophil recruitment limits expansion of segmented filamentous bacteria. *Mucosal Immunol.* **10**, 673–684 (2017).

83. Chen, Y. *et al.* Stimulation of airway mucin gene expression by interleukin (IL)-17 through IL-6 paracrine/autocrine loop. *J. Biol. Chem.* **278**, 17036–17043 (2003).

84. Xia, W. *et al.* Interleukin-17A Promotes MUC5AC Expression and Goblet Cell Hyperplasia in Nasal Polyps via the Act1-Mediated Pathway. *PLoS ONE* **9**, (2014).

85. Hymowitz, S. G. *et al.* IL-17s adopt a cystine knot fold: structure and activity of a novel cytokine, IL-17F, and implications for receptor binding. *EMBO J.* **20**, 5332–5341 (2001).

86. Kawaguchi, M., Adachi, M., Oda, N., Kokubu, F. & Huang, S.-K. IL-17 cytokine family. *J. Allergy Clin. Immunol.* **114**, 1265–1273 (2004).

87. Mildner, A. & Jung, S. Development and function of dendritic cell subsets. *Immunity* **40**, 642–656 (2014).

88. Smit, J. J., Rudd, B. D. & Lukacs, N. W. Plasmacytoid dendritic cells inhibit pulmonary immunopathology and promote clearance of respiratory syncytial virus. *J. Exp. Med.* **203**, 1153–1159 (2006).

89. Jang, S., Smit, J., Kallal, L. E. & Lukacs, N. W. Respiratory syncytial virus infection modifies and accelerates pulmonary disease via DC activation and migration. *J. Leukoc. Biol.* **94**, 5–15 (2013).

90. Tognarelli, E. I., Bueno, S. M. & González, P. A. Immune-Modulation by the Human Respiratory Syncytial Virus: Focus on Dendritic Cells. *Front. Immunol.* **10**, (2019).

91. Cormier, S. A. *et al.* Limited type I interferons and plasmacytoid dendritic cells during neonatal respiratory syncytial virus infection permit immunopathogenesis upon reinfection. *J. Virol.* **88**, 9350–9360 (2014).

92. Kallal, L. E., Schaller, M. A., Lindell, D. M., Lira, S. A. & Lukacs, N. W. CCL20/CCR6 blockade enhances immunity to RSV by impairing recruitment of DC. *Eur. J. Immunol.* **40**, 1042–1052 (2010).

93. Tourdot, S. *et al.* Respiratory syncytial virus infection provokes airway remodelling in allergen-exposed mice in absence of prior allergen sensitization. *Clin. Exp. Allergy J. Br. Soc. Allergy Clin. Immunol.* **38**, 1016–1024 (2008).

94. Larkin, E. K. & Hartert, T. V. Genes associated with RSV lower respiratory tract infection and asthma: the application of genetic epidemiological methods to understand causality. *Future Virol.* **10**, 883–897 (2015).

95. Bacharier, L. B. *et al.* Determinants of asthma after severe respiratory syncytial virus bronchiolitis. *J. Allergy Clin. Immunol.* **130**, 91-100.e3 (2012).

96. Asher, I. & Pearce, N. Global burden of asthma among children. *Int. J. Tuberc. Lung Dis. Off. J. Int. Union Tuberc. Lung Dis.* **18**, 1269–1278 (2014).

97. Almqvist, C., Worm, M., Leynaert, B. & working group of GA2LEN WP 2.5 Gender. Impact of gender on asthma in childhood and adolescence: a GA2LEN review. *Allergy* **63**, 47–57 (2008).

98. Lu, S. *et al.* Predictors of asthma following severe respiratory syncytial virus (RSV) bronchiolitis in early childhood. *Pediatr. Pulmonol.* **51**, 1382–1392 (2016).

99. Divekar, R. & Kita, H. Recent advances in epithelium-derived cytokines (IL-33, IL-25 and TSLP) and allergic inflammation. *Curr. Opin. Allergy Clin. Immunol.* **15**, 98–103 (2015).

100. Byers, D. E. Defining the Roles of IL-33, Thymic Stromal Lymphopoietin, and IL-25 in Human Asthma. *Am. J. Respir. Crit. Care Med.* **190**, 715–716 (2014).

101. Rhinovirus induced IL-25 in asthma exacerbation drives type-2 immunity and allergic pulmonary inflammation. Available at: https://www.ncbi.nlm.nih.gov/pmc/articles/PMC4246061/. (Accessed: 30th June 2018)

102. Verma, M. *et al.* Experimental asthma persists in IL-33 receptor knockout mice because of the emergence of thymic stromal lymphopoietin-driven IL-9+ and IL-13+ type 2 innate lymphoid cell subpopulations. *J. Allergy Clin. Immunol.* (2017). doi:10.1016/j.jaci.2017.10.020

103. Gauvreau, G. M. *et al.* Effects of an anti-TSLP antibody on allergen-induced asthmatic responses. *N. Engl. J. Med.* **370**, 2102–2110 (2014).

104. Ying, S. *et al.* Thymic stromal lymphopoietin expression is increased in asthmatic airways and correlates with expression of Th2-attracting chemokines and disease severity. *J. Immunol. Baltim. Md 1950* **174**, 8183–8190 (2005).

105. Torgerson, D. G. *et al.* Meta-analysis of Genome-wide Association Studies of Asthma In Ethnically Diverse North American Populations. *Nat. Genet.* **43**, 887–892 (2011).

106. Vicente, C. T., Revez, J. A. & Ferreira, M. A. R. Lessons from ten years of genome-wide association studies of asthma. *Clin. Transl. Immunol.* **6**, e165 (2017).

107. Levin, S. D. *et al.* Thymic stromal lymphopoietin: a cytokine that promotes the development of IgM+ B cells in vitro and signals via a novel mechanism. *J. Immunol. Baltim. Md 1950* **162**, 677–683 (1999).

108. Ziegler, S. F. *et al.* The biology of thymic stromal lymphopoietin (TSLP). *Adv. Pharmacol. San Diego Calif* **66**, 129–155 (2013).

109. Chien, C. D., Nguyen, S. M., Qin, H., Jacoby, E. & Fry, T. J. CRLF2 /Tslpr Overexpressing Acute Lymphoblastic Leukemia Relapse Is Driven By Chemotherapy-Induced TSLP from Bone Marrow Stromal Cells. *Blood* **126**, 1432–1432 (2015).

110. Collison, A. *et al.* TRAIL regulates MID1, TSLP, inflammation and remodelling in experimental eosinophilic oesophagitis. *J. Allergy Clin. Immunol.* **136**, 971–982 (2015).

111. Takai, T. TSLP expression: cellular sources, triggers, and regulatory mechanisms. *Allergol. Int. Off. J. Jpn. Soc. Allergol.* **61**, 3–17 (2012).

112. Zhong, J. *et al.* TSLP signaling pathway map: a platform for analysis of TSLP-mediated signaling. *Database J. Biol. Databases Curation* **2014**, bau007 (2014).

113. Ito, T., Liu, Y.-J. & Arima, K. Cellular and Molecular Mechanisms of TSLP Function in Human Allergic Disorders - TSLP Programs the "Th2 code" in Dendritic Cells. *Allergol. Int. Off. J. Jpn. Soc. Allergol.* **61**, 35–43 (2012).

114. Li, Y.-L. *et al.* Thymic stromal lymphopoietin promotes lung inflammation through activation of dendritic cells. *J. Asthma Off. J. Assoc. Care Asthma* **47**, 117–123 (2010).

115. Elder, M. J., Webster, S. J., Williams, D. L., Gaston, J. S. H. & Goodall, J. C. TSLP production by dendritic cells is modulated by IL-1β and components of the endoplasmic reticulum stress response. *Eur. J. Immunol.* **46**, 455–463 (2016).

116. Kashyap, M., Rochman, Y., Spolski, R., Samsel, L. & Leonard, W. J. Thymic Stromal Lymphopoietin is Produced by Dendritic Cells. *J. Immunol. Baltim. Md 1950* **187**, 1207–1211 (2011).

117. Lee, H.-C. *et al.* Thymic stromal lymphopoietin is induced by respiratory syncytial virus-infected airway epithelial cells and promotes a type 2 response to infection. *J. Allergy Clin. Immunol.* **130**, 1187-1196.e5 (2012).

118. Han, J. *et al.* Responsiveness to respiratory syncytial virus in neonates is mediated through thymic stromal lymphopoietin and OX40 ligand. *J. Allergy Clin. Immunol.* **130**, 1175-1186.e9 (2012).

119. Bohmwald, K. *et al.* Contribution of Cytokines to Tissue Damage During Human Respiratory Syncytial Virus Infection. *Front. Immunol.* **10**, 452 (2019).

120. Miller, A. L., Bowlin, T. L. & Lukacs, N. W. Respiratory syncytial virus-induced chemokine production: linking viral replication to chemokine production in vitro and in vivo. *J. Infect. Dis.* **189**, 1419–1430 (2004).

121. Lukacs, N. W. *et al.* Respiratory syncytial virus predisposes mice to augmented allergic airway responses via IL-13-mediated mechanisms. *J. Immunol. Baltim. Md 1950* **167**, 1060–1065 (2001).

122. Netea, M. G. *et al.* Trained immunity: a program of innate immune memory in health and disease. *Science* **352**, aaf1098 (2016).

123. Song, W. M. & Colonna, M. Immune Training Unlocks Innate Potential. *Cell* **172**, 3–5 (2018).

124. Bianchi, M. E. DAMPs, PAMPs and alarmins: all we need to know about danger. *J. Leukoc. Biol.* **81**, 1–5 (2007).

125. Kawai, T. & Akira, S. The role of pattern-recognition receptors in innate immunity: update on Toll-like receptors. *Nat. Immunol.* **11**, 373–384 (2010).

126. Foster, S. L., Hargreaves, D. C. & Medzhitov, R. Gene-specific control of inflammation by TLR-induced chromatin modifications. *Nature* **447**, 972–978 (2007).

127. Quintin, J. *et al.* Candida albicans Infection Affords Protection against Reinfection via Functional Reprogramming of Monocytes. *Cell Host Microbe* **12**, (2012).

128. Ramirez-Carrozzi, V. R. *et al.* Selective and antagonistic functions of SWI/SNF and Mi-2beta nucleosome remodeling complexes during an inflammatory response. *Genes Dev.* **20**, 282–296 (2006).

129. Ramirez-Carrozzi, V. R. *et al.* A unifying model for the selective regulation of inducible transcription by CpG islands and nucleosome remodeling. *Cell* **138**, 114–128 (2009).

130. Barski, A. *et al.* High-resolution profiling of histone methylations in the human genome. *Cell* **129**, 823–837 (2007).

131. Lee, G. R., Kim, S. T., Spilianakis, C. G., Fields, P. E. & Flavell, R. A. T helper cell differentiation: regulation by cis elements and epigenetics. *Immunity* **24**, 369–379 (2006).

132. Wei, G. *et al.* Global Mapping of H3K4me3 and H3K27me3 Reveals Specificity and Plasticity in Lineage Fate Determination of Differentiating CD4+ T Cells. *Immunity* **30**, 155–167 (2009).

133. Wen, H., Dou, Y., Hogaboam, C. M. & Kunkel, S. L. Epigenetic regulation of dendritic cell-derived interleukin-12 facilitates immunosuppression after a severe innate immune response. *Blood* **111**, 1797–1804 (2008).

134. De Santa, F. *et al.* Jmjd3 contributes to the control of gene expression in LPS-activated macrophages. *EMBO J.* **28**, 3341–3352 (2009).

135. Lee, M. G. *et al.* Demethylation of H3K27 regulates polycomb recruitment and H2A ubiquitination. *Science* **318**, 447–450 (2007).

136. Arcipowski, K. M., Martinez, C. A. & Ntziachristos, P. Histone demethylases in physiology and cancer: a tale of two enzymes, JMJD3 and UTX. *Curr. Opin. Genet. Dev.* **36**, 59–67 (2016).

137. Salminen, A., Kaarniranta, K., Hiltunen, M. & Kauppinen, A. Histone demethylase Jumonji D3 (JMJD3/KDM6B) at the nexus of epigenetic regulation of inflammation and the aging process. *J. Mol. Med. Berl. Ger.* **92**, 1035–1043 (2014).

138. Estarás, C., Fueyo, R., Akizu, N., Beltrán, S. & Martínez-Balbás, M. A. RNA polymerase II progression through H3K27me3-enriched gene bodies requires JMJD3 histone demethylase. *Mol. Biol. Cell* **24**, 351–360 (2013).

139. Doñas, C. *et al.* The histone demethylase inhibitor GSK-J4 limits inflammation through the induction of a tolerogenic phenotype on DCs. *J. Autoimmun.* **75**, 105–117 (2016).

140. Licona-Limón, P., Kim, L. K., Palm, N. W. & Flavell, R. A. TH2, allergy and group 2 innate lymphoid cells. *Nat. Immunol.* **14**, 536–542 (2013).

141. Zhou, B. *et al.* Thymic stromal lymphopoietin as a key initiator of allergic airway inflammation in mice. *Nat. Immunol.* **6**, 1047–1053 (2005).

142. Salter, B. M. A. *et al.* Human Bronchial Epithelial Cell-Derived Factors from Severe Asthmatic Subjects Stimulate Eosinophil Differentiation. *Am. J. Respir. Cell Mol. Biol.* (2017). doi:10.1165/rcmb.2016-0262OC

143. Mitchell, P. D. & O'Byrne, P. M. Epithelial-Derived Cytokines in Asthma. *Chest* **151**, 1338–1344 (2017).

144. Chauhan, A., Singh, M., Agarwal, A. & Paul, N. Correlation of TSLP, IL-33, and CD4 + CD25 + FOXP3 + T regulatory (Treg) in pediatric asthma. *J. Asthma Off. J. Assoc. Care Asthma* **52**, 868–872 (2015).

145. Moore, M. L. *et al.* A chimeric A2 strain of respiratory syncytial virus (RSV) with the fusion protein of RSV strain line 19 exhibits enhanced viral load, mucus, and airway dysfunction. *J. Virol.* **83**, 4185–4194 (2009).

146. Campbell, E. M. *et al.* Monocyte chemoattractant protein-1 mediates cockroach allergen-induced bronchial hyperreactivity in normal but not CCR2-/- mice: the role of mast cells. *J. Immunol. Baltim. Md 1950* **163**, 2160–2167 (1999).

147. Jang, S., Smit, J., Kallal, L. E. & Lukacs, N. W. Respiratory syncytial virus infection modifies and accelerates pulmonary disease via DC activation and migration. *J. Leukoc. Biol.* **94**, 5–15 (2013).

148. Wang, F. *et al.* RNAscope: A Novel in Situ RNA Analysis Platform for Formalin-Fixed, Paraffin-Embedded Tissues. *J. Mol. Diagn.* **14**, 22–29 (2012).

149. Saenz, S. A., Taylor, B. C. & Artis, D. Welcome to the neighborhood: epithelial cell-derived cytokines license innate and adaptive immune responses at mucosal sites. *Immunol. Rev.* **226**, 172–190 (2008).

150. Hammad, H. & Lambrecht, B. N. Barrier Epithelial Cells and the Control of Type 2 Immunity. *Immunity* **43**, 29–40 (2015).

151. Feng, S. *et al.* Role of the TSLP-DC-OX40L pathway in asthma pathogenesis and airway inflammation in mice. *Biochem. Cell Biol. Biochim. Biol. Cell.* **96**, 306–316 (2018).

152. Liu, Y.-J. Thymic stromal lymphopoietin and OX40 ligand pathway in the initiation of dendritic cell-mediated allergic inflammation. *J. Allergy Clin. Immunol.* **120**, 238–244; quiz 245–246 (2007).

153. Jang, S., Morris, S. & Lukacs, N. W. TSLP Promotes Induction of Th2 Differentiation but Is Not Necessary during Established Allergen-Induced Pulmonary Disease. *PLOS ONE* **8**, e56433 (2013).

154. Sigurs, N. *et al.* Severe respiratory syncytial virus bronchiolitis in infancy and asthma and allergy at age 13. *Am. J. Respir. Crit. Care Med.* **171**, 137–141 (2005).

155. Osman, M. *et al.* Changing trends in sex specific prevalence rates for childhood asthma, eczema, and hay fever. *Pediatr. Pulmonol.* **42**, 60–65

156. Hui, C. C. K. *et al.* Thymic stromal lymphopoietin (TSLP) secretion from human nasal epithelium is a function of TSLP genotype. *Mucosal Immunol.* **8**, 993–999 (2015).

157. Hunninghake, G. M. *et al.* TSLP polymorphisms are associated with asthma in a sex-specific fashion. *Allergy* **65**, 1566–1575 (2010).

158. Bunyavanich, S. *et al.* Thymic stromal lymphopoietin (TSLP) is associated with allergic rhinitis in children with asthma. *Clin. Mol. Allergy CMA* **9**, 1 (2011).

159. Camelo, A. *et al.* IL-33, IL-25, and TSLP induce a distinct phenotypic and activation profile in human type 2 innate lymphoid cells. *Blood Adv.* **1**, 577–589 (2017).

160. Halim, T. Y. F. Group 2 innate lymphoid cells in disease. *Int. Immunol.* **28**, 13–22 (2016).

161. Ramalingam, T. R. *et al.* Regulation of Helminth-Induced Th2 Responses by Thymic Stromal Lymphopoietin. *J. Immunol. Baltim. Md 1950* **182**, 6452–6459 (2009).

162. Huber, J. P. & Farrar, J. D. Regulation of effector and memory T-cell functions by type I interferon. *Immunology* **132**, 466–474 (2011).

163. Guo, B., Chang, E. Y. & Cheng, G. The type I IFN induction pathway constrains Th17-mediated autoimmune inflammation in mice. *J. Clin. Invest.* **118**, 1680–1690 (2008).

164. Ziegler, S. M. *et al.* Human pDCs display sex-specific differences in type I interferon subtypes and interferon α/β receptor expression. *Eur. J. Immunol.* **47**, 251–256 (2017).

165. Ye, L. *et al.* Interferon-λ enhances adaptive mucosal immunity by boosting release of thymic stromal lymphopoietin. *Nat. Immunol.* **20**, 593 (2019).

166. Uller, L. *et al.* Double-stranded RNA induces disproportionate expression of thymic stromal lymphopoietin versus interferon-beta in bronchial epithelial cells from donors with asthma. *Thorax* **65**, 626–632 (2010).

167. Robinson, R. F. Impact of respiratory syncytial virus in the United States. *Am. J. Health. Syst. Pharm.* **65**, S3–S6 (2008).

168. Lotz, M. T. & Peebles, R. S. Mechanisms of respiratory syncytial virus modulation of airway immune responses. *Curr. Allergy Asthma Rep.* **12**, 380–387 (2012).

169. Malinczak, C.-A. *et al.* Sex-associated TSLP-induced immune alterations following early-life RSV infection leads to enhanced allergic disease. *Mucosal Immunol.* **12**, 969–979 (2019).

170. Williams, J. W. *et al.* Transcription factor IRF4 drives dendritic cells to promote Th2 differentiation. *Nat. Commun.* **4**, 1–12 (2013).

171. Froidure, A. *et al.* Myeloid dendritic cells are primed in allergic asthma for thymic stromal lymphopoietin-mediated induction of Th2 and Th9 responses. *Allergy* **69**, 1068–1076 (2014).

172. Mohapatra, A. *et al.* Group 2 innate lymphoid cells utilize the IRF4-IL-9 module to coordinate epithelial cell maintenance of lung homeostasis. *Mucosal Immunol.* **9**, 275–286 (2016).

173. Buenrostro, J. D., Giresi, P. G., Zaba, L. C., Chang, H. Y. & Greenleaf, W. J. Transposition of native chromatin for fast and sensitive epigenomic profiling of open chromatin, DNA-binding proteins and nucleosome position. *Nat. Methods* **10**, 1213–1218 (2013).

174. Amaral, M. L., Erikson, G. A. & Shokhirev, M. N. BART: bioinformatics array research tool. *BMC Bioinformatics* **19**, 296 (2018).

175. Jenkins, S. J., Perona-Wright, G., Worsley, A. G. F., Ishii, N. & MacDonald, A. S. Dendritic cell expression of OX40 ligand acts as a costimulatory, not polarizing, signal for optimal Th2 priming and memory induction in vivo. *J. Immunol. Baltim. Md 1950* **179**, 3515–3523 (2007).

176. Reed, M. *et al.* Autophagy-inducing protein beclin-1 in dendritic cells regulates CD4 T cell responses and disease severity during respiratory syncytial virus infection. *J. Immunol. Baltim. Md 1950* **191**, 2526–2537 (2013).

177. Barnden, M. J., Allison, J., Heath, W. R. & Carbone, F. R. Defective TCR expression in transgenic mice constructed using cDNA-based alpha- and beta-chain genes under the control of heterologous regulatory elements. *Immunol. Cell Biol.* **76**, 34–40 (1998).

178. Robertson, J. M., Jensen, P. E. & Evavold, B. D. DO11.10 and OT-II T Cells Recognize a C-Terminal Ovalbumin 323–339 Epitope. *J. Immunol.* **164**, 4706–4712 (2000).

179. Kaneko, Y. *et al.* The search for common pathways underlying asthma and COPD. *Int. J. Chron. Obstruct. Pulmon. Dis.* **8**, 65–78 (2013).

180. Gabay, C., Lamacchia, C. & Palmer, G. IL-1 pathways in inflammation and human diseases. *Nat. Rev. Rheumatol.* **6**, 232–241 (2010).

181. Dinarello, C. A. Interleukin-1 in the pathogenesis and treatment of inflammatory diseases. *Blood* **117**, 3720–3732 (2011).

182. Molteni, M., Gemma, S. & Rossetti, C. The Role of Toll-Like Receptor 4 in Infectious and Noninfectious Inflammation. *Mediators Inflamm.* **2016**, (2016).

183. Miller, S. I., Ernst, R. K. & Bader, M. W. LPS, TLR4 and infectious disease diversity. *Nat. Rev. Microbiol.* **3**, 36–46 (2005).

184. van Tol, S., Hage, A., Giraldo, M. I., Bharaj, P. & Rajsbaum, R. The TRIMendous Role of TRIMs in Virus–Host Interactions. *Vaccines* **5**, (2017).

185. van Gent, M., Sparrer, K. M. J. & Gack, M. U. TRIM Proteins and Their Roles in Antiviral Host Defenses. *Annu. Rev. Virol.* **5**, 385–405 (2018).

186. Rajsbaum, R., García-Sastre, A. & Versteeg, G. A. TRIMmunity: The roles of the TRIM E3-ubiquitin ligase family in innate antiviral immunity. *J. Mol. Biol.* **426**, 1265–1284 (2014).

187. Patil, G. & Li, S. Tripartite motif proteins: an emerging antiviral protein family. *Future Virol.* **14**, 107–122 (2019).

188. Cantor, H. & Shinohara, M. L. Regulation of T-helper-cell lineage development by osteopontin. *Nat. Rev. Immunol.* **9**, 137–141 (2009).

189. Ashkar, S. *et al.* Eta-1 (Osteopontin): An Early Component of Type-1 (Cell-Mediated) Immunity. *Science* **287**, 860–864 (2000).

190. Antonelli, A. *et al.* Interferon-α, -β and -γ induce CXCL11 secretion in human thyrocytes: modulation by peroxisome proliferator-activated receptor γ agonists. *Immunobiology* **218**, 690–695 (2013).

191. Noah, T. L. *et al.* Chemokines and inflammation in the nasal passages of infants with respiratory syncytial virus bronchiolitis. *Clin. Immunol. Orlando Fla* **104**, 86–95 (2002).

192. Haeberle, H. A. *et al.* Inducible Expression of Inflammatory Chemokines in Respiratory Syncytial Virus-Infected Mice: Role of MIP-1α in Lung Pathology. *J. Virol.* **75**, 878–890 (2001).

193. Monick, M. M. *et al.* Activation of the Epidermal Growth Factor Receptor by Respiratory Syncytial Virus Results in Increased Inflammation and Delayed Apoptosis. *J. Biol. Chem.* **280**, 2147–2158 (2005).

194. Gao, Y. *et al.* Control of T helper 2 responses by transcription factor IRF4-dependent dendritic cells. *Immunity* **39**, 722–732 (2013).

195. Stritesky, G. L. *et al.* The transcription factor STAT3 is required for T helper 2 cell development. *Immunity* **34**, 39–49 (2011).

196. Cao, L. *et al.* TSLP promotes asthmatic airway remodeling via p38-STAT3 signaling pathway in human lung fibroblast. *Exp. Lung Res.* **44**, 288–301 (2018).

197. Liu, J. & Ma, X. Interferon regulatory factor 8 regulates RANTES gene transcription in cooperation with interferon regulatory factor-1, NF-kappaB, and PU.1. *J. Biol. Chem.* **281**, 19188–19195 (2006).

198. Yamamoto, M. *et al.* Shared and Distinct Functions of the Transcription Factors IRF4 and IRF8 in Myeloid Cell Development. *PLOS ONE* **6**, e25812 (2011).

199. Ozato, K., Shin, D.-M., Chang, T.-H. & Morse, H. C. TRIM family proteins and their emerging roles in innate immunity. *Nat. Rev. Immunol.* **8**, 849–860 (2008).

200. Tait Wojno, E. D., Hunter, C. A. & Stumhofer, J. S. The Immunobiology of the Interleukin-12 Family: Room for Discovery. *Immunity* **50**, 851–870 (2019).

201. Yamaguchi, T., Takizawa, F., Fischer, U. & Dijkstra, J. M. Along the Axis between Type 1 and Type 2 Immunity; Principles Conserved in Evolution from Fish to Mammals. *Biology* **4**, 814–859 (2015).

202. Liu, Y.-J. TSLP in epithelial cell and dendritic cell cross talk. *Adv. Immunol.* **101**, 1–25 (2009).

203. Mitchell, C., Provost, K., Niu, N., Homer, R. & Cohn, L. Interferon-gamma acts on the airway epithelium to inhibit local and systemic pathology in allergic airway disease. *J. Immunol. Baltim. Md 1950* **187**, 3815–3820 (2011).

204. Han, M. *et al.* IFN-γ Blocks Development of an Asthma Phenotype in Rhinovirus-Infected Baby Mice by Inhibiting Type 2 Innate Lymphoid Cells. *Am. J. Respir. Cell Mol. Biol.* **56**, 242–251 (2016).

205. Ban, J. *et al.* Human Respiratory Syncytial Virus NS 1 Targets TRIM25 to Suppress RIG-I Ubiquitination and Subsequent RIG-I-Mediated Antiviral Signaling. *Viruses* **10**, 716 (2018).

206. Du, H. *et al.* MID1 Catalyzes the Ubiquitination of Protein Phosphatase 2A and Mutations within Its Bbox1 Domain Disrupt Polyubiquitination of Alpha4 but Not of PP2Ac. *PLOS ONE* **9**, e107428 (2014).

207. Zhang, L. *et al.* MID1-PP2A complex functions as new insights in human lung adenocarcinoma. *J. Cancer Res. Clin. Oncol.* **144**, 855–864 (2018).

208. Guergnon, J. *et al.* PP2A targeting by viral proteins: A widespread biological strategy from DNA/RNA tumor viruses to HIV-1. *Biochim. Biophys. Acta BBA - Mol. Basis Dis.* **1812**, 1498–1507 (2011).

209. Kouzarides, T. Chromatin Modifications and Their Function. *Cell* **128**, 693–705 (2007).

210. Allis, C. D. & Jenuwein, T. The molecular hallmarks of epigenetic control. *Nat. Rev. Genet.* **17**, 487–500 (2016).

211. Fischle, W. *et al.* Molecular basis for the discrimination of repressive methyl-lysine marks in histone H3 by Polycomb and HP1 chromodomains. *Genes Dev.* **17**, 1870–1881 (2003).

212. Zhang, Y. & Reinberg, D. Transcription regulation by histone methylation: interplay between different covalent modifications of the core histone tails. *Genes Dev.* **15**, 2343–2360 (2001).

213. De Santa, F. *et al.* The histone H3 lysine-27 demethylase Jmjd3 links inflammation to inhibition of polycomb-mediated gene silencing. *Cell* **130**, 1083–1094 (2007).

214. Tekkanat, K. K. *et al.* RANTES (CCL5) production during primary respiratory syncytial virus infection exacerbates airway disease. *Eur. J. Immunol.* **32**, 3276–3284 (2002).

215. Kruidenier, L. *et al.* A selective jumonji H3K27 demethylase inhibitor modulates the proinflammatory macrophage response. *Nature* **488**, 404–408 (2012).

216. Bermick, J. R. *et al.* Neonatal monocytes exhibit a unique histone modification landscape. *Clin. Epigenetics* **8**, 99 (2016).

217. Bayarsaihan, D. Epigenetic Mechanisms in Inflammation. *J. Dent. Res.* **90**, 9–17 (2011).

218. Morandini, A. C., Santos, C. F. & Yilmaz, Ö. Role of epigenetics in modulation of immune response at the junction of host–pathogen interaction and danger molecule signaling. *Pathog. Dis.* **74**, (2016).

219. Shanmugam, M. K. & Sethi, G. Role of epigenetics in inflammation-associated diseases. *Subcell. Biochem.* **61**, 627–657 (2013).

220. Das, N. D. *et al.* Gene networking and inflammatory pathway analysis in a JMJD3 knockdown human monocytic cell line. *Cell Biochem. Funct.* **30**, 224–232 (2012).

221. Das, A. *et al.* Proteomic changes induced by histone demethylase JMJD3 in TNF alpha-treated human monocytic (THP-1) cells. *Mol. Immunol.* **56**, 113–122 (2013).

222. Ishii, M. *et al.* Epigenetic regulation of the alternatively activated macrophage phenotype. *Blood* **114**, 3244–3254 (2009).

223. Pham, D. *et al.* Opposing roles of STAT4 and Dnmt3a in Th1 gene regulation. *J. Immunol. Baltim. Md 1950* **191**, 902–911 (2013).

224. Estarás, C. *et al.* Genome-wide analysis reveals that Smad3 and JMJD3 HDM co-activate the neural developmental program. *Dev. Camb. Engl.* **139**, 2681–2691 (2012).

225. Wei, Y. *et al.* KDM6B overexpression activates innate immune signaling and impairs hematopoiesis in mice. *Blood Adv.* **2**, 2491–2504 (2018).

226. Worgall, S. Editorial: RSV, dendritic cells, and allergens—a bad combination. *J. Leukoc. Biol.* **94**, 1–3 (2013).

227. Heinemann, B. *et al.* Inhibition of demethylases by GSK-J1/J4. *Nature* **514**, E1–E2 (2014).

228. Acosta, P. L., Caballero, M. T. & Polack, F. P. Brief History and Characterization of Enhanced Respiratory Syncytial Virus Disease. *Clin. Vaccine Immunol. CVI* **23**, 189–195 (2016).

229. Connors, M. *et al.* Pulmonary histopathology induced by respiratory syncytial virus (RSV) challenge of formalin-inactivated RSV-immunized BALB/c mice is abrogated by depletion of CD4+ T cells. *J. Virol.* **66**, 7444–7451 (1992).

230. Connors, M. *et al.* Enhanced pulmonary histopathology induced by respiratory syncytial virus (RSV) challenge of formalin-inactivated RSV-immunized BALB/c mice is abrogated by depletion of interleukin-4 (IL-4) and IL-10. *J. Virol.* **68**, 5321–5325 (1994).

231. Blanchet, M.-R., Gold, M., Bennett, J. & McNagny, K. CD103 in the development of experimental asthma. *Allergy Asthma Clin. Immunol. Off. J. Can. Soc. Allergy Clin. Immunol.* **6**, P11 (2010).

232. Halim, T. Y. F. *et al.* Tissue-Restricted Adaptive Type 2 Immunity Is Orchestrated by Expression of the Costimulatory Molecule OX40L on Group 2 Innate Lymphoid Cells. *Immunity* **48**, 1195-1207.e6 (2018).

233. Wu, J. *et al.* Critical role of OX40/OX40L in ILC2-mediated activation of CD4+T cells during respiratory syncytial virus infection in mice. *Int. Immunopharmacol.* **76**, 105784 (2019).

234. Mullard, A. Vaccine failure explained. *Nature* news.2008.1302 (2008). doi:10.1038/news.2008.1302

235. Delgado, M. F. *et al.* Lack of antibody affinity maturation due to poor Toll-like receptor stimulation leads to enhanced respiratory syncytial virus disease. *Nat. Med.* **15**, 34–41 (2009).

236. Barrios, C. *et al.* The costimulatory molecules CD80, CD86 and OX40L are up-regulated in Aspergillus fumigatus sensitized mice. *Clin. Exp. Immunol.* **142**, 242–250 (2005).

237. Achuthan, A. *et al.* Granulocyte macrophage colony-stimulating factor induces CCL17 production via IRF4 to mediate inflammation. *J. Clin. Invest.* **126**, 3453–3466 (2016).

238. Hsu, A. T. *et al.* Epigenetic and transcriptional regulation of IL4-induced CCL17 production in human monocytes and murine macrophages. *J. Biol. Chem.* **293**, 11415–11423 (2018).

239. Wang, S.-P. *et al.* A UTX-MLL4-p300 Transcriptional Regulatory Network Coordinately Shapes Active Enhancer Landscapes for Eliciting Transcription. *Mol. Cell* **67**, 308-321.e6 (2017).

240. Cho, Y.-W. *et al.* PTIP associates with MLL3- and MLL4-containing histone H3 lysine 4 methyltransferase complex. *J. Biol. Chem.* **282**, 20395–20406 (2007).

241. Van der Meulen, J., Speleman, F. & Van Vlierberghe, P. The H3K27me3 demethylase UTX in normal development and disease. *Epigenetics* **9**, 658–668 (2014).

242. Li, Q. *et al.* Critical role of histone demethylase Jmjd3 in the regulation of CD4+ T-cell differentiation. *Nat. Commun.* **5**, 5780 (2014).

243. Liu, Z. *et al.* The histone H3 lysine-27 demethylase Jmjd3 plays a critical role in specific regulation of Th17 cell differentiation. *J. Mol. Cell Biol.* **7**, 505–516 (2015).

244. LaMere, S. A. *et al.* H3K27 Methylation Dynamics during CD4 T Cell Activation: Regulation of JAK/STAT and IL12RB2 Expression by JMJD3. *J. Immunol. Baltim. Md 1950* **199**, 3158–3175 (2017).

245. Manna, S. *et al.* Histone H3 Lysine 27 demethylases Jmjd3 and Utx are required for T-cell differentiation. *Nat. Commun.* **6**, (2015).

246. Schmidt, M. E. *et al.* Memory CD8 T cells mediate severe immunopathology following respiratory syncytial virus infection. *PLoS Pathog.* **14**, e1006810 (2018).

247. Openshaw, P. J. & Chiu, C. Protective and dysregulated T cell immunity in RSV infection. *Curr. Opin. Virol.* **3**, 468–474 (2013).

248. Rosenberg, H. F. & Domachowske, J. B. Inflammatory responses to Respiratory Syncytial Virus (RSV) infection and the development of immunomodulatory pharmacotherapeutics. *Curr. Med. Chem.* **19**, 1424–1431 (2012).

249. Openshaw, P. J. M. & Tregoning, J. S. Immune Responses and Disease Enhancement during Respiratory Syncytial Virus Infection. *Clin. Microbiol. Rev.* **18**, 541–555 (2005).

250. Bueno, S. M. *et al.* Host immunity during RSV pathogenesis. *Int. Immunopharmacol.* **8**, 1320–1329 (2008).

251. Li, Y. *et al.* Therapeutic potential of GSK-J4, a histone demethylase KDM6B/JMJD3 inhibitor, for acute myeloid leukemia. *J. Cancer Res. Clin. Oncol.* **144**, 1065–1077 (2018).

252. Pawlyn, C. *et al.* Histone Demethylase Inhibition As a Novel Therapeutic Strategy in Myeloma. *Blood* **124**, 2087–2087 (2014).

253. Thinnes, C. C. *et al.* Targeting histone lysine demethylases — Progress, challenges, and the future. *Biochim. Biophys. Acta* **1839**, 1416–1432 (2014).

254. Boila, L. D., Chatterjee, S. S., Banerjee, D. & Sengupta, A. KDM6 and KDM4 histone lysine demethylases emerge as molecular therapeutic targets in human acute myeloid leukemia. *Exp. Hematol.* **58**, 44-51.e7 (2018).

255. Souyris, M. *et al.* TLR7 escapes X chromosome inactivation in immune cells. *Sci. Immunol.* **3**, (2018).

256. O'Driscoll, D. *et al.* Expression of X chromosome-linked TLR4 signalling molecules in female versus male neonatal cord blood. *Eur. Respir. J.* **48**, PA3968 (2016).

257. Uematsu, S. & Akira, S. Toll-like Receptors and Type I Interferons. *J. Biol. Chem.* **282**, 15319–15323 (2007).

258. Yang, K. *et al.* Human TLR-7-, -8-, and -9-Mediated Induction of IFN-α/β and -λ Is IRAK-4 Dependent and Redundant for Protective Immunity to Viruses. *Immunity* **23**, 465–478 (2005).

259. Smith, N. *et al.* Control of TLR7-mediated type I IFN signaling in pDCs through CXCR4 engagement—A new target for lupus treatment. *Sci. Adv.* **5**, eaav9019 (2019).

260. Jacob, C. O. *et al.* Identification of IRAK1 as a risk gene with critical role in the pathogenesis of systemic lupus erythematosus. *Proc. Natl. Acad. Sci.* **106**, 6256–6261 (2009).

261. Souyris, M., Mejía, J. E., Chaumeil, J. & Guéry, J.-C. Female predisposition to TLR7-driven autoimmunity: gene dosage and the escape from X chromosome inactivation. *Semin. Immunopathol.* **41**, 153–164 (2019).

262. Farrugia, M. & Baron, B. The Role of Toll-Like Receptors in Autoimmune Diseases through Failure of the Self-Recognition Mechanism. *Int. J. Inflamm.* **2017**, (2017).

263. Singer, J. W. *et al.* Inhibition of interleukin-1 receptor-associated kinase 1 (IRAK1) as a therapeutic strategy. *Oncotarget* **9**, 33416–33439 (2018).

264. Quigley, C. A. The Postnatal Gonadotropin and Sex Steroid Surge—Insights from the Androgen Insensitivity Syndrome. *J. Clin. Endocrinol. Metab.* **87**, 24–28 (2002).

265. Bouvattier, C. *et al.* Postnatal changes of T, LH, and FSH in 46,XY infants with mutations in the AR gene. *J. Clin. Endocrinol. Metab.* **87**, 29–32 (2002).

266. Robledo-Aceves, M. *et al.* Risk factors for severe bronchiolitis caused by respiratory virus infections among Mexican children in an emergency department. *Medicine (Baltimore)* **97**, (2018).

267. Buchwald, A. G. *et al.* Epidemiology, Risk Factors, and Outcomes of Respiratory Syncytial Virus Infections in Newborns in Bamako, Mali. *Clin. Infect. Dis.* doi:10.1093/cid/ciz157

268. Jepsen, M. T. *et al.* Incidence and seasonality of respiratory syncytial virus hospitalisations in young children in Denmark, 2010 to 2015. *Eurosurveillance* **23**, 17–00163 (2018).

269. Lanari, M. *et al.* Risk factors for bronchiolitis hospitalization during the first year of life in a multicenter Italian birth cohort. *Ital. J. Pediatr.* **41**, 40 (2015).

270. Shang, T. *et al.* Toll-Like Receptor-Initiated Testicular Innate Immune Responses in Mouse Leydig Cells. *Endocrinology* **152**, 2827–2836 (2011).

271. Sun, B. *et al.* Sertoli cell-initiated testicular innate immune response through toll-like receptor-3 activation is negatively regulated by Tyro3, Axl, and mer receptors. *Endocrinology* **151**, 2886–2897 (2010).

272. Cephus, J. *et al.* Testosterone attenuates group 2 innate lymphoid cell-mediated airway inflammation. *Cell Rep.* **21**, 2487–2499 (2017).

273. Keselman, A. & Heller, N. Estrogen Signaling Modulates Allergic Inflammation and Contributes to Sex Differences in Asthma. *Front. Immunol.* **6**, (2015).

274. Chang, K.-K. *et al.* TSLP induced by estrogen stimulates secretion of MCP-1 and IL-8 and growth of human endometrial stromal cells through JNK and NF-κB signal pathways. *Int. J. Clin. Exp. Pathol.* **7**, 1889–1899 (2014).

275. Wu, H.-X., Guo, P.-F., Jin, L.-P., Liang, S.-S. & Li, D.-J. Functional regulation of thymic stromal lymphopoietin on proliferation and invasion of trophoblasts in human first-trimester pregnancy. *Hum. Reprod.* **25**, 1146–1152 (2010).

276. Köhler, A. *et al.* A hormone-dependent feedback-loop controls androgen receptor levels by limiting MID1, a novel translation enhancer and promoter of oncogenic signaling. *Mol. Cancer* **13**, 146 (2014).

277. Mabjeesh, N. J., Willard, M. T., Frederickson, C. E., Zhong, H. & Simons, J. W. Androgens stimulate hypoxia-inducible factor 1 activation via autocrine loop of tyrosine kinase receptor/phosphatidylinositol 3'-kinase/protein kinase B in prostate cancer cells. *Clin. Cancer Res. Off. J. Am. Assoc. Cancer Res.* **9**, 2416–2425 (2003).

278. Haeberle, H. A. *et al.* Oxygen-Independent Stabilization of Hypoxia Inducible Factor (HIF)-1 during RSV Infection. *PLoS ONE* **3**, (2008).

279. Jang, Y. *et al.* UVB Induces HIF-1α-Dependent TSLP Expression via the JNK and ERK Pathways. *J. Invest. Dermatol.* **133**, 2601–2608 (2013).

280. Mitani, T. *et al.* Hypoxia enhances transcriptional activity of androgen receptor through hypoxia-inducible factor-1α in a low androgen environment. *J. Steroid Biochem. Mol. Biol.* **123**, 58–64 (2011).

281. Sumi, Y. & Hamid, Q. Airway remodeling in asthma. *Allergol. Int. Off. J. Jpn. Soc. Allergol.* **56**, 341–348 (2007).

282. Zaiss, D. M. W., Gause, W. C., Osborne, L. C. & Artis, D. Emerging functions of amphiregulin in orchestrating immunity, inflammation and tissue repair. *Immunity* **42**, 216–226 (2015).

283. Monticelli, L. A. *et al.* Innate lymphoid cells promote lung tissue homeostasis following acute influenza virus infection. *Nat. Immunol.* **12**, 1045–1054 (2011).

284. Liu, T., Ding, L., Wu, Z., Santos, F. G. D. L. & Phan, S. Role of dendritic cell-derived amphiregulin in pulmonary fibrosis (CCR5P.203). *J. Immunol.* **194**, 186.5-186.5 (2015).

285. Chen, Z.-G. *et al.* Neutralization of TSLP inhibits airway remodeling in a murine model of allergic asthma induced by chronic exposure to house dust mite. *PloS One* **8**, e51268 (2013).

286. Fehrenbach, H., Wagner, C. & Wegmann, M. Airway remodeling in asthma: what really matters. *Cell Tissue Res.* **367**, 551–569 (2017).

287. Malmström, K. *et al.* Lung function, airway remodelling and inflammation in symptomatic infants: outcome at 3 years. *Thorax* **66**, 157–162 (2011).

288. Williams, P. V. Lung Function, Airway Remodeling, and Inflammation in Infants: Outcome at 8 Years. *Pediatrics* **136**, S257–S257 (2015).

289. Roncolato, F. T. *et al.* The effect of pulmonary function testing on bleomycin dosing in germ cell tumours. *Intern. Med. J.* **46**, 893–898 (2016).

290. Sleijfer, S., van der Mark, T. W., Schraffordt Koops, H. & Mulder, N. H. Decrease in pulmonary function during bleomycin-containing combination chemotherapy for testicular cancer: not only a bleomycin effect. *Br. J. Cancer* **71**, 120–123 (1995).

291. Dishop, M. K. Diagnostic Pathology of Diffuse Lung Disease in Children. *Pediatr. Allergy Immunol. Pulmonol.* **23**, 69–85 (2010).

292. Hrycaj, S. M. *et al.* Hox5 genes direct elastin network formation during alveologenesis by regulating myofibroblast adhesion. *Proc. Natl. Acad. Sci. U. S. Am. Wash.* **115**, E10605 (2018).